N°Ordre……/Faculté/UMBB/2024.

ALGERIAN DEMOCRATIC AND POPULAR REPUBLIC
MINISTRY OF HIGHER EDUCATION AND SCIENTIFIC RESEARCH

University of M`Hamed Bougara -Boumerdes
Faculty of Hydrocarbons and Chemistry
Department of Mining and Petroleum Deposits

Thesis for the completion of studies Towards obtaining the diploma of
MASTER

Presented by:

BERGHEUL Ania

Field: Hydrocarbons

Major: petroleum geology

Forward Stratigraphic Modeling of Fluvio-Deltaic Environments: Case Studies from the F3 Block, Netherlands Offshore, and TAGI reservoir (blocks 401a,402a), Berkine Basin

In front of the jury:

Mr.	CHAOUCHI	Rabah	Prof	President
Ms.	YAHIAOUI	Lamia	MAA	Supervisor
Mr.	AMROUCHE	Mohamed	Geoscientist	Co-Supervisor
Mr.	SADAOUI	Moussa	Prof	Examiner
Mr.	BENAYED	Soumya	MCA	Examiner

Academic year : 2023/2024

Acknowledgments

First and foremost, praise and thanks to Allah the Almighty and Merciful for giving me the strength and patience to accomplish this modest work.

All my heartfelt thanks to my university supervisor, Ms. Yahiaoui Lamia for her exceptional guidance and insightful feedback throughout the completion of this thesis. Her expertise has been crucial to my research.

I would like to express my sincere thanks to my mentor at SLB, Dr. Amrouche Mohamed for guiding me on this topic and providing continuous support throughout the completion of this project, as well as being an inspirational figure and mentor. His expertise, advice, and patience have been invaluable.

My gratitude also extends to the SLB company team who welcomed me into their organization. I would like to particularly thank Ms. Asma Chekroune for granting me this invaluable opportunity. My thanks also go to the D&I segment and G&G team for their heartfelt welcome, a special thanks to Mr. Nabil Meddour, Sylvain le Tourneur, Amine Bali, Tanina Lounissi, Meriem Lhasbellaoui, Yacine Sahar, for their availability, feedback and kindness.

I am grateful to the entire teaching staff of the Geology Department for their guidance throughout these incredible and challenging years. A special mention to Dr Benayed Soumya for her kindness, availability, and guidance. All my warm thanks go to my dear family and friends for being my support throughout this journey.

I would like to extend my gratitude to all those who, directly or indirectly, contributed to the completion of this work.

Dedication

To my dearest parents, to whom I owe many of my successes and accomplishments, I dedicate this work to you.

To my **dad**, for being my ultimate inspiration and instilling in me the importance of hard work and perseverance in the pursuit of my dreams.

To my beloved **mom**, whose boundless love has been my refuge in difficult times. This work is a humble tribute to your devotion and constant support

To my exceptional **siblings** Linda, Sofia, Faouzi, Beka, and Cherif for their unwavering support and love and to my beloved **nieces** and **nephews**

To the **friends** who became family.

To the friends encountered along this journey and my peers from MAGL19.

Last but not least, to **myself**

Abstract

The discovery of petroleum reservoirs relies heavily on understanding the evolutionary processes shaping sedimentary basins and their sedimentary infill over geological time. Accurately simulating this dynamic evolution is a primary challenge for petroleum geologists, especially as exploration moves towards deeper and more technically challenging areas with low seismic resolution.

Amid these challenges, enhancing predictive capabilities for reservoir and facies distribution at regional and basin scales is crucial for quantifying risk and uncertainty. A promising approach to address these difficulties is the use of stratigraphic forward models, which are calibrated to observed data using inverse modeling techniques.

This study utilizes PETREL's Geological Process Modeling (GPM) technology to understand basin evolution, depositional settings, and reservoir distribution in fluvio-deltaic environments. GPM integrates various inputs and field data to reconstruct stratigraphic sequences, enhancing the comprehension of subsurface geology from early exploration to development phase.

The research focuses on modeling the Pliocene fluvio-deltaic system in the F3 block of the North Sea. It examines how variables like sediment supply, eustasy, and tectonics affect sedimentation patterns and stratigraphic architecture. Additionally, it introduces GPM technology to Algeria, specifically targeting the TAGI reservoir's siliciclastic deposits in the Berkine Basin. The study provides insights into the geological processes shaping the evolution of this reservoir, demonstrating a strong correlation between model outputs and real-world seismic and well data. This correlation enables the identification of sequence boundaries, lithologies, and the timing of significant geological events.

The study aims to showcase the potential and limitations of Geological Process Modeling (GPM) in reconstructing past geological scenarios, ultimately enhancing the predictive capabilities in petroleum exploration.

Key words: geological process modeling, numerical modeling, Sedimentary basins, Berkine basin, F3 block, fluvio-deltaic environments, GPM

Résumé

La découverte des réservoirs pétroliers repose fortement sur la compréhension des processus évolutifs qui façonnent les bassins sédimentaires et leur remplissage sédimentaire au fil du temps géologique. Simuler avec précision l'évolution dynamique de ces bassins représente un défi majeur pour les géologues pétroliers, particulièrement à mesure que l'exploration des hydrocarbures conventionnels évolue vers des gisements plus profondes et techniquement plus complexes, caractérisées par une résolution sismique limitée.

Dans ce contexte, l'amélioration des capacités prédictives concernant la distribution des réservoirs et des faciès à l'échelle régionale et des bassins est essentielle pour quantifier les risques et les incertitudes. Une approche efficace et novatrice pour relever ces défis consiste à recourir aux modèles stratigraphiques avancés, qui sont ajustés aux données observées grâce à l'utilisation de techniques de modélisation inverse.

Cette étude utilise la technologie de Modélisation des Processus Géologiques (GPM) de PETREL pour comprendre l'évolution des bassins, les environnements de dépôt et la distribution des réservoirs dans les environnements fluvio-deltaïques. GPM intègre diverses données pour reconstruire les séquences stratigraphiques, enrichissant ainsi la compréhension de la géologie du sous-sol dans le cadre de l'exploration pétrolière

La recherche se concentre sur la modélisation du système fluvio-deltaïque pliocène dans le bloc F3 de la mer du Nord. Elle examine comment des variables telles que l'apport sédimentaire, l'eustatisme et la tectonique influencent les schémas de sédimentation et l'architecture stratigraphique. En outre, elle introduit la technologie GPM en Algérie, en se focalisant spécifiquement sur les dépôts siliclastiques du réservoir TAGI dans le bassin de Berkine. L'étude offre des perspectives sur les processus géologiques qui façonnent l'évolution de ce réservoir, démontrant une corrélation solide entre les résultats du modèle et les données sismiques et de puits réelles. Cette corrélation permet d'identifier les limites des séquences, les lithologies et la chronologie des événements géologiques significatifs.

L'objectif de cette étude est de mettre en évidence le potentiel et les limitations de la Modélisation des Processus Géologiques (GPM) pour reconstruire les scénarios géologiques passés, augmentant ainsi les capacités prédictives dans le domaine de l'exploration pétrolière.

Mots clés : modélisation géologiques, modélisation numérique, bassins sédimentaires, bassin de Berkine, bloc F3, environnements fluvio-deltaïques, GPM

Table of contents

General introduction:.....1
CHAPTER 1: Generalities
1 Geological Numerical Modeling.....4
1.1 Geological Process Modeling (GPM).....5
1.1.1 The Need for Geological Process Modeling (GPM).....6
1.1.2 Advantages over Geostatistical Methods.....7
1.1.3 Applications of GPM.....7
1.2 Research Motivation.....8
CHAPTER II: Geological Process Modeling (GPM) technology
2 Overview of GPM in Petrel software:.....10
2.1 GPM data input types:.....12
2.1.1 Soft data.....12
2.1.2 Hard data.....12
2.2 Elements and guiding principles of GPM.....13
2.2.1 Guiding principles:.....13
2.2.2 Elements of GPM:.....14
2.3 Key model inputs for a GPM model.....15
2.3.1 Paleo-topography:.....15
2.3.2 Sea level variations:.....15
2.3.3 Sediment types:.....16
2.3.4 Tectonics:.....16
2.4 Geological processes.....16
2.5 Domain of applications of GPM:.....19
2.6 Conclusion:.....23
CHAPTER III: North Sea “F3 BLOCK” case study
3 Introduction.....25
3.1 Study area.....25
3.2 Regional geology.....26
3.2.1 Tectonic framework:.....26
3.2.2 Stratigraphy:.....27
3.3 Data and methodology.....29
3.4 Sequence stratigraphy.....32
3.4.1 Sequence Breakdown.....33
3.5 Model set up and Calibration.....33
3.5.1 Paleo Topography.....34

3.5.2 Sediment types 37
3.5.3 Sea level 37
3.5.4 Tectonics 38
3.5.5 Sediment diffusion 39
3.5.6 Post modeling conversion 40
3.6 Simulation result and discussion 41
3.7 Alternative scenarios 45
3.7.1 Scenario a: varying diffusion coefficient and constant diffusion function 45
3.7.2 Scenario b: Impact of the diffusion coefficient 46
3.7.3 Scenario c: Impact of the diffusion function 47
3.7.4 Scenario d: No tectonics 48
3.7.5 Scenario E: Varying the sea level curve 49
3.8 Conclusion 51
CHAPTER IV: GPM case application in Algeria Block 401a/402a, Berkin basin
4 Introduction 53
4.1 Geological setting 53
4.1.1 Berkine basin 53
4.1.2 Tectonic History 54
4.1.3 Stratigraphy 55
4.2 Area of study: 56
4.2.1 The Triassic Argilo-Gréseux Inférieur “TAGI” in the Blocks Blocks 401a and 402a 57
4.2.2 Study sequence stratigraphy 57
4.3 Data preparation and experiments 60
4.3.1 Importing data for the initialization of the simulation model 60
4.3.2 Implementing wells 61
4.3.3 Well correlations: 64
4.4 Model building 65
4.4.1 Initial topography: 66
4.4.2 Sea level: 67
4.4.3 Sediment types: 68
4.4.4 Tectonics 69
4.5 Simulation result and discussion 71
4.6 Experiment 2: modeling sequences separately 74
4.7 Conclusion 76
5 General conclusion 78
5.1 Recommendations 79
References 80
APPENDIX 82

List of figures

Figure 1. GPM simulated model. The GPM model demonstrates the detailed incorporation of dynamic factors such as paleo-environmental settings and tectonic effects, Sergio Courtade 2017 5
Figure 2. Comparison between forward stratigraphic modeling (GPM) and conventional 6
Figure 3. cross-section through GPM simulation result showing sands in the deep part of the Campos basin, Brazil representing basin floor fans deposited by turbidity currents originating in the upper end of the basin (upper left of the figure). from Acevedo et al., 2014 10
Figure 4. Evolution and development timeline of GPM software (Geological Process Modeling for Petrel 2018, Schlumberger) 11
Figure 5. GPM software general workflow 14
Figure 6. Comparison of two sea level reconstructions during the last 560 Myr according to Exxon et al and Haq et al (1987). 15
Figure 7. variation of diffusion in function of sediment type and sea level depth (Sergio Courtade © 2017 Schlumberger) 17
Figure 8. GPM Model of the Ferron sandstone outcrop in Henry Mountains, Utah. Geologic model on the left and Wheeler diagram on the right. From Li et al, 2012 20
Figure 9. Arial view of an unconfined submarine fan system simulated in GPM showing submarine canyons, amalgamated turbidite channels and turbidite fans, M.Radzi, 2019 21
Figure 10. Alaska North Slope model. The present-day shoreline is shown in red. Upper left: Initial surface (contours in meters). Upper right: Final model in plan view and location of cross section. Bottom: Cross section showing predicted stratigraphy and sediment composition (coarse sediments in red and green, fines in blue and black).Christ, Alina-Berenice & Schenk, Oliver & Salomonsen, Per. (2016). 22
Figure 11. GPM carbonate reservoir model tied to well data (stromatolite lithology), Publication from Petrobras and Schlumberger, 2016 23
Figure 12. Location of Block F3 in the Dutch sector of the North Sea, marked with a blue box, and the positions of utilized wells shown on Google Earth 25
Figure 13. Structural map of the North Sea Dutch Offshore, indicating the location of the F3 block (highlighted by a red box) adapted from Schroot and Schuttenhelm, 2003; and Nelskamp et al.). 26
Figure 14. Generalized lithologic column of the survey area based on available well reports (www.nlog.nl) 27
Figure 15. Seismic 2D line description in PETREL 29
Figure 16. NE-SW 2D seismic line running across the Pliocene fluvio-deltaic system,NAM 1989 29
Figure 17. Location of the wells F02-01, F06-1, F03-4, F03-2 in 2D window 30
Figure 18. Flowchart showing the general workflow required to run a GPM Simulation 32
Figure 19. interpreted systems tracts overlaid on seismic by Qayyum et al (2013) 33
Figure 20. SW-NE 2D seismic line, featuring the base and top surfaces of the sequences, Both date 5 Ma. 34
Figure 21. SW-NE 2D seismic line flattened on the ‘Paleowater depth’ horizon (blue line) 35
Figure 22. Calculations pane in the surface settings 36
Figure 23. Restored ‘Water depth’ surface (top) and ‘Paleotopography’ surface (bottom) at 5 Ma 36
Figure 24. Haq global sea-level curve in GPM software 38
Figure 25. Uplift tectonic map rates and function 39
Figure 26. Diffusion curve, X axis shows sea level Elevation depth, Y axis is the multiplier 40

Figure 27. Trimming process in PETREL 41
Figure 28. Trimmed result of the GPM model overlaid on seismic 2D line (reference model) 42
Figure 29. 2D seismic line and the main sequences horizons of the GPM model 43
Figure 30. apparent polarity applied in 2D section line and the model's horizons in black 43
Figure 31. Diffusion coefficient rates and constant function used for the simulation 45
Figure 32. scenario (a) GPM model 45
Figure 33. scenario (b) GPM model with diffusion coefficient of 5m²/y 46
Figure 34. GPM model after varying the diffusion function, Top model showing an aggradational pattern, bottom showing a progradational pattern 47
Figure 35. Top: GPM model without the influence of tectonic movements. Bottom: GPM model affected by uplift to the Eastern part. 48
Figure 36. GPM model varying the sea level curve input 49
Figure 37. trimmed simulations result of the previous scenarios overlaid on seismic 2D line 50
Figure 38. Map showing the location of the Berkine Basin (yellow circle) on the northern part of the Saharan Platform, related structural highs and the main oil and gas fields of Algeria, modified from Turner et al 2001. 53
Figure 39. NNW-SSW generalized cross section through the Berkine Basin, showing the location of major oil fields of the central part of the basin. Boote et al. (1998) 54
Figure 40. Generalized stratigraphy of the Berkine Basin and the different units of the TAGI. Turner et al 2001 55
Figure 41. Location of the Blocks 401a and 402a and Hydrocarbon Accumulations in eastern part of Berkine Basin and the section of used wells for the GPM model, modified from Turner et al 2001 56
Figure 42. Sequence stratigraphy of the TAGI based on Blocks 401a and 402a Turner et al (2001) 59
Figure 43. Petrel data types with their formats, categories, and template 60
Figure 44. Map georeferencing information in PETREL 61
Figure 45. the location of the wells BKE-1, SFNE-1, ROD-2, ROD-4, RER-1, RERN-1 in Petrel 2D window 62
Figure 46. well tops position on studied wells representing the sequence boundaries 62
Figure 47. Make/edit Surface process in PETREL 63
Figure 48. Surfaces corresponding to sequence boundaries 63
Figure 49. well correlation SW-NE through the wells (BKE-1, SFNE-1, ROD-2, ROD-4, RER-1, RERN-1) 64
Figure 50. Color codes for different facies of the studied area 64
Figure 51. Study area polygon in 2D window 66
Figure 52. Base model topography elevation variations in the topography editor 67
Figure 53. Exxon global sea-level curve of the simulation interval in GPM software 67
Figure 54. Sediment proportions and corresponding code names 68
Figure 55. subsidence map rates in mm/a 69
Figure 56. Uplift event map rates in mm/a 70
Figure 57. Diffusion function 71
Figure 58. GPM model for the TAGI reservoir in the study area 72
Figure 59. GPM dynamic evolution of TAGI reservoir in different time intervals 72
Figure 60. GPM model for the TAGI reservoir with each sequence simulated separately 74
Figure 61. left: Stratigraphic column of TAGI from ROD-2 logs right: GPM model of TAGI at the level of ROD-2 75

List of Tables

Table 1. Summary of available wells and well logs used in the study..... 30
Table 2. Grain properties and fractions of the sediment types used as input.....37
Table 3. Used wells names and coordinates.....61
Table 4. Sediment types and properties 68
Table 5. Tectonic rates along geological times 70
Table 6. Sediment diffusion values in m2/y.....71
Table 7. Input parameters for the simulation of experiment 2 with GPM 74

General introduction

General introduction:

In the exploration phase, the discovery of petroleum reservoirs is critically dependent on constructing accurate geological models. These models integrate diverse data sources, such as seismic surveys, well logs, and geological maps, to provide a comprehensive understanding of subsurface geological structures and properties. Despite significant advancements in seismic imaging techniques and deep-sea drilling over the past decades, reproducing the dynamic evolution of the subsurface filling history remains a substantial challenge.

A relatively recent and underutilized tool in geological modeling is Geologic Process Modeling (GPM), also known as Forward Stratigraphic Modeling (FSM). GPM offers an alternative approach to subsurface modeling by enabling the chronological reconstruction of a basin's geological history based on forward stratigraphy modeling. This method simulates sedimentary deposition over time, accounting for processes such as erosion, transport, and deposition of clastic sediments and carbonates. By numerically simulating these physical and geological processes, GPM allows for the creation of 3D models that add layers of sediment in several time steps, resulting in physically and geologically constrained models.

The strength of GPM lies in its ability to produce models that closely approximate reality, showing expected sediment geometries and predicting lithology distributions. This method provides geologists with a powerful quantitative tool to build accurate and realistic subsurface models, which are essential for identifying optimal drilling locations, estimating hydrocarbon reserves, and designing efficient production strategies. Consequently, GPM significantly enhances the understanding and prediction of subsurface environments, contributing to the overall success and profitability of hydrocarbon exploration projects.

This study aims to provide a thorough understanding of the potential and constraints associated with the utilization of Geological Process Modeling (GPM) in reconstructing geological scenarios from the past. The well analyzed F3 block in the North Sea is selected as an exemplary case study due to its rich documentation through seismic surveys and well data. Furthermore, the application of GPM techniques will be explored in the TAGI reservoir within the Berkin Basin. Accordingly, this study is organized into four chapters:

Chapter 1 introduces geological numerical modeling and focuses on the emergence of Geological Process Modeling (GPM) as a specialized technique for simulating sedimentary processes. The chapter contextualizes GPM among other modeling approaches, highlighting its unique contributions, and sets the stage for exploring its applications in fluvio-deltaic environments in later chapters.

Chapter 2 provides an overview of Geological Process Modeling (GPM), focusing on its essential inputs, parameters, and practical applications through real-world case studies.

Chapter 3 outlines the geological context of the "F3 block" in the Netherlands offshore and introduces a model using GPM technology. It aims to reconstruct the sequence and geometry of the defined deep-seated sedimentary units of the deltaic complex dominated by clastic sediments. The study includes running alternative scenarios to test the influence of key parameters on the simulated delta architecture and its interactions with sea level changes, tectonics, and sediment supply.

Chapter 4 introduces the inaugural use of GPM in the Berkin Basin, focusing on the TAGI reservoir in Algeria. It outlines the geological context of the Berkin Basin, explains the methodology employed for GPM application, and presents the simulations results. These findings are anticipated to offer fresh perspectives on the basin's evolutionary trajectory and its prospects for hydrocarbon exploration.

CHAPTER I:
Generalities

1 Geological Numerical Modeling

Geological numerical modeling uses mathematical and computational techniques to simulate and analyze various geological processes. These models represent the intricate interactions within geological systems, such as sedimentary basin evolution, fluid flow in porous media, tectonic activities, and resource exploration. This approach transforms geological analysis from descriptive to theoretical, providing insights into the underlying mechanisms of complex basin phenomena.

To transform qualitative analysis into quantitative characterization, researchers incorporate experimental and field data, remote sensing data, and geophysical data into the models. This enhances the realism of the models and reduces uncertainties. The development of hybrid modeling techniques, which combine different numerical methods, takes advantage of their individual strengths while mitigating their weaknesses. Additionally, advancements in high-performance computing have enabled large-scale geological modeling simulations, allowing for more detailed and comprehensive analyses.

The shift toward quantification has been driven by the availability of high-quality data, such as 3D and 4D seismic data, increased computational power, and a competitive environment where finer margins are critical. Traditionally, numerical modeling in geology has relied on geostatistical methods, using statistical techniques to estimate geological properties between wells. Methods such as Kriging or Stochastic interpolation are commonly used in the upstream industry to model reservoir characteristics. However, these conventional methods have limitations, particularly in simulating the realistic timeline distribution of facies, as they often omit the chronological sequence of depositional processes controlled by paleo-environmental and tectonic factors.

Sedimentary process modeling, and geologic process modeling in general, can be done intuitively, but it becomes more powerful and quantitative with the assistance of a process simulation model. These models place constraints based on physical and geological knowledge on the simulated sedimentary deposits. For example, given certain sea-level variations, paleoclimate, and paleogeographic conditions, only certain types, sizes, and geometries of fluvial deposits, deltas, or turbidites are possible. An ideal geologic process model is used similarly to a reservoir simulator. In a reservoir simulator we first estimate many reservoir parameters (porosity, permeability, saturations, etc.). We run the simulator forward and try to match well-production histories and then iteratively adjust the reservoir parameters to perfect the match. Once satisfied, the simulator can predict future production in existing or proposed wells.

Similarly, this thesis employs Geological Process Modeling (GPM) software to simulate paleogeographic conditions, including basin size and shape, sediment influx rate, paleoclimate, and tectonic settings. Initially, these conditions are hypothesized based on available data. The model is then iteratively adjusted by modifying the boundary conditions until it approximately matches observations (well logs and seismic data). The output of the model can then be used to predict the geology between and beyond the available data points.

By using GPM, we can create more accurate and realistic subsurface models, which are essential for identifying optimal drilling locations, estimating hydrocarbon reserves, and designing efficient production strategies, contributing to the overall success and profitability of hydrocarbon exploration projects.

1.1 Geological Process Modeling (GPM)

Geological Process Modeling (GPM) offers an alternative approach to traditional geological modeling by reconstructing the geological history of a basin in chronological order using Forward Stratigraphy Modeling (FSM). GPM simulates sedimentary deposition over time, considering processes such as erosion, transport, and deposition for both clastic and carbonate sediments. This method has seen rapid development and extensive application in academia and the petroleum industry over the last years.

GPM builds physically and geologically constrained 2D and 3D models. These models closely resemble natural sediment geometries and lithology distributions. The detailed nature of GPM allows for the inclusion of various dynamic factors, such as paleo-environmental settings and tectonic effects, resulting in more accurate and realistic geological models.

The strength of GPM lies in its ability to produce models that closely approximate reality, depicting expected sediment geometries and predicting lithology distributions. By simulating the interactions of various geological processes over time (Figure 1), GPM provides geologists with a powerful tool to build accurate and realistic subsurface models.

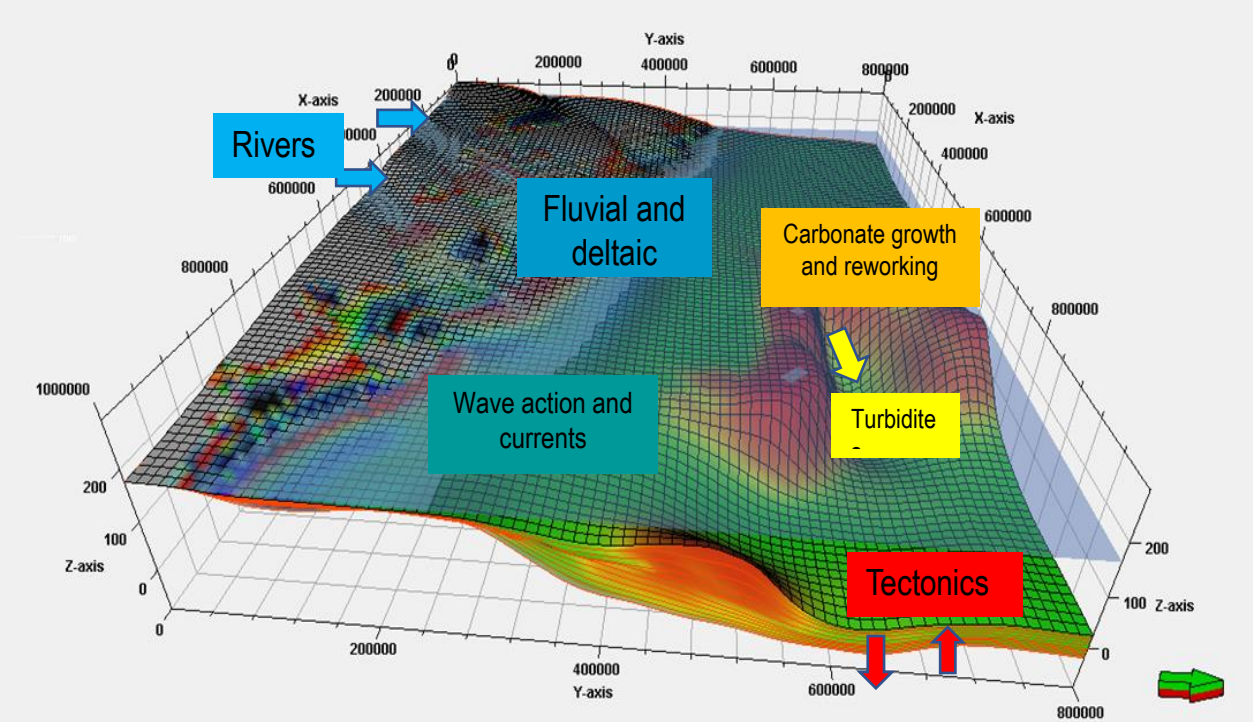

Figure 1. GPM simulated model. The GPM model demonstrates the detailed incorporation of dynamic factors such as paleo-environmental settings and tectonic effects, Sergio Courtade 2017

1.1.1 The Need for Geological Process Modeling (GPM)

A dynamic deterministic modeling method (Figure 2) is crucial for recreating past geologic events. For example, processes that created ancient evaporite deposits can be represented by dynamic models that allow for the adjustment of basin topography, circulation patterns, inflow rates, and evaporation rates as experiments are performed.

The challenge in adopting sedimentary process modeling as a standard industry technique lies in the general unfamiliarity with modeling practices. Traditionally, hard data such as well logs and seismic data have been the primary sources for delineating hydrocarbon reservoir characteristics. These data are processed in a straightforward manner, with raw data fed into a processing module to yield refined data. The interpretation of geological features observed in this data often relies on intuition.

Forward Stratigraphic Models (FSMs), however, bridge the gap between observed strata (either in subsurface hydrocarbon reservoirs or in outcrop analogues) and the geological processes that generated them (Burgess, 2012; Harris et al., 2016; Zhang et al., 2019). It enhances our understanding of the processes that control architecture and facies distribution in deltas, thus allowing for better predictions in subsurface cases with limited data (Burgess, 2012). This understanding is vital for reservoir evaluation and risk assessment during hydrocarbon exploration.

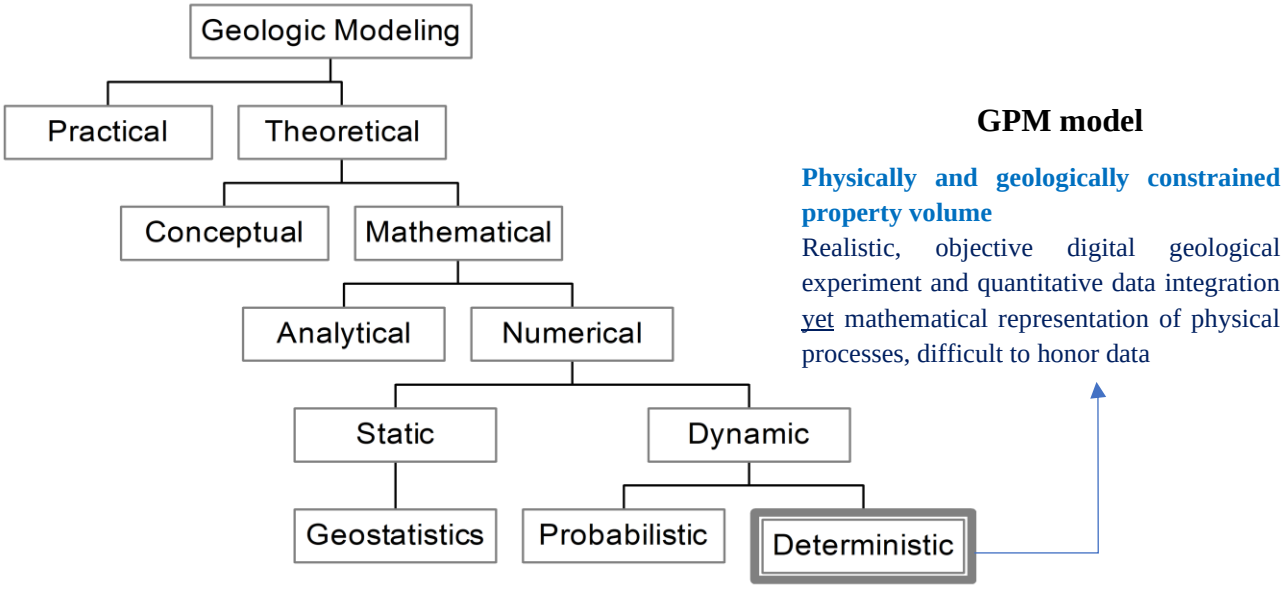

Figure 2. Comparison between forward stratigraphic modeling (GPM) and conventional geological modeling approaches.

1.1.2 Advantages over Geostatistical Methods

While geostatistical methods have been the norm in geological modeling, they primarily use statistical algorithms to estimate geology between wells, these methods focus on geometric and spatial correlations of present-day properties without considering the basin's depositional history often resulting in unrealistic subsurface models. In contrast, Geological Process Modeling (GPM) reconstructs the chronological geological history of a basin, employing a deterministic approach to build 3D models by sequentially adding sediment layers over multiple timesteps. This approach simulates the physical and geological processes occurring in nature, generating models that closely reflect reality.

Geological Process Modeling (GPM) offers a more complete understanding than data and spatial statistics-based models by incorporating physical sedimentary processes. This enhances predictive capabilities beyond existing data points. Even if GPM models don't perfectly align with the data, their ability to predict geology between and beyond data locations is valuable in exploration. Additionally, GPM supports basin modeling programs with crucial inputs on sediment accumulation rates, types, and conditions.

1.1.3 Applications of GPM

GPM software has versatile applications across various stages of petroleum exploration and development:

1. **Early Exploration Phase**:
    - Validates conceptual models.
    - Critically evaluates regional seismic interpretations.
    - Assists in reservoir prediction prior to drilling the first exploration well.

2. **Development Phase**:
    - Refines well correlations.
    - Contributes to basin modeling studies.
    - Constrains static geostatistical models with geological data.
    - Enhances reservoir characterization workflows.
    - Informs field development strategies.

3. **Educational Tool**:
    - The results from Stratigraphic Forward Models (SFMs) act as an effective educational tool, enabling the visualization and explanation of the stratigraphic evolution of sedimentary systems over time. This is particularly valuable at the scale of reservoir and seal development.

1.2 Research Motivation:

The objectives of this thesis are to explore the application of Geological Process Modeling (GPM) in siliciclastic depositional environments, with a focus on fluvial and deltaic settings. Specifically, the research aims to:

1. Predict facies distribution in a Prograding Deltaic System: Utilize boundary conditions calibrated with seismic data from the Dutch Sector, North Sea F3 Block, to gain insights into the geological processes that formed the observed sedimentary sequences and features.
2. Estimate the influence of key variables such as sediment supply, eustasy, and tectonics on the sedimentation patterns and stratigraphic architecture.
3. Implement GPM technology in Algeria to the TAGI reservoir's siliciclastic deposits in the Berkine Basin, providing new insights into the geological processes shaping the reservoir.

By achieving these objectives, the research aims to enhance the understanding of geological processes in fluvial and deltaic environments, improve predictive capabilities in subsurface modeling, and support more effective exploration and production strategies in the petroleum industry.

CHAPTER II:

Geological Process Modeling (GPM) technology

2 Overview of GPM in Petrel software:

Petrel E&P is a software platform developed by SLB (Schlumberger) that integrates various disciplines together, such as geoscience, reservoir engineering, production engineering, and drilling. This technology provides a comprehensive set of tools and functionalities for geoscientists and engineers, supporting the entire exploration-to-production workflow. Petrel E&P allows users to integrate diverse data types, such as seismic, well logs, and reservoir performance data, to construct detailed 3D models of the subsurface. These models are crucial for understanding reservoir characteristics, optimizing drilling and production strategies, and maximizing hydrocarbon recovery by enabling better decision-making.

A relatively recent and underutilized addition to the geologist's toolkit is Geological Process Modeling (GPM). This technology aims to model the processes of erosion, transport, and deposition of clastic sediments, as well as carbonate growth and redistribution, based on quantitative deterministic physical principles (Cross, 1990; Tetzlaff & Priddy, 2001; Merriam & Davis, 2001). GPM enable the construction of enhanced petroleum systems and forward reservoir models illustrating stratigraphic sequences and litho-facies, predicting the associated sedimentation processes (figure 3). In exploration, it aids in more accurately predicting reservoir presence, connectivity, and shape. The GPM approach to geological modeling is applicable across various geological settings and throughout the entire upstream business, from early exploration to improved oil recovery. It can be applied at the basin scale for siliciclastic, carbonate, and mixed lithologies.

When geological conceptual models are represented and documented digitally through GPM, geologists can achieve a better understanding of their prospects. This digital representation enhances confidence and traceability in both ongoing and completed projects, leading to more reliable and reproducible geological interpretations.

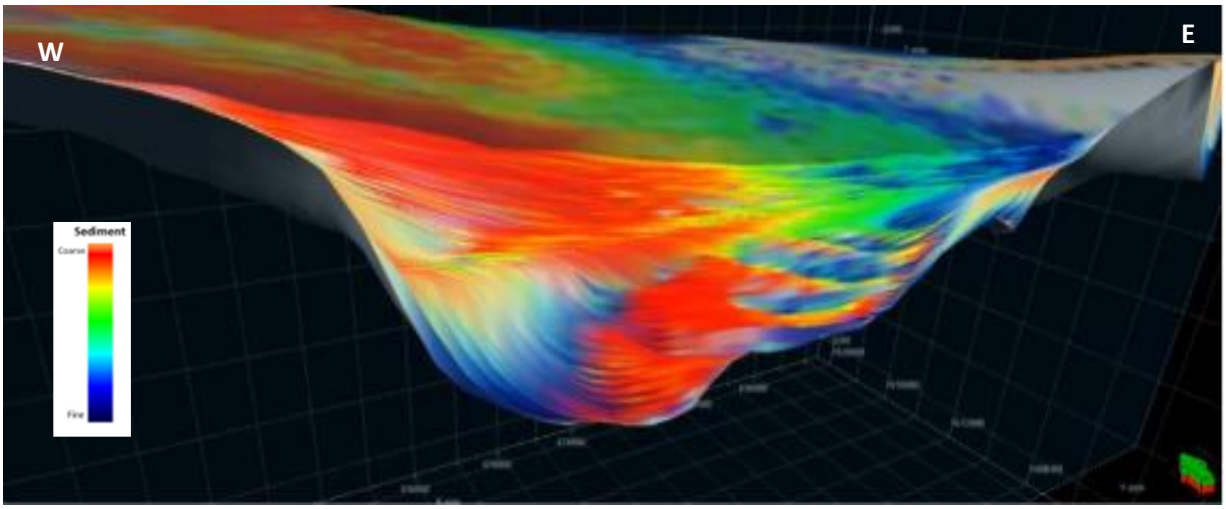

Figure 3. cross-section through GPM simulation result showing sands in the deep part of the Campos basin, Brazil representing basin floor fans deposited by turbidity currents originating in the upper end of the basin (upper left of the figure). from Acevedo et al., 2014

GPM operates as a digital sedimentary 'sandbox' laboratory, simulating the formation of sedimentary sequences based on user-defined conditions such as basin topography, sea level variations, and sediment inputs. It models the erosion, transport, and deposition of both clastic and carbonate sediments across various geological settings, including channels, rivers, turbidity flows, and shoreline systems. Additionally, it incorporates processes such as carbonate growth, wave action, meteoric diagenesis, and sediment compaction, which help to constrain the outputs by understanding the processes that may have formed a sedimentary sequence.

The GPM software generates geological models through the numerical simulation of physical processes combined with well-documented empirical rules. These resulting models are highly realistic and closely approximate real-world conditions when all boundary conditions are accurately defined.

Originally developed by Daniel Tetzlaff as part of his Ph.D. project at Stanford University, GPM was one of the first 3D simulators of sedimentary processes. Initially existing as a standalone software package, GPM was integrated into the Petrel platform and commercialized in 2017. Since then, it has undergone continuous improvements, with major new features planned for future releases (Figure 4).

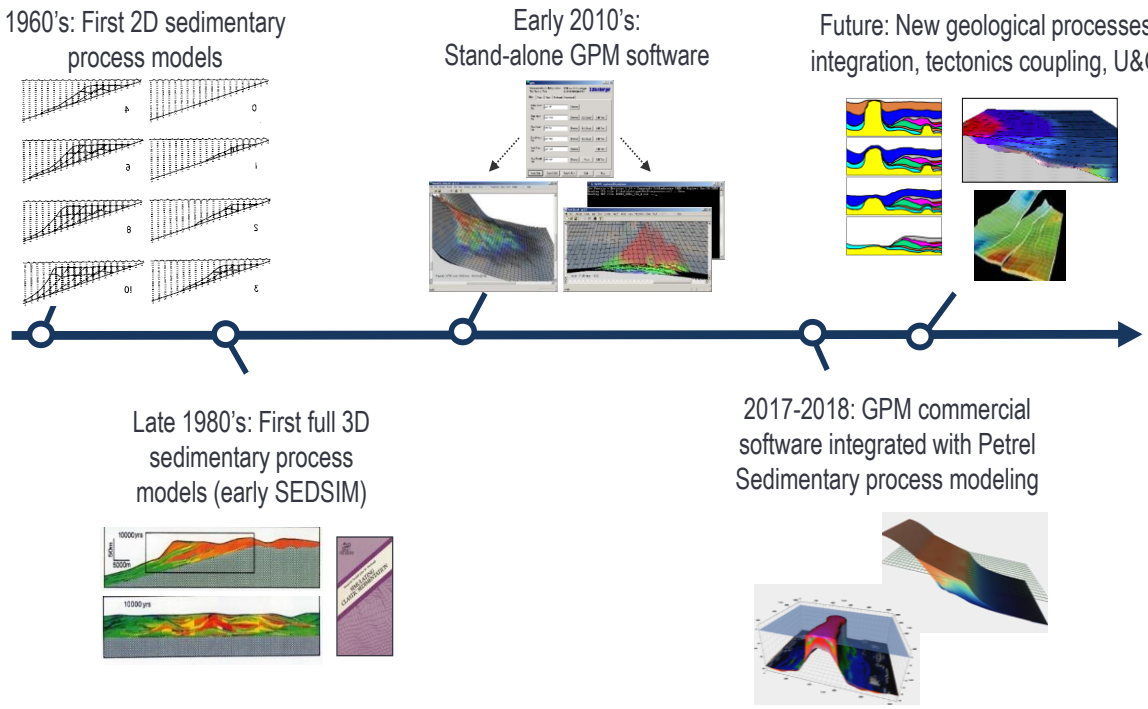

Figure 4. Evolution and development timeline of GPM software (*Geological Process Modeling for Petrel 2018,* Schlumberger)

2.1 GPM data input types:

GPM software primarily utilizes soft data rather than hard data as its main input. Its purpose is to explore various geological scenarios based on the available data and challenge existing interpretations. Through simulation, different geological scenarios and hypotheses are tested and refined, allowing the final versions of the models to match the hard data.

2.1.1 Soft data

- **Eustatic curve**: Obtained from standard published curves and refined later with local knowledge.
- **Wave action**: Direction, amplitude, and period for fair weather and storm waves.
- **Tectonics**: knowledge of major uplift, subsidence, tilting, and gentle folding as a function of time is important to obtain a better model.
- **Paleoclimate:** Precipitation patterns, wind climate, ocean currents and weathering effect all influence the model.
- **Sediment provenance**: For siliciclastic, the amount, type, and direction of external sediment flow into the model are crucial factors.

2.1.2 Hard data

- **Seismic**: Provides images of subsurface structures and stratigraphy, revealing fault systems, folds, and depositional patterns, preferably, picked surfaces should be converted to depth.
- **Well logs**. The most useful logs are processed lithology logs in which the main lithotypes have been classified into major groups. Also important are porosity logs because they may be helpful in establishing the compaction history and, in the case of carbonates, post-depositional dissolution.
- **Cores**: Available cores are important as they can confirm the lithologies and possibly the depositional environments predicted by the model. They also provide "compacted porosity" and "compacted permeability," which are important when modeling compaction.
- **Topographic and Bathymetric Data**: High-resolution elevation and depth data are essential for modeling surface processes and basin morphology.
- **Other data:** Outcrop data from the same formation, as well as analogs serve as a general non-quantitative guideline to refine the final model.

2.2 Elements and guiding principles of GPM:

2.2.1 Guiding principles:

The GPM software necessitates user input for all initial and boundary conditions, including paleogeographic factors like basin topography, tectonic movements, sea-level fluctuations, sediment influx, river flow dynamics, and sediment properties. These inputs are crucial for predicting sediment accumulations while adhering to the principles of mass and energy conservation, thereby modeling physical concepts locally.

Numerically, GPM employs the Navier-Stokes equation to simulate both steady and unsteady flow, including wave longshore currents, ensuring a robust and accurate representation of geological processes. Depth-averaged horizontal flow in free surface flow is tackled using finite differences for steady flow and the particle-in-cell method for unsteady flow. The latter method involves numerous particles, each representing a finite volume of fluid, while a grid tracks local depth and average flow velocity. Additionally, waves and wave-induced currents are simulated using a first-arrival algorithm that respects Snell's law and diffraction effects.

GPM comprehensively simulates geological processes such as sediment formation, erosion, transport, deposition, and post-deposition effects like tectonics and compaction. This functionality aids users in understanding and constraining sedimentary sequences based on physical principles. Importantly, GPM does not impose stratigraphic geometry rules; instead, it allows stratigraphy to emerge naturally from geological processes, ensuring that models are grounded in physics rather than solely relying on data or spatial variability properties.

2.2.2 Elements of GPM:

Building a stratigraphic forward model for a sedimentary body involves a procedure of simplification and conceptualization of its genetic processes, an overview of the workflow is shown in figure 5 below.

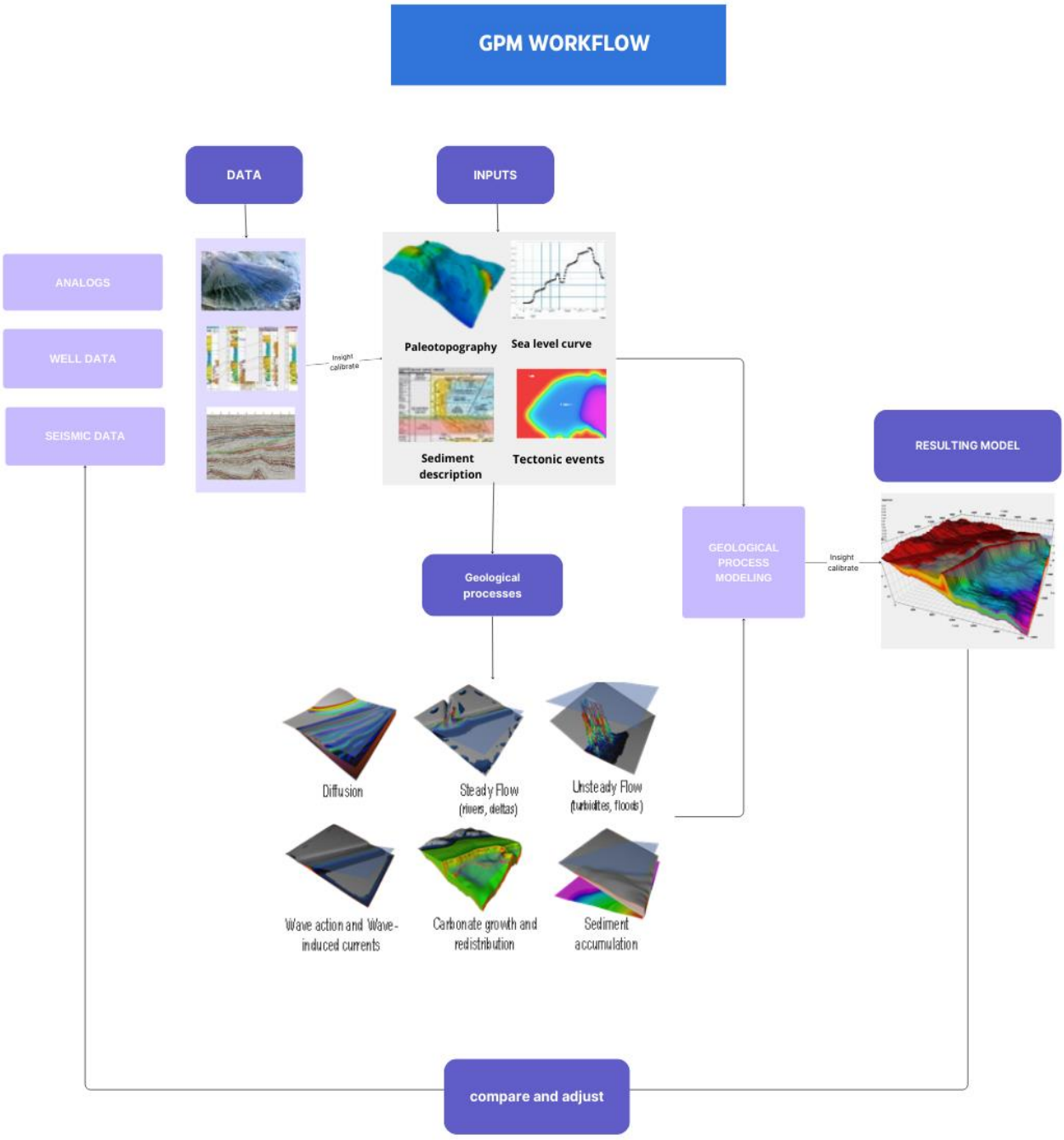

Figure 5. GPM software general workflow

2.3 Key model inputs for a GPM model

2.3.1 Paleo-topography:

The topographic surface, or 'basement,' represents the initial surface upon which erosion, transport, and deposition will occur. To reconstruct the initial topography and sedimentary thickness accurately, one must reverse both the compaction and structural deformations

This reconstruction relies on seismic data indicating structural features, well correlations with restoration tools for structural history and water depth, isopach maps for sediment thickness variations, and conceptual basin geometry for overall basin shape.

2.3.2 Sea level variations:

Eustatic sea-level changes occur over billions of years due to factors like glacial ice volume variations and plate tectonic processes altering the seafloor shape. In GPM, sea level is a dynamic factor reflecting eustatic evolution. Rising sea levels increase accommodation space, leading to thick sediment deposition, while falling levels reduce space, causing erosion. Sea level changes also impact sediment transport, forming coastal deposits or coastal plains and deltas. These variations create distinct stratigraphic sequences like transgressive and regressive sequences, with specific sedimentary structures reflecting sea level history. GPM offers options to define sea level, including using predefined global curves like Haq and Exxon's, importing data, creating custom curves in Petrel, or manually drawing them.

The Exxon Sea level curve, also called the Vail curve, and the Haq Sea level curve are widely used models depicting global sea level changes over geological time (figure 6). The Vail curve, developed by ExxonMobil researchers led by Peter Vail, is based on seismic stratigraphy analysis, offering insights into sea level variations over the Phanerozoic Eon. The Haq curve, developed by Bilal Haq and colleagues, is a refined version providing updated and detailed sea level change data.

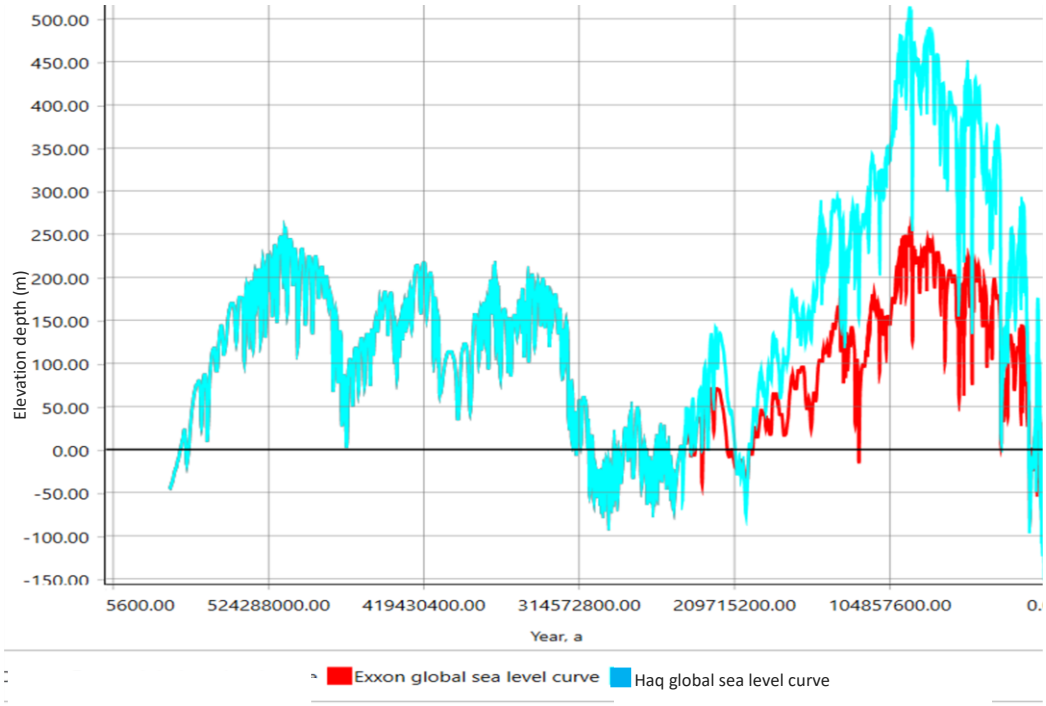

Figure 6. Comparison of two sea level reconstructions during the last 560 Myr according to Exxon et al and Haq et al (1987).

2.3.3 Sediment types:

sediment types are defined as aggregates of particles with identical size, shape, and density characteristics. GPM operates with various sediment types and their mixtures in continuous proportions, along with porosity considerations, resulting in a wide range of lithologies. Moreover, GPM captures paleoenvironmental conditions such as depositional depth, relative sea level changes, and wave energy, leading to the formation of diverse depositional facies.

Typically, GPM utilizes four main sediment components: "gravel," "sand," "silt," and "clay," or alternatively "reef." Each component is specified by its physical properties, including:

- Grain size
- Grain density
- Compaction coefficient
- Initial depositional porosity
- Permeability

In the case of carbonates, additional properties include dependencies on growth rates influenced by light and wave action.

By accurately defining these sediment types, GPM enables the modeling of various depositional environments and helps in predicting the distribution and characteristics of sedimentary facies within a basin.

2.3.4 Tectonics:

In GPM, tectonic activities are modeled to reflect syn-depositional movements of various structural elements such as platforms, basins, and slopes during sedimentation. This modeling approach captures how sedimentation occurs concurrently with tectonic events. Additionally, the software allows for the incorporation of post-depositional tectonics using trimming tools after running the model. This functionality is governed by two main sets of parameters:

- **Areal Map**: provides information on the spatial variations of tectonic movements across the modeled area, detailing how different regions have experienced tectonic shifts.

- **Stratigraphic Curve**: illustrates the temporal variation of tectonic movements over time, enabling users to understand the evolution of tectonic influences and their impact on sedimentary processes throughout geological history.

2.4 Geological processes

A realistic geological model requires a thorough understanding of all sedimentary processes involved in deposition (Warrlich et al., 2008). Once the genesis of the sedimentary body is comprehended, the deposition mechanisms must be translated into several key parameters. GPM allows access to various geological processes:

Diffusion: Diffusion plays a fundamental role in simulating the movement of sediments from higher slopes (source locations) to lower parts of the model area. The principle of diffusion

states that sediment moves downslope at a rate proportional to the slope and sediment characteristics; finer sediments travel further from the shoreline compared to coarser ones. GPM employs a vertical curve to describe the diffusion coefficient, which varies with depth relative to sea level at each time increment.

The calculation of sediment diffusion in GPM is simplified using the expression:

$$\frac{\partial z}{\partial t} = k\nabla^2 z$$

Where Z is the topographic elevation, K diffusion coefficient, t is the time, $\nabla^2 z$ is Laplacian of z.

The diffusion coefficient (k) is estimated based on known grain sizes for each sediment component and assumes uniform grain diameter (D) in the flow mix.

Sediment diffusion depends on three key parameters: sediment grain size and turbulence, a diffusion curve serving as a unitless multiplier in the algorithm, and the diffusion coefficient influenced by sediment type and the energy of the depositional environment. Notably, the highest depth-dependent diffusion coefficient occurs near sea level, where energy is highest over geological time. (Dashtgard et al., 2007) (figure 7)

Diffusion modeling in GPM encompasses various geological processes, including shoreline dynamics, mass movements, transgressive deposits, erosion, and soil creeping down slopes. If wave action is not explicitly modeled, it can be approximated using a diffusion curve with high values near sea level that decrease exponentially with depth. Diffusion can also simulate the erosion of high mountains due to glacial action.

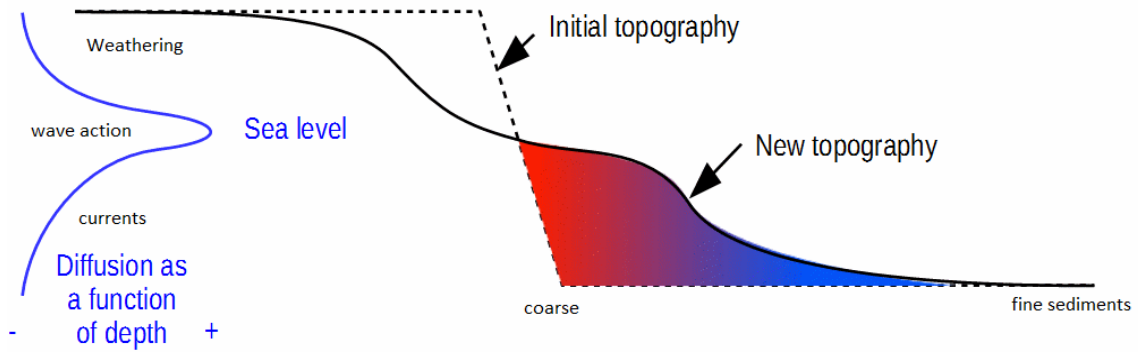

Figure 7. variation of diffusion in function of sediment type and sea level depth (Sergio Courtade © 2017 Schlumberger)

- **Compaction:** An algorithm for sediment compaction based on simple load is included in GPM. It simulates the sediment's elastic compression due to overlying load. This algorithm captures the rise in accommodation space resulting from compaction, leading to changes in sedimentation patterns, thickness, and geometry. It specifically accounts for the varying rates of compaction observed in different lithologies.

- **Sediment accumulation:** This feature allows modeling intervals without many details, such as overburden load over the sequence of interest, e.g., deposition of ashes created by

volcanic activity and accumulation of evaporites, eolianites, or pelagic shales. It is also used to simulate the deposition of sediments by mechanisms that are not covered by the other GPM software processes. The sediment supply curve and areal input rates are necessary to accurately model sediment accumulation in the desired geological setting.

- **Steady flow:** This process simulates flows that vary slowly over time where flow velocity and channel depth do not vary abruptly, e.g. rivers at a normal stage, deltas, and sea currents. Steady flow has a transport capacity determined by flow velocity and depth; it erodes sediment until this capacity is reached and transports sediment until the transport capacity diminishes to the point at which it can no longer carry its load and models the erosion, transport, and deposition of sediment at each point in the flow.

Numerically, the process uses a finite difference scheme within a rectangular grid for faster computation and to illustrate the frequency of flow that is characteristic in channel flow such as rivers. This method assumes constant flow velocity from the channel bottom to the surface.

Flows in GPM are controlled by point sources, identified by a source ID in the source position map. These flows start at specified cells in the source map where the cell value is equal to the point source ID.

A point sediment source needs four key parameters:

- Source ID (corresponds to the number given to the source in the Source map.)
- Water supply curve
- Sediment supply curve
- Sediment sizes and compositions for predicting transport and deposition.

The channel width, sediment load, and fan size in the modeled channel are influenced by parameters such as surface slope, sediment erodibility, transport coefficient, and water discharge.

Water Discharge (m^3/s) = Water Supply (m/s) * Source Area (m^2)

To define the source Area:

Source Area = Water Discharge / Water Supply

- **Unsteady flow:** simulates periodic flows that occur for a limited time, such as turbidity currents in deep-water settings, river floodplains, estuaries, coastal zones, and events like dam failures where flow velocity and depth rapidly change. This process requires inputting time-varying values for flow velocity, discharge rate, and sediment load, which can be derived from historical data, climate models, or hypothetical scenarios.

The algorithm for unsteady flow in GPM uses a "particle-in-cell" method, where numerous fluid elements or particles represent small volumes of fluid influenced by gravity, local slope, the local water surface (affected by nearby fluid elements), and friction against the bottom and other fluid elements (showing dynamic viscosity effects).

This method helps determine the sediment concentration in flow and sediment transport capacity (Tetzlaff and Harbaugh, 1989). The particle method equation relies on the assumption that erosion and deposition depend on the balance between the flow's transport capacity and the

"effective sediment concentration". The equation for multiple sediment transport in flow is given as follows:

$$A_{em} = \Sigma_{ks} \frac{I_{ks}}{f_{1ks}}$$

where A_{em} is the effective sediment concentration of mixture, l_{ks} is the sediment concentration of each type, and f_1,k_s is the transportability of each sediment type.

- **Waves:** The model simulates waves with varying positions, periods, and amplitudes. This process is applicable in areas where the sediment surface is below sea level. GPM employs formulas for wave celerity, which is the velocity of wave groups, to calculate wave trajectory, considering refraction and diffraction based on wave amplitude, period, and depth distribution.

When waves reach shallow areas, the following effects on the sediment occur:

  - Increased diffusion because of turbulence.
  - Net sediment movement of particles occurs in a direction perpendicular to shore (shoreface aggradation or degradation).
  - A longshore current occurs near the shore, creating water acceleration in the direction of wave propagation that can, in turn, move more sediment.

- **Carbonate growth:** This feature models the growth and erosion of carbonates based on the input of up to four sediment types. The growth of each sediment type is simulated according to the carbonate growth parameters.

2.5 Domain of applications of GPM:

Reservoir connectivity and traps prediction: Case Study Coastal Ferron Sandstones, Utah, USA

A study by S.F. Courtade, C. Warren, P. Salomonsen, and J. Tveiten utilized GPM to reconstruct the deposits of the Turonian fluvial and deltaic Ferron Sandstone from the Cretaceous foreland basin in North America. The Ferron Sandstone Member, which is 100 to 160 meters thick, consists of six depositional sequences separated by five sequence boundaries. The model incorporated tectonic uplift, basin subsidence, vertical faulting, sea level variations, and sediment diffusion processes. The resulting model (figure 8) accurately reproduced the sequences and boundaries identified in the outcrop and predicted reservoir discontinuities in the progradational and down stepping forced regressive deposits of Sequence 03, as well as low connectivity risks in the sandstones. This highlights GPM's potential for predicting reservoir continuity and stratigraphic traps.

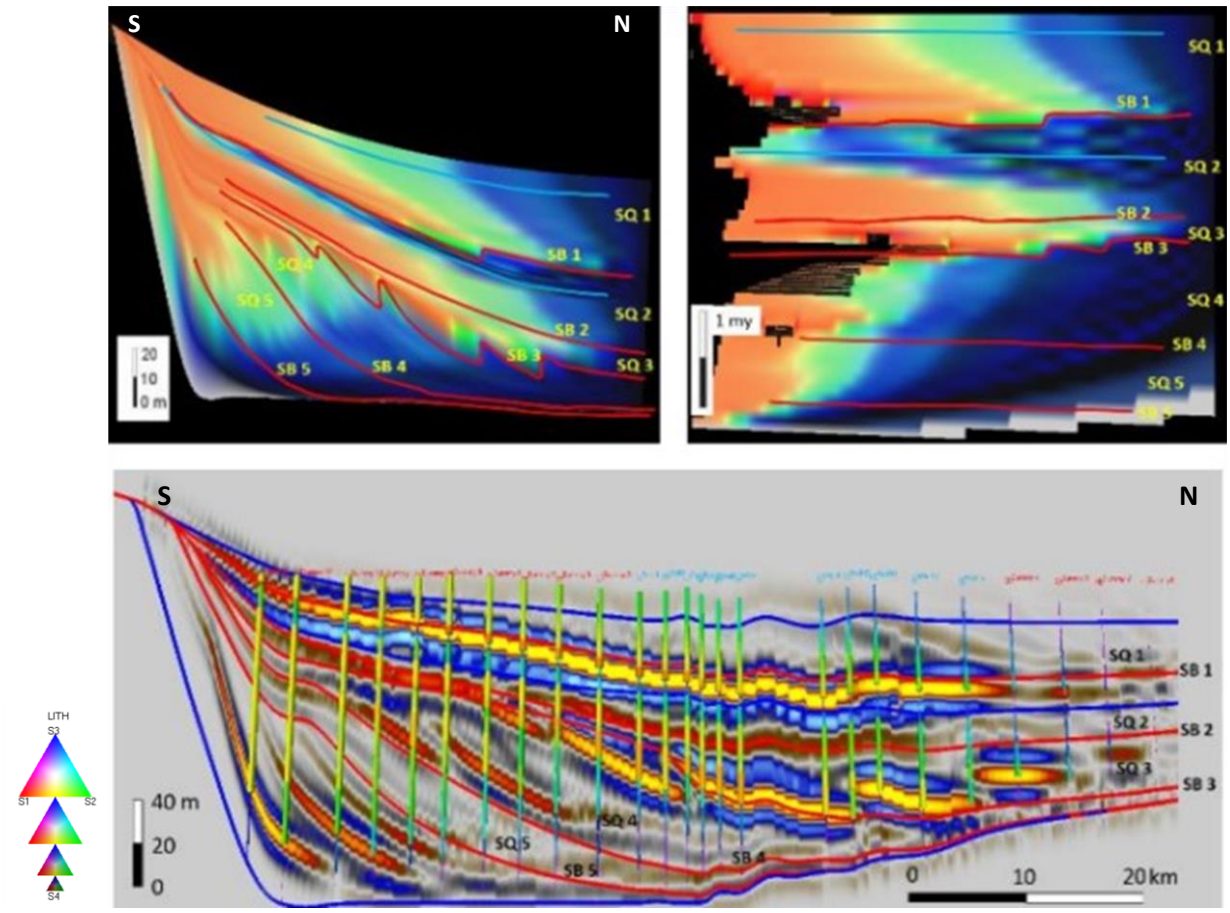

Figure 8. GPM Model of the Ferron sandstone outcrop in Henry Mountains, Utah. Geologic model on the left and Wheeler diagram on the right. From Li et al, 2012

Predict reservoir heterogeneity submarine fan of deepwater Sabah

In this study by M Radzi et al, GPM was used for 3D modeling over an area of 64 km × 102 km with 500 m grid spacing. Simulations covered 126 timesteps from 13.1 Ma to 6.7 Ma using the Haq et al. (1988) sea level model, incorporating sediment diffusion, accumulation, tectonics, and unsteady flow processes. Lithological and transport parameters were defined based on well and seismic data, with iterative calibration to align with observed data. The modeling results (fig 9) reveal depositional features typical of submarine fan systems, including canyons, turbidite channels, levees, and fans. Sand deposits were found in a new prospect area, influenced by sea level, accommodation space, and turbidite flow velocity, validating sequence stratigraphic predictions. High-quality reservoirs are expected in sandstone-rich, multi-layered basin floor fans and channel levee complexes, particularly in paleo low relief areas.

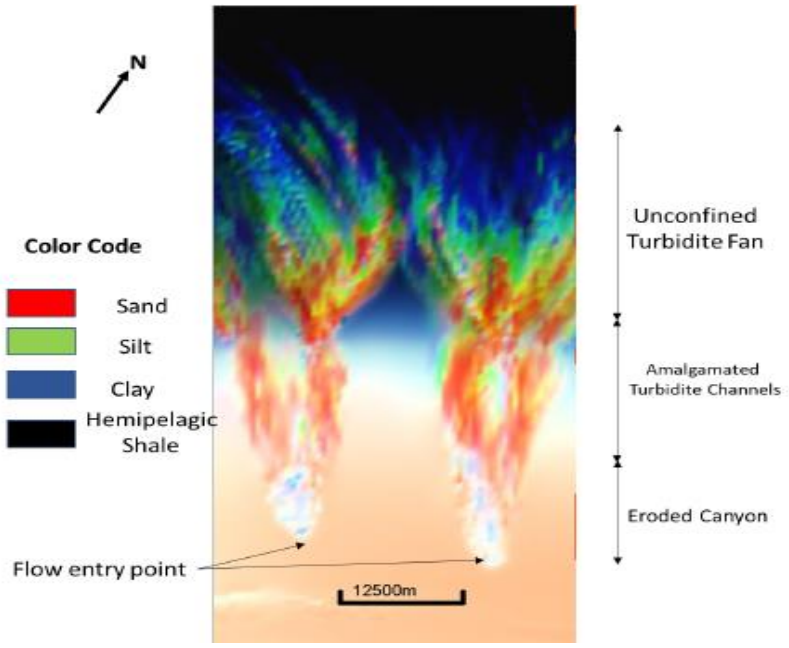

Figure 9. Arial view of an unconfined submarine fan system simulated in GPM showing submarine canyons, amalgamated turbidite channels and turbidite fans, M.Radzi, 2019

Using Stratigraphic Forward Modeling to Model the Brookian Sequence of the Alaska North Slope

Christ, Alina-Berenice & Schenk, Oliver & Salomonsen, Per. (2016). utilized GPM to reconstruct parts of the progradational Brookian sequence from the Early Cretaceous. The model covers an area of 2.11 million square kilometers and spans a length of 1,600 kilometers, modeling a time span from 122 Ma to 115 Ma. The GPM input included a base surface reconstructed from seismic data used in a previous basin model by Schenk et al. (2012), aiding in the understanding of sediment deposition and distribution patterns during the Early Cretaceous.

The study extended the surface to include sediment provenance areas and reconstruct the paleotopography at 122 Ma, placing four sedimentary point sources based on topography and paleocurrent data. A tectonic map was created with uplift rates of 0.05 mm/a in the Brooks Range and subsidence rates of 0.2 mm/a in the basin, derived from a previous basin modeling study.

The model (fig 10) shows prograding foresets from the Brooks Range into the basin, with grain sizes decreasing with distance from the sources. Coarser grains take about 3 million years to reach the center of the Colville foreland basin. The modeled sequences' extent and thickness were validated by comparing them to surfaces from the basin model.

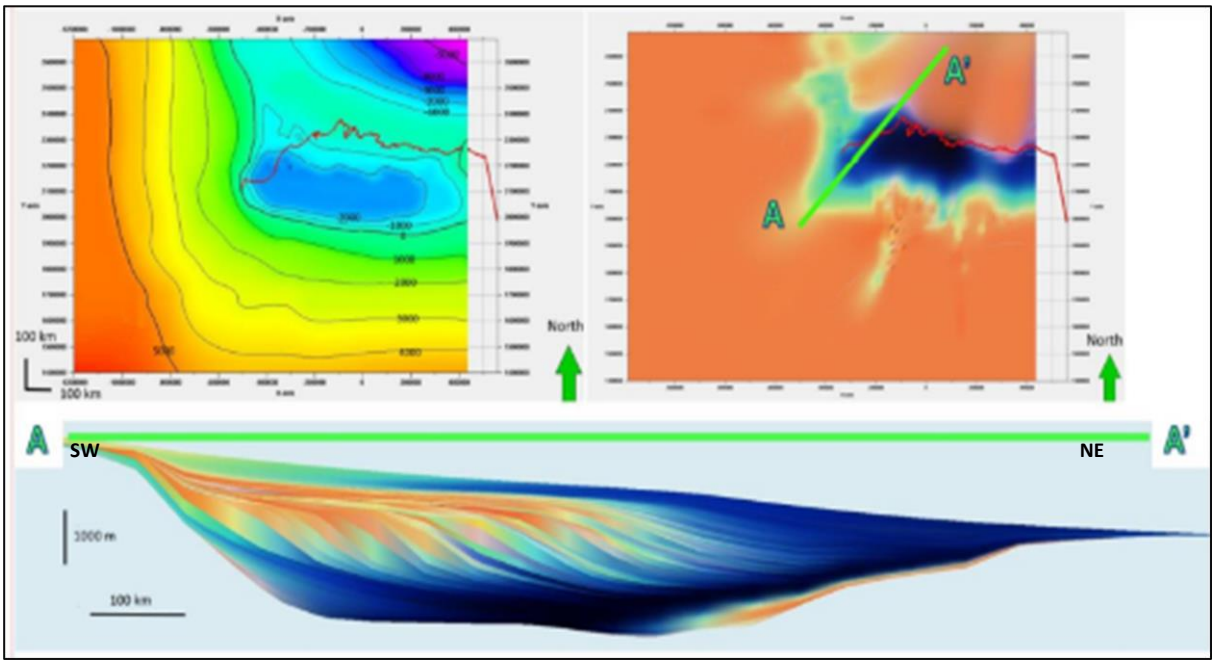

Figure 10. Alaska North Slope model. The present-day shoreline is shown in red. Upper left: Initial surface (contours in meters). Upper right: Final model in plan view and location of cross section. Bottom: Cross section showing predicted stratigraphy and sediment composition (coarse sediments in red and green, fines in blue and black).Christ, Alina-Berenice & Schenk, Oliver & Salomonsen, Per. (2016).

Reservoir Characterization: Case of the Brazilian East Margin Pre-salt carbonate reefs

This study by Souza Jr, Olinto G., et al. aimed to characterize carbonate facies in deep offshore fields to select effective Enhanced Oil Recovery (EOR) strategies, focusing on providing a more realistic description of Petrobras' pre-salt carbonate reservoirs. Geological Process Modeling (GPM) software was utilized to forward model these carbonate reservoirs (figure 11).

The study involved correlating the GPM results with traditional petrophysical and facies models, which were integrated with existing well data. This approach ensured that the generated carbonate models met the reservoir characterization goals effectively. By integrating geological, petrophysical, and well data, the study produced meaningful and realistic models that enhanced the understanding of reservoir heterogeneity. These models were crucial for optimizing EOR strategies, ultimately aiming to improve hydrocarbon recovery from these complex reservoirs.

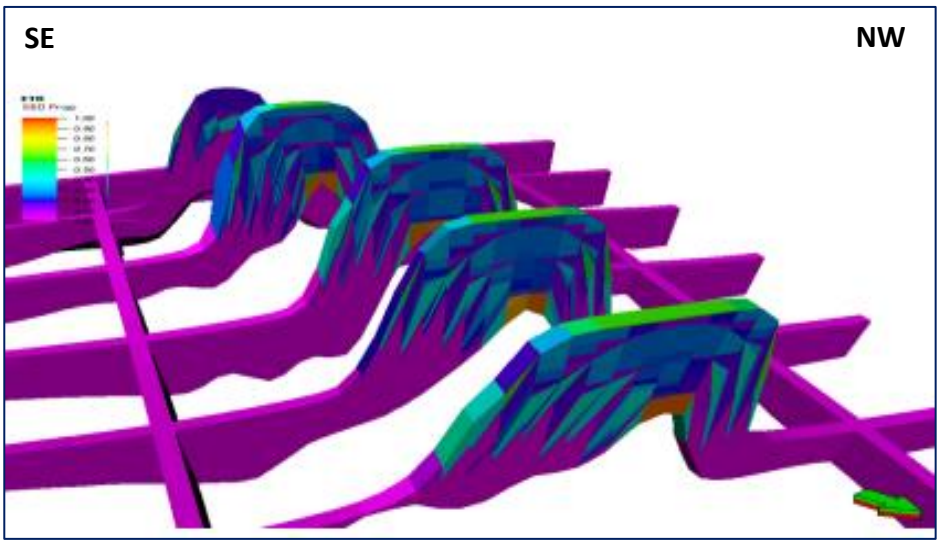

Figure 11. GPM carbonate reservoir model tied to well data (stromatolite lithology), Publication from Petrobras and Schlumberger, 2016

2.6 Conclusion:

Geological Process Modeling (GPM) technology represents a significant advancement in our ability to understand and predict the behavior of sedimentary systems over geological time scales. By integrating geological concepts with quantitative data, GPM provides detailed reconstructions of sediment deposition and erosion processes, enabling a more accurate interpretation of subsurface geology.

CHAPTER III

North Sea “F3 BLOCK” case study

3 Introduction

This chapter provides an overview of the geologic settings of the survey area "F3 block" of the Netherland offshore and introduces a geological model using GPM technology. The objective is to reconstruct the structural architecture and sedimentation patterns of the deltaic complex dominated by clastic sediments. Additionally, departing from the parameters used for the base case model, a set of alternative scenarios was run to test the influence of important parameters on the simulated architecture of the delta and its interactions with eustatic changes, tectonics, and sediment supply.

3.1 Study area

The North Sea basin, located at the inland edge of the North Atlantic, covers an area of approximately 625,000 km². It is bounded to the South by the Netherlands, to the East by Norway, Sweden, and Denmark, and to the West by England. The basin is divided into several sub-basins known as blocks.

Our study area “Block F3”, is situated in the Dutch Offshore sector of the North Sea continental shelf within the territory of the Netherlands (figure 12). Covering an area of 16 km x 24 km, it is in the southern part of the North Sea Dutch Central Graben, between latitudes 54° 52’ 0.86” N and longitudes 4° 48’ 47.07” E, it features a diverse geological composition ranging from Upper Jurassic to late Tertiary deposits. A prominent geological feature of the study area is a large Pliocene fluvio-deltaic system characterized by sigmoidal bedding geometries with downlap, toplap, onlap, and truncation structures. In 1987, a 3D seismic survey was conducted to identify geological structures and hydrocarbon reservoirs in this region.

Figure 12. Location of Block F3 in the Dutch sector of the North Sea, marked with a blue box, and the positions of utilized wells shown on Google Earth

3.2 Regional geology

3.2.1 Tectonic framework:

The structural framework of the North Sea basin is primarily shaped by extensional tectonics resulting from failed rifting during the Mesozoic and Variscan orogeny. Major rifting occurred during the Carboniferous-Permian period, accompanied by volcanism, which led to the formation of basins and evaporite deposits influenced by salt tectonics. In the Triassic period, there was further rifting oriented NW-SE to SW-NE (figure 13), followed by a widespread marine transgression during the Jurassic. During the Jurassic, volcanic dome growth and continued rifting created local topography and thick shale sequences within anoxic basins. Rifting activity ceased in the Cretaceous, leading to thermal subsidence and contrasting patterns of sediment deposition. In the Cenozoic era, the initiation of sea floor spreading, and mountain building resulted in uplift, submarine fan development, and significant sediment accumulation from the Miocene onward. These processes buried Jurassic source rocks and contributed to the formation of effective hydrocarbon seals.

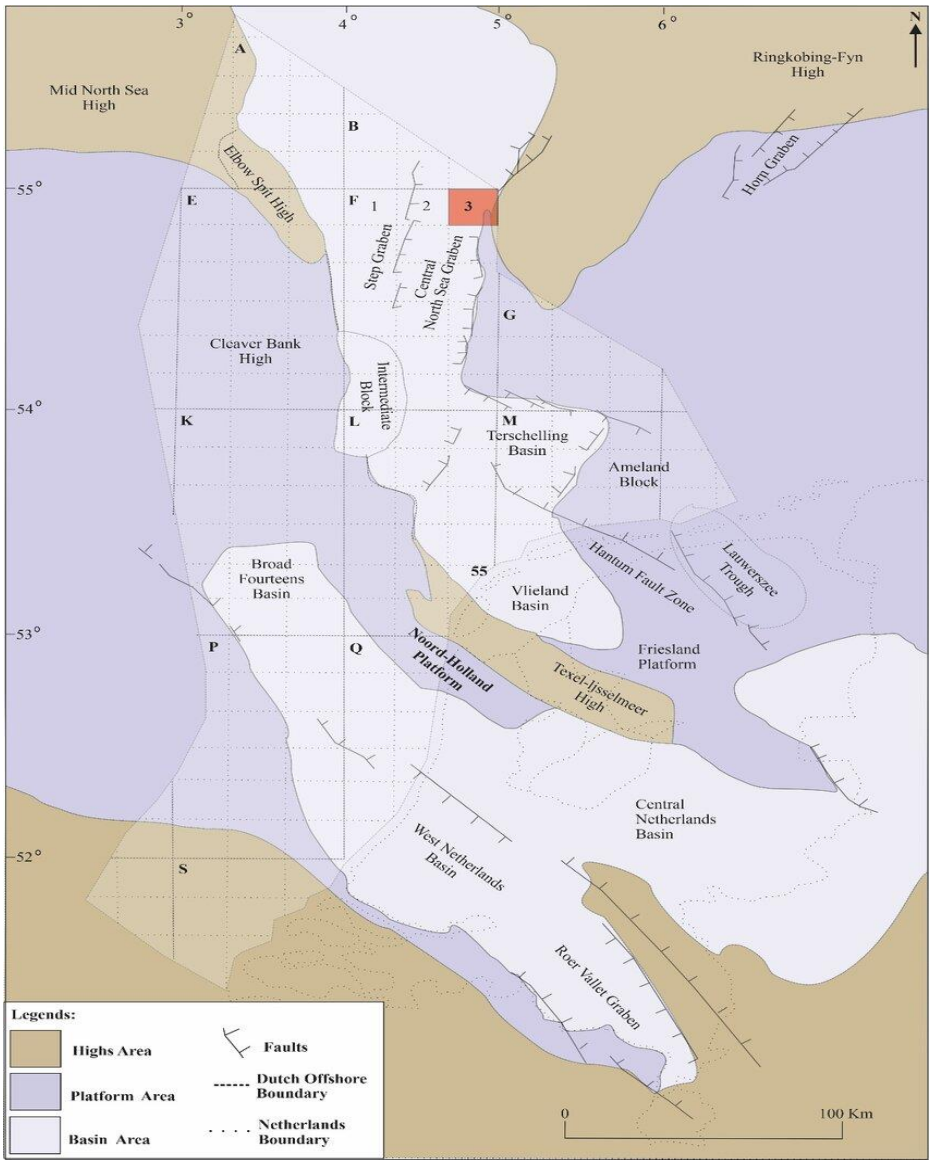

Figure 13. Structural map of the North Sea Dutch Offshore, indicating the location of the F3 block (highlighted by a red box) adapted from Schroot and Schuttenhelm, 2003; and Nelskamp et al.).

3.2.2 Stratigraphy:

The stratigraphy of the study area is documented by the composite well log reports of the wells F02-1, F06-1, and F03-4. The figure 14 below shows nine main lithostratigraphic units, listed below from oldest to youngest:

1- Zechstein Group (Late Permian)
2- Upper Germanic Trias Group (Middle-Late Triassic)
3- Schieland Group (Late Jurassic)
4- Scruff Group (Late Jurassic)
5- Rijnland Group (Early Cretaceous)
6- Chalk Group (Late Cretaceous)
7- Lower North Sea Group (Paleocene-Eocen
9- Upper North Sea Group (Neogene-Quaternary)

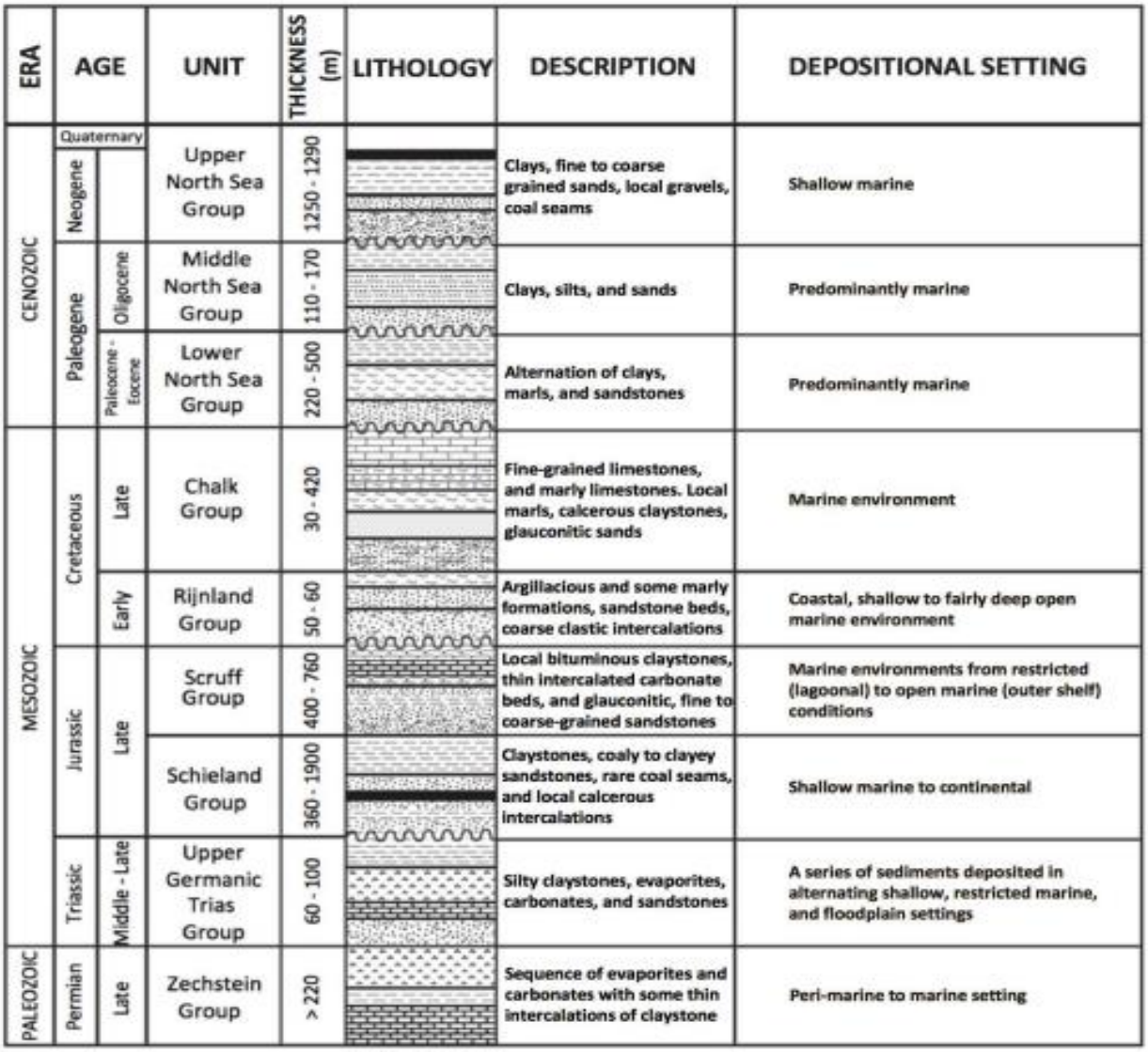

Figure 14. Generalized lithologic column of the survey area based on available well reports (www.nlog.nl)

The present study focuses on the units comprising prograding deposits of the deltaic system that falls under the North Sea Group, assembled during the Tertiary and Quaternary periods and prograding mainly towards the west-southwest. The North Sea Group can be divided into three sub-formations: the Lower North Sea (Paleogene), the Middle North Sea (Paleogene), and Upper North Sea (Neogene).

The sedimentation rate significantly accelerated during the Quaternary period, with approximately half of the total thickness deposited in just 2% of the Cenozoic deposition time. These sediments were primarily deposited under shallow marine and fluvial conditions, with increased subsidence during glacial periods (De Gans, 2007).

The Lower North Sea Group mainly consists of relatively fine-grained gradational Paleogene sediments, including grey sands, sandstones, and clays. These sediments represent several clastic sedimentation cycles in a marine environment at the edge of the North Sea Basin. The upper boundary of this group is marked by unconformably overlying deposits of the Middle North Sea Group, while the lower boundary is characterized by a sharp lithologic break marking the top of the Chalk Group. The depositional setting of this group is predominantly marine.

The Middle North Sea consists of formations of sands, silts, and clays with the main sand deposits along the southern margin of the North Sea Basin. The depositional environment of this group is predominantly marine with some lagoon and coastal plain sediments.

The Upper North Sea Group, which is of interest in our study, is interpreted as a sequence of Neogene shallow-marine sediments. It includes clays and fine- to coarse-grained sands with gravel, peat, and brown coal seams. There is a general trend from coarse- to fine-grained sands towards the north and west regions of the North Sea Basin. The lower boundary of this subgroup is defined by the Middle North Sea Group and older beds, while the upper boundary is overlain by the present land surface or seafloor. The overall depositional setting includes shallow marine environments and terrestrial beds of fluvial and lacustrine origins. The uppermost part of this group may contain glacial deposits.

3.3 Data and methodology:

To construct the 3D geological model of the F3 block, both well logs and seismic data were used, the principal data of this study is a high-quality 3D cube (depth) from the block F3 covering an area of approximately 24 × 16 km² realized by NAM in 1987, and specifically a NE-SW 2D seismic line running across a prograding delta known to be from the Pliocene (figure 16) that was imported in SEG-Y format into Petrel in a seismic main folder containing all seismic related data. The data volume consists of 462 inlines and 951 crosslines and the line spacing for both is 25 m with a 4 ms sample rate, the settings are shown in the figure 15.

Axis	Min	Max	Delta
X	605831.12	629142.46	23311.34
Y	6073712.20	6089751.20	16039.00
Depth	-1842.00	6.00	1848.00
Lat	54°47'33.9467"N	54°56'32.2517"N	0°08'58.3050"
Long	4°38'46.2096"E	5°00'56.5898"E	0°22'10.3801"
Trace	-1840.00	4.00	1844.00
Seismic (templa...	~-24486.33	~19214.57	~43700.90
Amplitude (data)	~-24486.33	~19214.57	~43700.90

Description	Value
Original CRS:	ED50-UTM31 ("MEN...
Vintage:	Seismic Depth 1
Seismic type:	2D
Number of 2D lines:	1
Number of traces:	951
Number of samples per trace:	462
Number of cells total:	439362
Sample interval:	4
Volume value format:	Floating point 32 bit
Is storage OK?	Yes
Bytes consumed by samples:	1716.3 KB
Line id:	M00001 "C:\Users\S...
Line unique id:	e1990aeb-d549-406b...
Geometry line name:	Original Random line...

Figure 15. Seismic 2D line description in PETREL

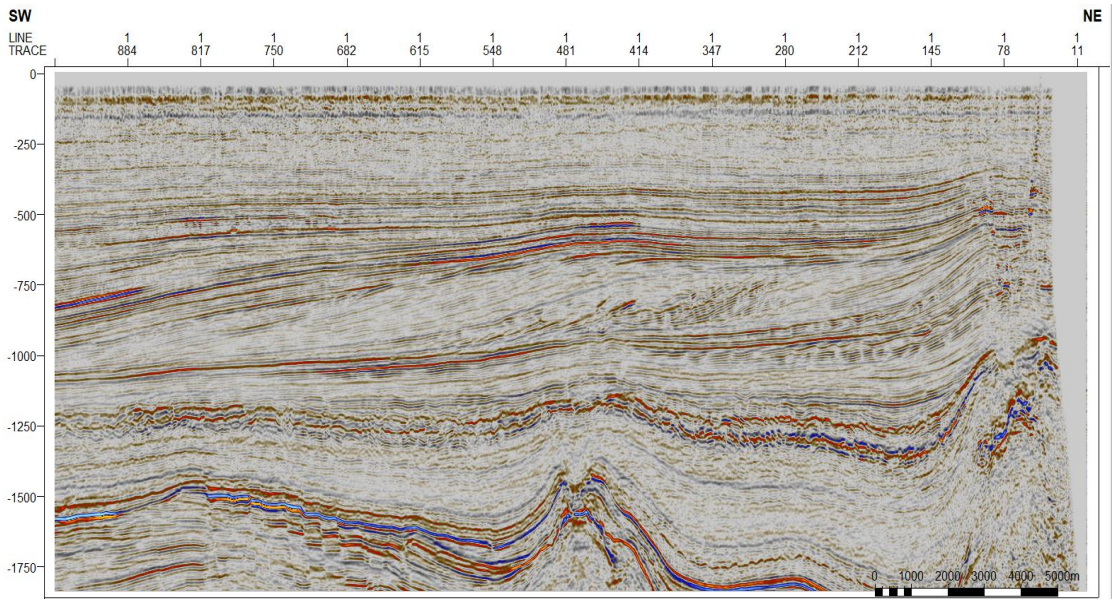

Figure 16. NE-SW 2D seismic line running across the Pliocene fluvio-deltaic system, *NAM 1987*

The dataset also consists of four vertical wells; F02-1, F06-1, F03-2 and F03-4 in NE-SW direction (figure 17) with relevant logs available (table 1) (gamma ray, density, sonic, and porosity in true vertical depth).

All wells had sonic and gamma ray logs. Only two wells (F2-1 and F3-2) had density logs. These logs were used to train a neural network that was then applied to the other two wells (F3-4 and F6-1) to predict density from sonic and gamma-ray logs. Porosity in all cases was calculated from density using the formula: Porosity = (2.65 - Density) / (2.65 - 1.05).

Both seismic and well data were provided by dGB Earth Sciences through its open-source seismic repository portal, ensuring access to high-quality and well-documented datasets.

Well name	X-coordinate	Y-coordinate	Acoustic impedance AI	Gamma (GR)	Density (RHOB)	Caliper	Sonic (DT)	Porosity (PHIE)
F02-01	606554	6080126	x	√	√	√	√	√
F03-2	619101	6089491	√	√	√	x	√	√
F03-4	623255.98	6082586.87	√	√	√	x	√	√
F06-1	607903	6077213	√	√	√	x	√	√

Table 1. Summary of available wells and well logs used in the study

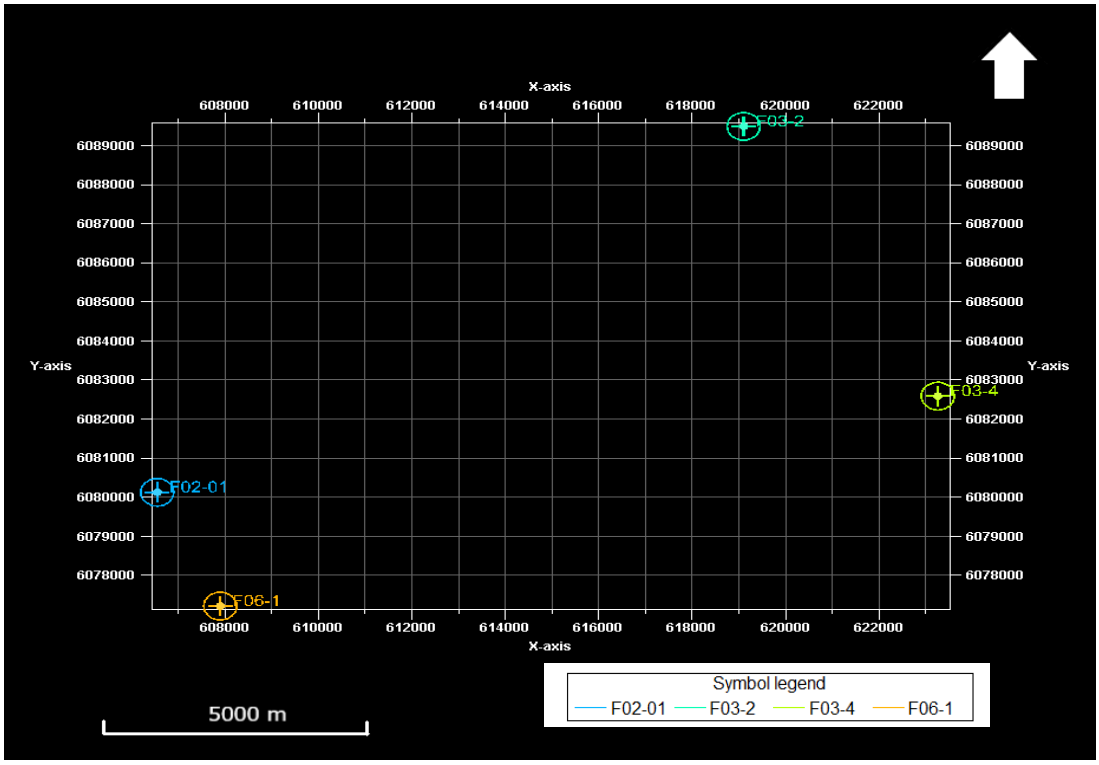

Figure 17. Location of the wells F02-01, F06-1, F03-4, F03-2 in 2D window

Due to the important spacing between the two group of utilized wells (F06-2, F02-1 and F03-4, F03-2), the sampling distribution statistic method was used to verify the heterogeneity of the geological area to correlate the wells. For this assessment, we selected wells F02-1 and F03-4, separated by 16822m.

In this case the two group of wells are called two populations H1, H2 are their measured depth at the top of the reservoir.

H1= {782.71 ;775.75}

H2= {637.09 ;634.99}

J1=2, J2=2, J Is the population volume

$$\delta = \sqrt{\frac{\sum_{i=1}^{J}(h_{1i}-\bar{h}_1)^2+\sum_{i=1}^{J}(h_{2i}-\bar{h}_2)^2}{J_1+J_2-2}}$$

$$\delta = 3.64$$

With δ being the average difference between two populations

Hi current value of each population , $\bar{h}$ *is the mean value of the population*

$$\bar{h}1 = 779.23$$

$$\bar{h}2 = 636.04$$

$$\delta h = \delta\sqrt{\frac{j_2+j_1}{j_2 \cdot j_1}} = 3.64$$

Distinction criteria

$$t = \frac{\bar{h}_2-\bar{h}_1}{\delta h} = \frac{636{,}04-779{,}23}{3{,}64} = -39{,}32$$

t <3 => The variability observed is stochastic; as the samples originate from the same overarching population, we can thus establish correlation among the wells, as there are no significant geological events separating the two well populations and affecting their geological history.

To achieve the objectives of this study, Geological Process Modeling (GPM) software integrated into the Petrel E&P software platform was used. The workflow involved multiple steps, seismic interpretation, well log analysis, model building, and validation. The diagram below (fig 18) provides a brief summary of the workflow, highlighting the key stages and processes involved in developing the 3D geological model.

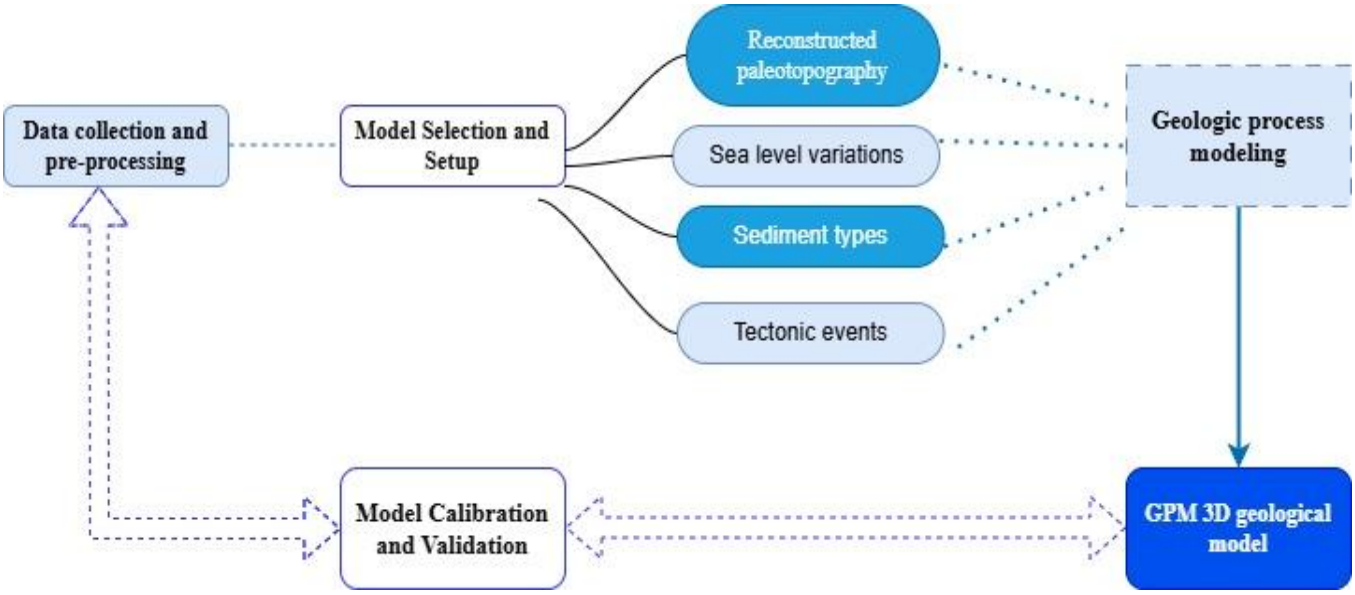

Figure 18. Flowchart showing the general workflow required to run a GPM Simulation

3.4 Sequence stratigraphy:

When paired with seismic data, well logs provide comprehensive vertical stratigraphic information essential for creating accurate stratigraphic models of sedimentary deposits (Van Wagoner, 1991). Well log sequence analysis typically begins with gamma ray (GR) logs from available wells. The fundamental interpretation guideline for gamma ray logs, developed by Luthi (2001), identifies shale or clay layers with higher values and sandy layers with lower values. Mojeddifar et al. (2015) further categorized four lithologies based on gamma ray values: coarse sand (<20 API), sand (20-45 API), fine sand (45-70 API), and shale (>70 API).

Changes in sedimentary facies stacking patterns are reflected in variation patterns found in gamma ray (GR) logs. These patterns include upward coarsening, upward fining, or constant grain size variations. Correspondingly, GR log trends may show upward decreasing, upward increasing, or upward constant trends, aligning with prograding (upward coarsening), aggrading (constant), and retrograding (upward fining) deltaic systems.

Three depositional episodes are identified in the study interval (Figure 19), synchronized through structural and wheeler domains analysis, integrating seismic reflection terminations and GR log patterns. This approach aligns with interpretations by Quayyum et al. (2012, 2013) and Amosu and Sun (2017) (figure 19). These episodes encompass the Highstand System Tract (HST), Transgressive System Tract (TST), and Lowstand System Tract (LST), each comprising a complete set of packages. These packages are delineated by maximum flooding surfaces

(MFS), basal surface of forced regression (BSFR), correlative conformity and sub-aerial conformity (CC/SU), and maximum regressive surface (MRS) markers at their tops.

A typical base-level cycle is characterized by a full suite of TST, HST, FSST (Falling Stage System Tract), and LST packages, assuming a constant amplitude of base level rise and fall. However, variations in base level across geological time may result in packages occurring in different sequences.

3.4.1 Sequence Breakdown

- The lower sequence (Sequence 1) comprises TST, HST, and FSST.
- The second sequence (Sequence 2) consists of LST, HST, and FSST.
- The last sequence (Sequence 3) includes LST, TST, and HST

The basal unit of Sequence 1 consists of a set of parallel and landward restricted reflectors (Quayyum et al., 2013). The GR log for this interval shows an upward increasing trend ending with a peak interpreted as a maximum flooding surface. Based on the reflection terminations and the GR response, this unit is interpreted as a TST**.**
Each of these sequences provides insights into the depositional history and environmental changes within the study interval, helping to reconstruct the geologic evolution of the area.

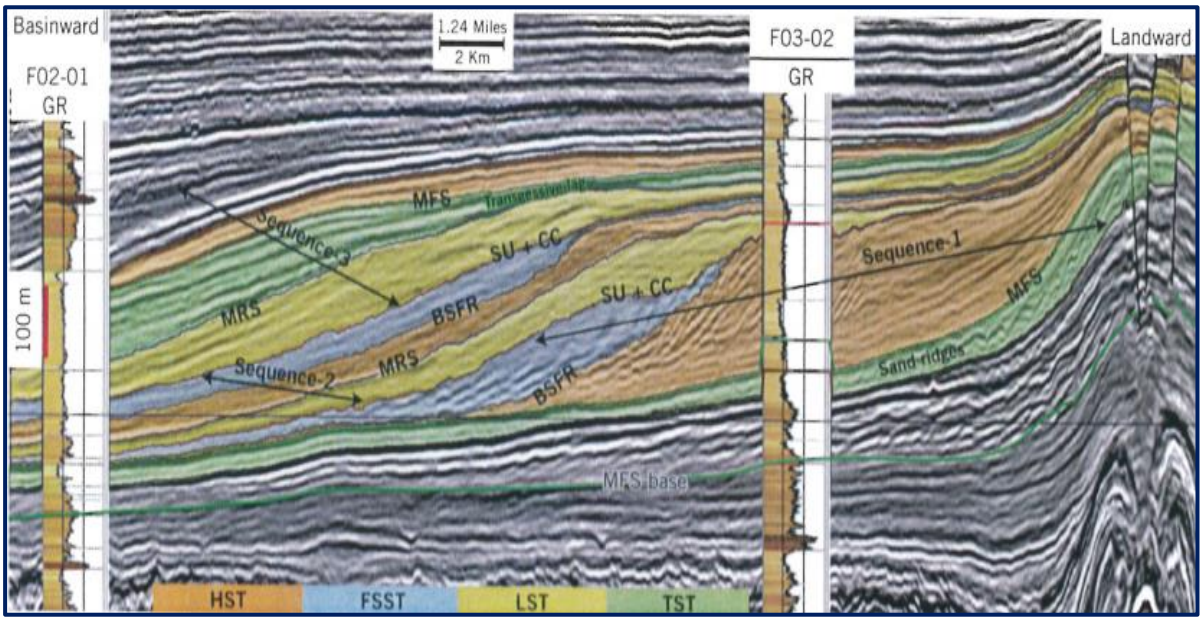

Figure 19. interpreted systems tracts overlaid on seismic by Qayyum et al (2013)

3.5 Model set up and Calibration:

In this research, the parameters of the stratigraphic forward model are subject to uncertainty and are systematically tested to identify the best-fit model. To save computation time, a low-spacial extent model is employed, consisting of a grid increment of 50 m x 50m and covering an area of 2km width and 50 km based on the distribution of modern sediments, the known

evolutionary history of the delta, and other available datasets. The temporal span of the model extends over a period of 3.8 million years, ranging from 5 million years to 1.2 million years.

While GPM software uses internal timesteps of varying duration adjusting the iterative solution for the differential equations to simulate sediment transport and deposition, we specified results to be output every 100,000 years resulting in a total of 380 layers. To save computation time, a low-resolution model is employed, consisting of a grid increment of 50 m x 50m.

3.5.1 Paleo Topography:

In Geological Process Modeling (GPM), "Topography" refers to the initial paleotopographic surface used to construct the model for the subsequent stratigraphic interval. This surface represents the Earth's topographic elevation at a specific past geological time, reconstructed from outcrop, well, or seismic data.

Post-depositional modifications like compaction, tectonic deformation, and erosion require structural restoration and decompaction to restore the present-day geometry to its original depositional state. To reconstruct the paleotopography of the sequence being modeled, a depth-converted seismic section (NE-SW 2D seismic line across the Pliocene fluvio-deltaic system) is used.

The first step is interpreting the base surface of the sequence and a datum surface representing the same geological time (e.g., onlap surface, maximum flooding surface). This datum surface serves as the top surface of the progradational sequence. The paleo-topography is extrapolated northeast to allow additional sediments to enter the basin and recreate the Pliocene delta, with material originating from the erosion of distal sediment sources. Since the base and top surfaces extend beyond the seismic section to the northeast, the slope and platform shape is assumed from regional geological information and observed progradation from seismic. (fig 20)

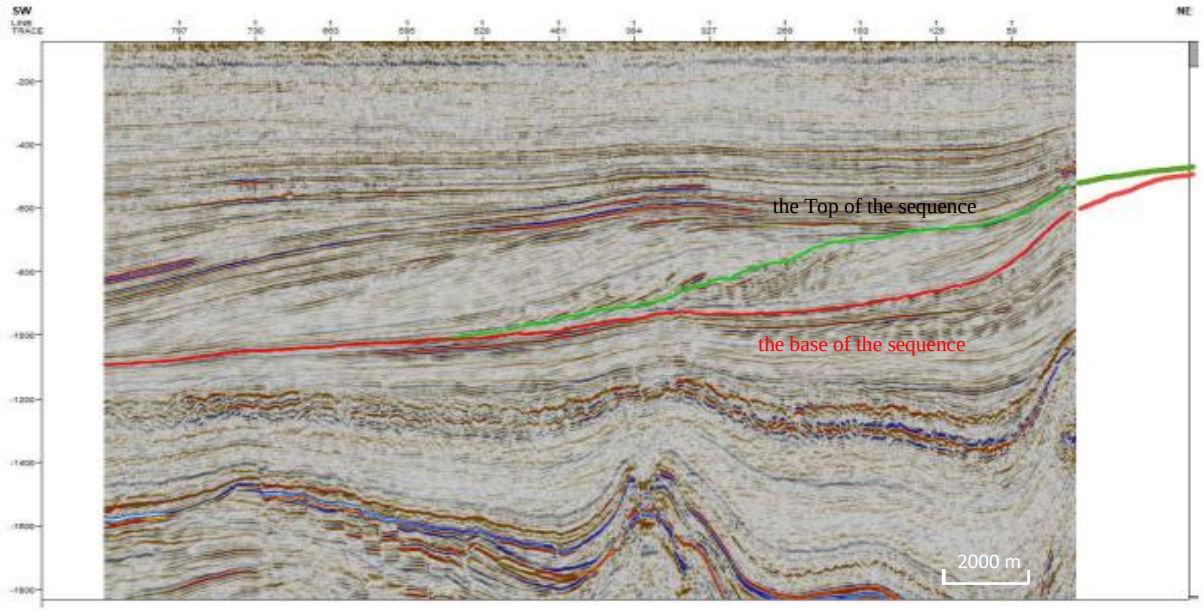

Figure 20. SW-NE 2D seismic line, featuring the base and top surfaces of the sequences, Both date 5 Ma.

The second step involves creating the paleo sea level (figure 21) using water depth information from the time of deposition of the datum surface. This information is derived from microfossil data, lithology, sedimentary structures, and seismic interpretation. Proxy relationships between paleosea level and the top and base surfaces guide manual interpretation. In this case, regional geological information indicates a paleowater depth of about 25 meters on the shelf. The paleosea level is assumed to be parallel to the base surface in the distal part (southwest) and parallel to the top surface in the proximal part (northeast), representing the shelf area.

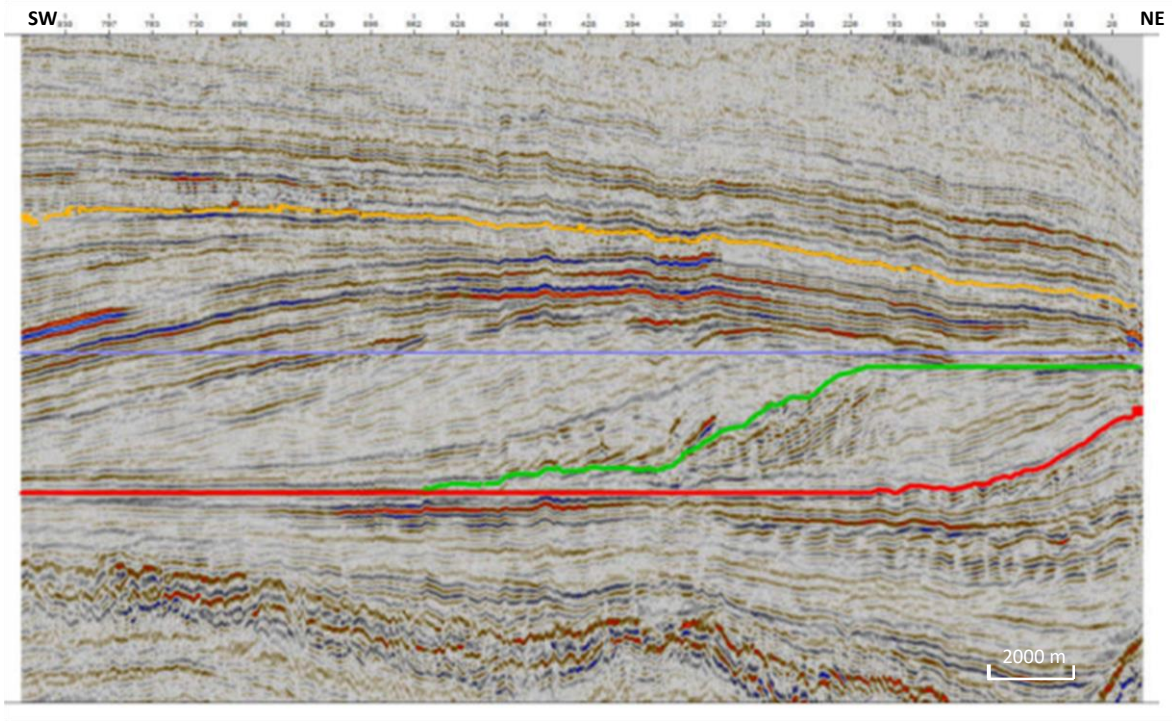

Figure 21. SW-NE 2D seismic line flattened on the 'Paleowater depth' horizon (blue line)

The next step involves creating the initial topography surface (not restored, at present day) by subtracting the 'Base' surface from the 'Paleowater depth' surface, which removes the water depth influence from the basal stratigraphic horizon to identify the initial topographic elevation. Then, the paleo sea-level surface at 5 million years ago (Ma) is created at 85 meters using the 'Calculator' tool (figure 22) with the equation 'Paleosea_level_5Ma=85'.

Finally, the 'Paleotopography' surface is copied and renamed to 'Paleotopography_5Ma'. An 85-meter bulk shift is applied using the 'Z = Z + A with A = 85' operation from the 'Calculations' tab to restore the paleotopography to its correct location at 5 million years ago (Ma) (figure23).

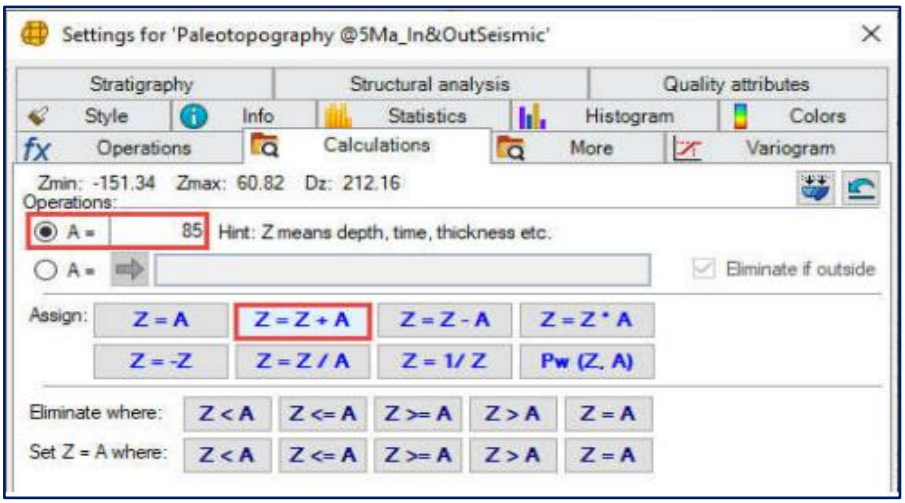

Figure 22. calculations pane in the surface settings

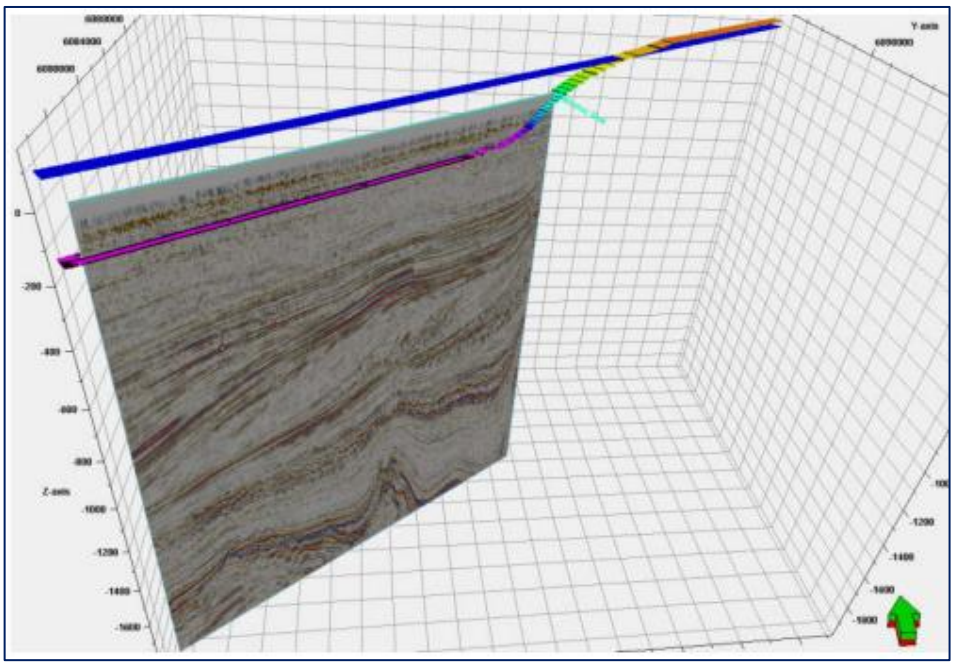

Figure 23. Restored 'Water depth' surface (top) and 'Paleotopography' surface (bottom) at 5 Ma

A decompaction workflow, based on equations from Sclater and Christie (1980) and adapted from Allen and Allen (1990), was employed to mitigate the effects of sediment compaction over time. This workflow enables the decompaction of the thickness between the paleo sea level and the paleo topography.

The workflow starts by computing the sediment thickness of the unit at its current depth and then calculates its thickness at the time of deposition. Essential information for this process includes the current depth and thickness of the unit being decompacted, along with its primary sedimentary composition.

Three inputs were needed:

- The paleo water depth, corresponds to the sea level elevation depth at the start of the deposited unit, here it was +85 meters at 5 Ma
- The compacted paleo topography at 5 Ma that we created previously
- The compacted paleo topography at present day depth that corresponds to the base surface that we interpreted.

A new folder named 'Decompaction results' is created in the 'Input' pane, containing two new surfaces: a. The 'SedTh' surface, representing the thickness of the unit composed only of sediment matrix. b. The 'DepoZ' surface, representing the decompacted paleo topography at the time of deposition.
The 'DepoZ' surface is used as the 'Topography' input for creating the GPM model.

3.5.2 Sediment types:

The target zone of this analysis contains siliciclastic shelf deposits comprising sand and shale (Overeem et al., 2001).

Four sediment types are modeled: coarse sand, fine sand, silt, and clay (table 2). GPM models each lithology and assigns to them a distinctive color depending on the composition. The color is a single color if the lithology is not mixed, e.g. coarse sand (red), fine sand (green), silt (blue) and clay (black), but if the sediments comprise mixed lithologies they are represented as additive color mixtures (Schlumberger, 2016).

Lithology	**Grain Properties**			
	Diameter (mm)	**Density (g/cm^3)**	**Transportability**	**Fraction ranges**
Coarse Sand	1	2.7	0.8	0.25
Fine Sand	0.5	2.65	1.6	0.25
Silt	0.01	2.6	3.2	0.25
Clay	0.02	2.55	6.4	0.25

Table 2. Grain properties and fractions of the sediment types used as input

3.5.3 Sea level

For the sea level we used the pre-existing Haq global sea-level curve (Figure 24); a stratigraphic curve of the age in millions of years with the sea level in meters, relative to the model's datum.

Figure 24. Haq global sea-level curve in GPM software

3.5.4 Tectonics

By comparing the paleo and present-day topography we observe that only simple vertical motions of subsidence and uplifts were applied to the paleo topography. To recreate these movements, GPM software requires tectonic maps and rates as the main inputs (figure 25).

Considering that the sedimentation of the F3 block delta was provided by an uplift event triggered by faults and salt domes in the eastern part of the area, an uplift map was created to illustrate this deformation and the uplift rates were deduced from literature and seismic data.

The initial increase of the subsidence rate occurred in the early Pliocene creating an accommodation space of 300 meters, this requires a subsidence rate of 1.5 mm per year at the start of the simulation.

The decompacted thickness of the delta is about 400 or 500 meters, its deposition happened during Pliocene for about 2.8 m years, which gives an average subsidence rate of 0.1 to 0.2 mm per year.

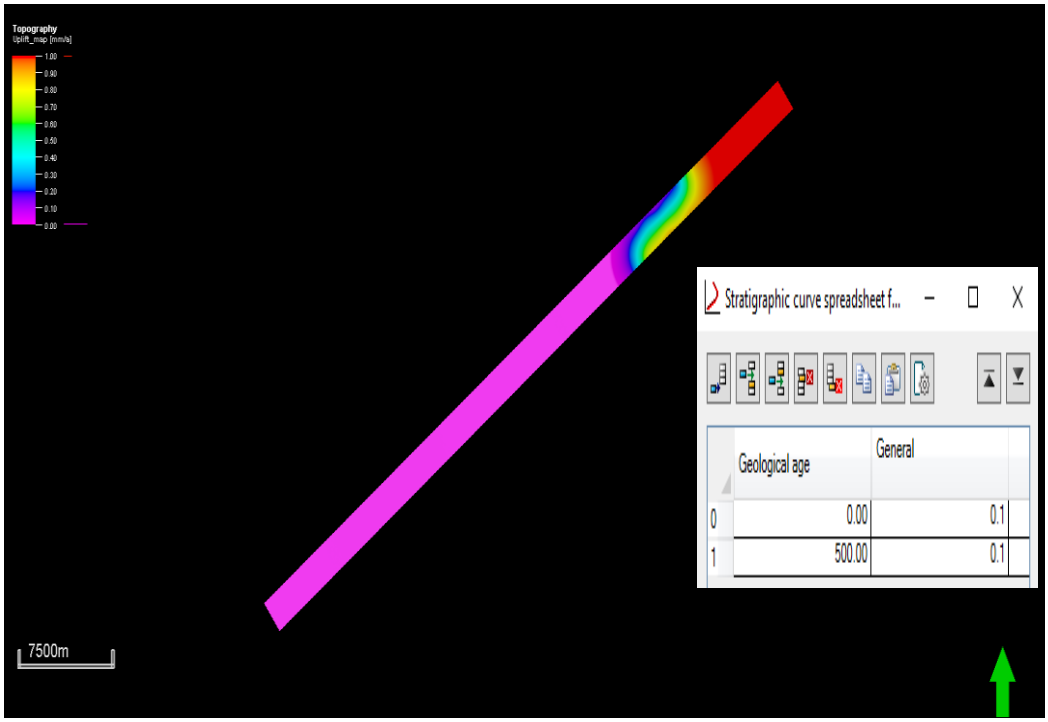

Figure 25. uplift tectonic map rates and function

3.5.5 Sediment diffusion:

To model diffusion in GPM both a diffusion coefficient and a diffusion curve along the elevation depth and relative sea level are needed.

The diffusion curve acts as a unitless multiplier that models stronger erosion and transportation of the sediments in the sea level zone, which has a strong impact on erosion, sequence thickness and the delta front slope, using an inappropriate diffusion curve can lead to a lack of sediments in the distal region of the model.

The default diffusion curve was tested first, however the resulting delta lacked sediments in its distal regions, increasing the diffusion coefficient alone did not give better results. Instead, we tried modifying the diffusion curve (figure 26).

- Higher diffusion at high altitudes gave us the best results for our simulation as it increased the sediment outputs and gave us the expected thickness.

- Increasing the diffusion curve at sea level flattens the top of the delta which is consistent with the erosional process associate with HST.

The diffusion coefficient controls the strength of the diffusion equation. The diffusion rate is measured in m^2/a. This is the amount of sediment in square meters passing through the vertical line on a slide that is 1 meter wide each year.

A diffusion coefficient of 15 m^2/year was used.

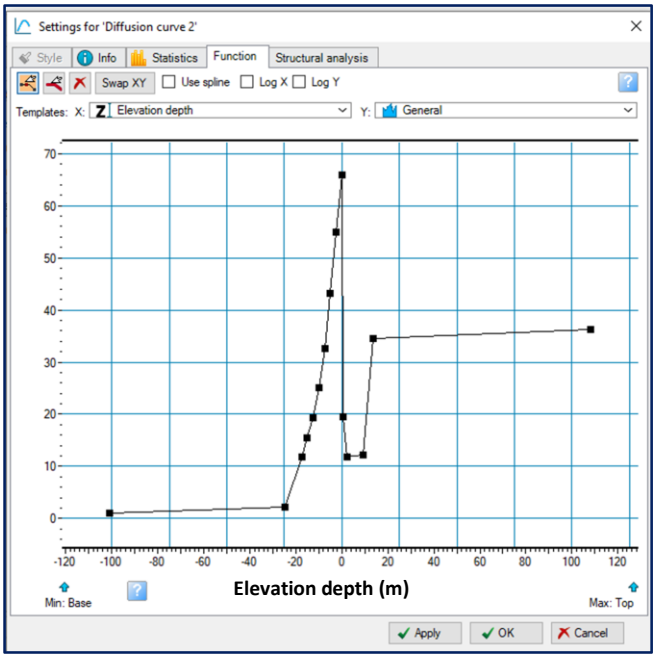

Figure 26. Diffusion curve, X axis shows sea level Elevation depth, Y axis is the multiplier

3.5.6 Post modeling conversion:

GPM software models sedimentation processes and stratigraphic boundaries for a specified time interval, in order to compare the results of the obtained model with really well and depth-converted seismic data, we needed to reposition it into the present-day location

The "Trim simulation results to right position and age" process enables that, it updates the stratigraphic model by applying the following operations to the modeled sequence: vertical translation, repositioning, and thickness compensation.

This process enables to transpose (shift and deform) the base of an existing GPM software model to a specific surface. Using the calculator, the “base surface” created previously was used as the base for the model at present day and a thickness of 1000 meters was chosen in order to not cut into the model’s real thickness.
Both the base surface and the paleotopography surfaces need to have the same grid geometry, limits, rotation, and x and y increments.

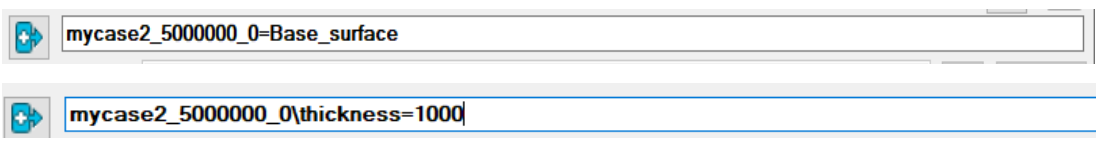

The surface used a target to trim the base of the model and the thickness map are inserted in the corresponding boxes (figure 27).
“Cut top” option was selected to cut the model where it is thicker than the isopach map.

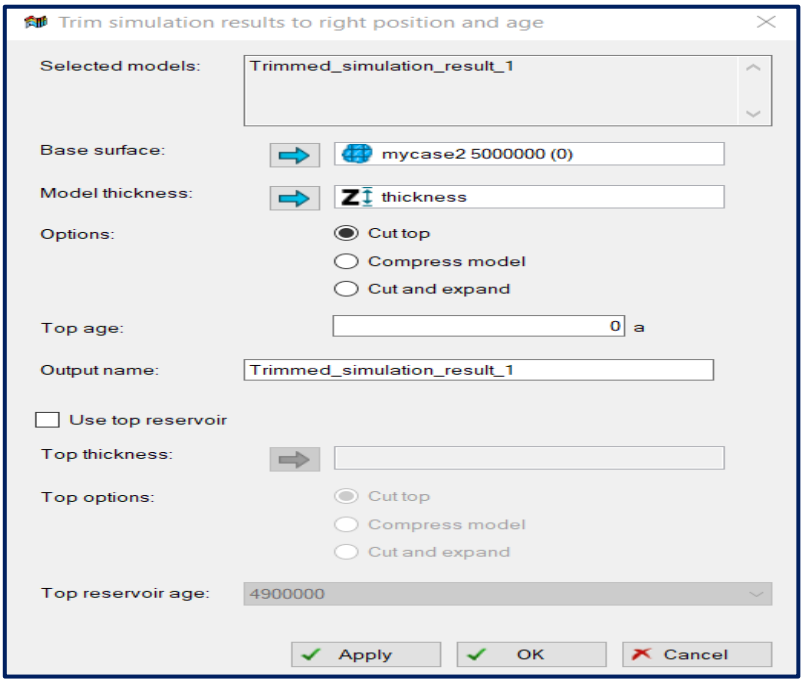

Figure 27. Trimming process in PETREL

3.6 Simulation result and discussion

The simulation (Fig 28) was conducted to gain insights into the evolution of a large Plio-Pleistocene delta in the southern Central Graben offshore basin of the Netherlands. Three main sequences were identified (fig 29) each containing lowstand, transgressive, and highstand system tracts. Seismic interpretation reveals that the delta structure consists of three sequences bounded by two maximum flooding surfaces, overlaid by a thick sediment cover. The first group of sediments shows continuous high-amplitude reflectors onlapping the prograding delta and becoming conformable towards the top. The second group consists of subparallel, discontinuous low-amplitude reflectors.

Detailed fluid dynamics were not considered in this model. Despite using a very simple process-based model, both allogenic and autogenic cycles were reproduced. At a large scale, three main sedimentary units were deposited: a first prograding unit from 5 to 3.8 Ma, a second unit from 3.8 to 2.9 Ma, and an aggradational third unit from 2.9 to 1.2 Ma. These units were controlled by sediment diffusion driven by gravity and sea level fluctuations.

The base of the first unit starts with shaly deposits grading into coarser textures in the slope area. The geometries of sequences 1 and 2 match the prograding and regressive patterns observed in the seismic data. The early forced regressive phase of sequence 1 leads to the development of sigmoid oblique prograding clinoforms (Fig 29) due to low subsidence rates and sea level fall with sufficient detrital supply. Erosion and sediment bypass at the shelf edge result in sediment deposition on the lower slope and basin floor when sedimentation rates exceed accommodation space. This causes each parasequence to become progressively shallower than the previous one, leading to a seaward shift in shoreline position (regression). A

rapid rise in sea level subsequently drowns the deltaic system, covering it with transgressive marine sediments due to a rapid eustatic rise or high subsidence rate.

Shelf-edge deposition and accretion resulting in lower slope and basin floor sediment starvation occur when there is no net shift in shoreline position or average water depth, as observed in sequence 3.

The model shows lateral texture heterogeneities with a southwest deepening trend. Lateral facies vary from higher energy deposits along the slope to finer deposits basinward to the east. These variations allowed the accumulation of coarse grains and bioconstructions in structurally higher zones (higher energy/lower bathymetry) and finer grains and mud in the surrounding depressions (lower energy/higher bathymetry). This approach successfully reproduced the overall architecture of reservoir units, honoring well data. Finally, the upward aggrading trend is respected, coupled with lateral variability in texture.

Bioturbated fine sediments accumulate, and deltaic accumulation progresses on the platform, forming a thick sequence as progradation reaches the platform edge and continues down the slope. The creeping of prodeltaic clays, crushed by overlying sands and the slope, leads to the formation of diapirs, slumps, and normal faults, creating a structural setup favorable for hydrocarbon trapping.

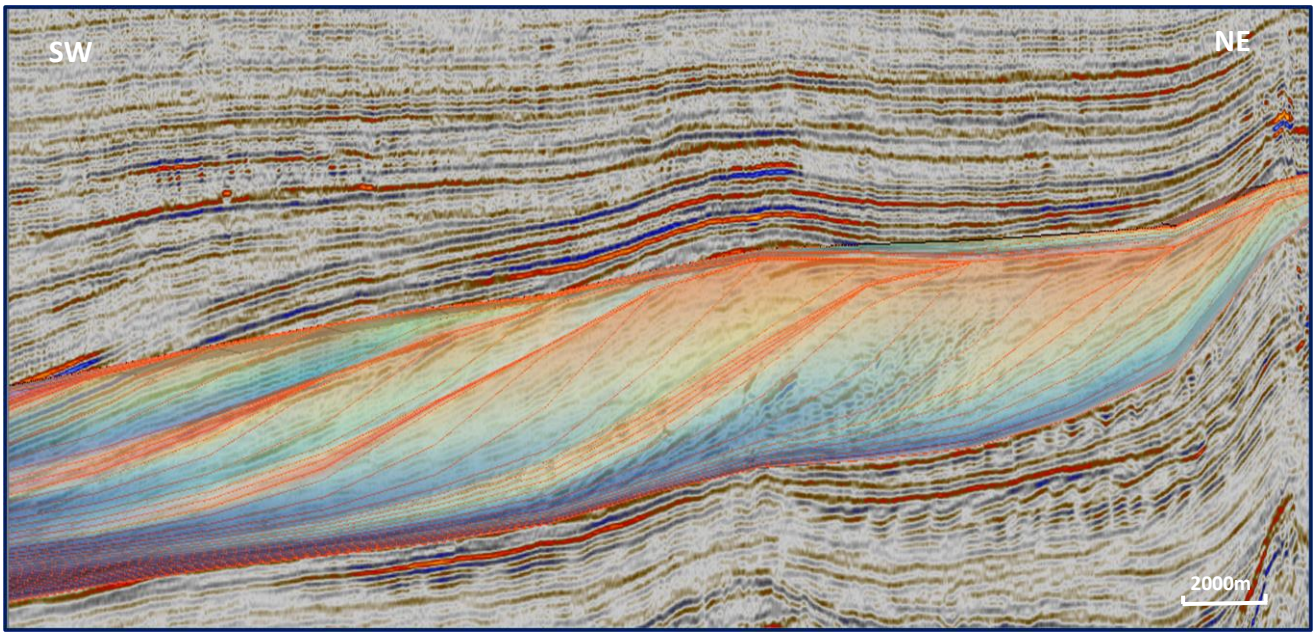

Figure 28. trimmed result of the GPM model overlaid on seismic 2D line (reference model)

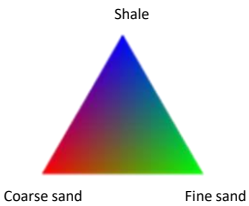

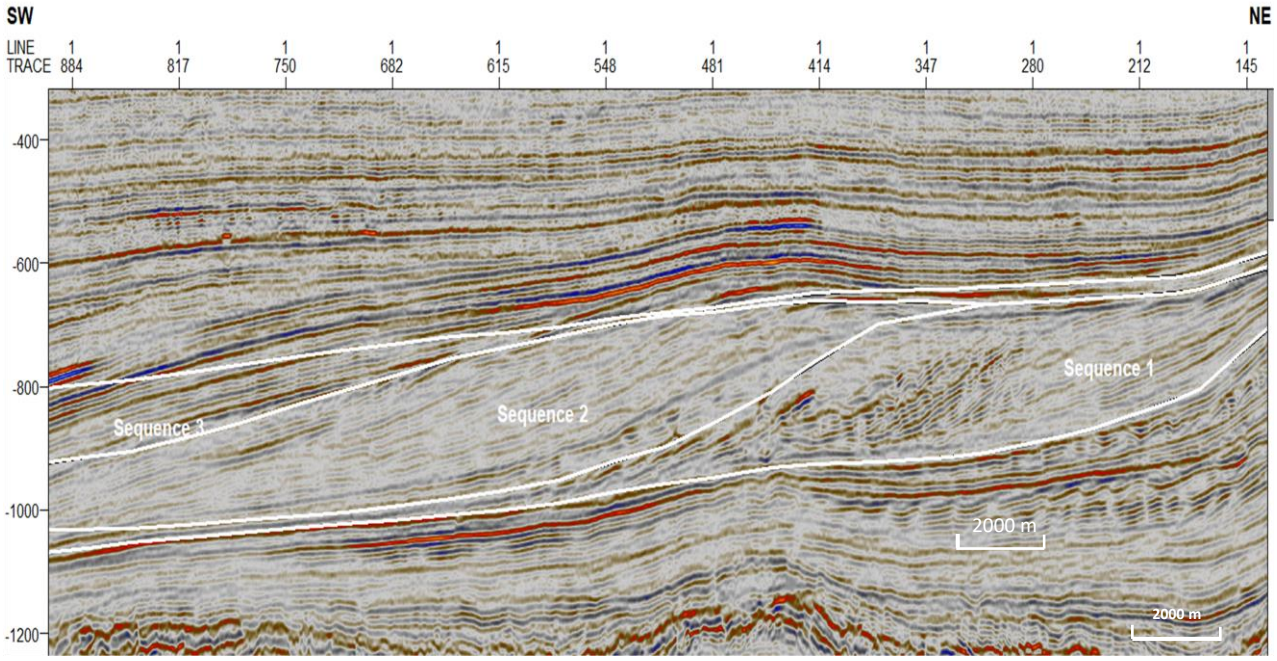

Figure 29. 2D seismic line and the main sequences horizons of the GPM model

In Petrel, "apparent polarity" is a way to visually represent seismic reflection data based on the direction of the seismic wavelet (peak or trough). It helps reveal features like unconformities by showing the sign of the reflection coefficient. This representation is valuable for checking the lateral variation of polarity along a reflection layer. On noisy seismic sections, apparent polarity can show event continuity better than the original seismic section, especially in good-quality data. It's crucial for interpreting subsurface geology, aiding in fault detection and improving the delineation of hydrocarbon reservoir extent and properties. This feature helped distinguishing between different stratigraphic units and understanding depositional environments for the study area (figure 30).

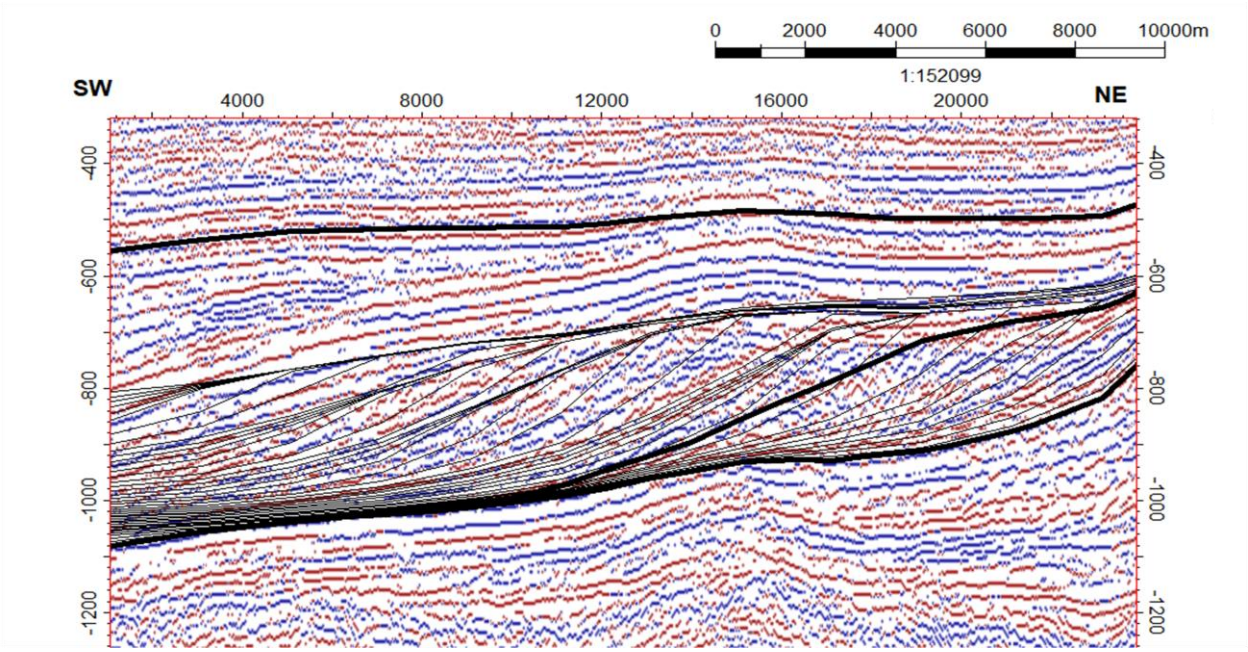

Figure 30. apparent polarity applied in 2D section line and the model's horizons in black

Lower Sequence #1: It began with a high sedimentation rate during a late normal regression, forming a Highstand System Tract (HST). Landward uplift caused erosion and a base level drop, forming a Forced Regressive Wedge (FSST) as a Falling Stage System Tract (FSST). This created a composite surface that marks the first sequence boundary (SB) separating it from Upper Sequence #2.
Upper Sequence #2: Deposition started with slowly rising base levels and relatively slower sedimentation rates. It included Normal Regressive Deposits subdivided into Lowstand System Tract (LST) and HST, separated by a Maximum Regressive Surface (MRS). Salt movement caused another FSST, marking the end of Sequence #2.
Third Sequence: It was more wave-tide dominated, starting with an LST and transitioning into a Transgressive Systems Tract (TST) with large-scale wave and tidal erosion. The Healing Phase ended at a Maximum Flooding Surface (MFS), above which normal regressive deposits formed the HST.

Additional details on specific stratigraphic units within the early Pliocene interval reveal distinct characteristics:

• Sequence 1 exhibits a clear forced regression (FR), with a base unit showing landward restriction and primarily comprising sand ridges overlain by thin transgressive shale. It is further overlain by aggrading to prograding parasequences.

• Sequence 2 represents normal transgressive system tracts.

• Sequence 3 marks a stage where the basin starts rising transgression and healing phase.

3.7 Alternative scenarios

Several alternative scenarios were tested in this study to assess sensitivity to changes in input parameters. These scenarios included changes in sediment diffusion rates, tectonic activity and the eustatic variations. The respective model results are presented in the following sections, showcasing the variations in sediment distribution and stratigraphic architecture under different scenarios.

3.7.1 Scenario a: varying diffusion coefficient and constant diffusion function:

To evaluate the impact of the diffusion coefficient on the model outcome (fig 32), a constant diffusion function was applied throughout the entire simulation interval, as illustrated in the figure 31.

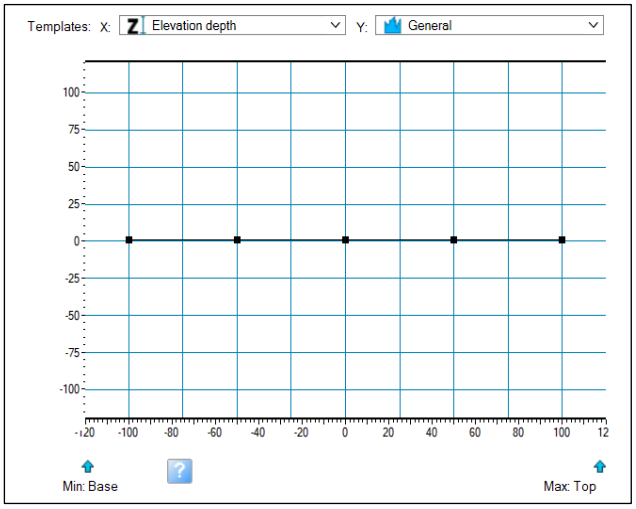

X, a	Value, m2/a
2500000.00	15.00
3750000.00	15.00
3750000.00	1.00
5000000.00	1.00

Figure 31. Diffusion coefficient rates and constant function used for the simulation

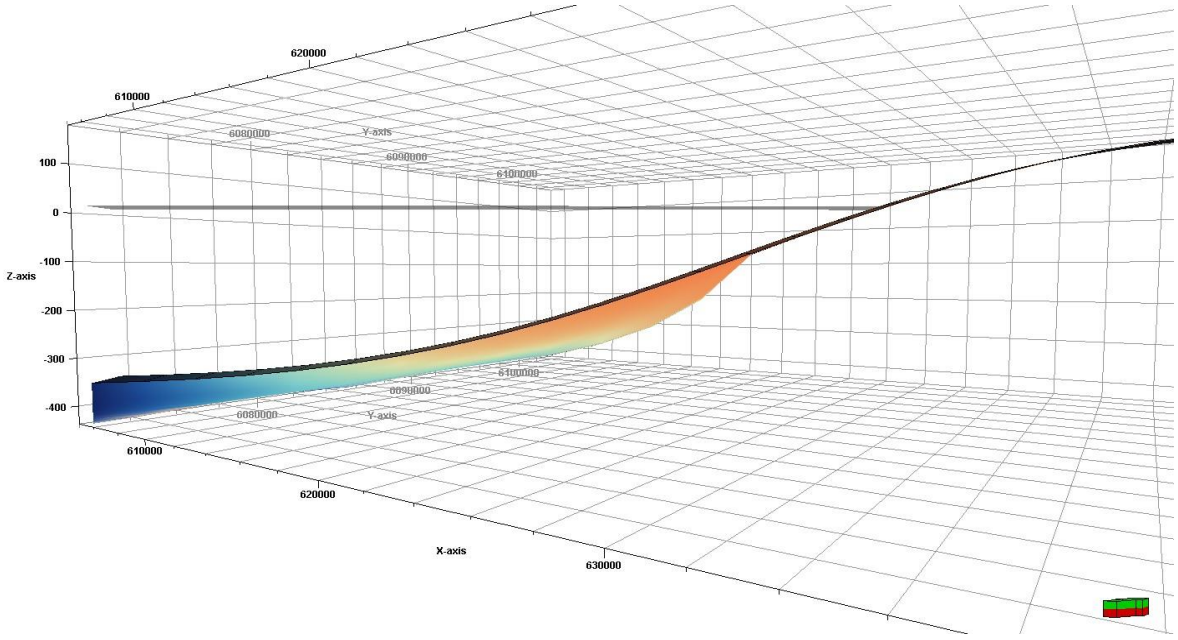

Figure 32. scenario (a) GPM model

Between 5 and 3.75 Ma: The low diffusion coefficient (1m2/y) is responsible for little erosion, transport and deposition of sediments into the basin; the overall sequences thickness is small and the sediments do not travel far from the base of the slope area into the basin.

Between 3.75 and 2.5 Ma: High diffusion coefficient (15) is responsible for higher erosion, transport and deposition of sediments into the basin, both the overall sediment thickness and the sediment thickness per time step are larger and the sediments travel far into the basin reaching way beyond the base of slope area and extending western beyond of the model

3.7.2 Scenario b: Impact of the diffusion coefficient

For this simulation (figure 32) we only varied the diffusion coefficient from 15m²/y to 5m²/y.

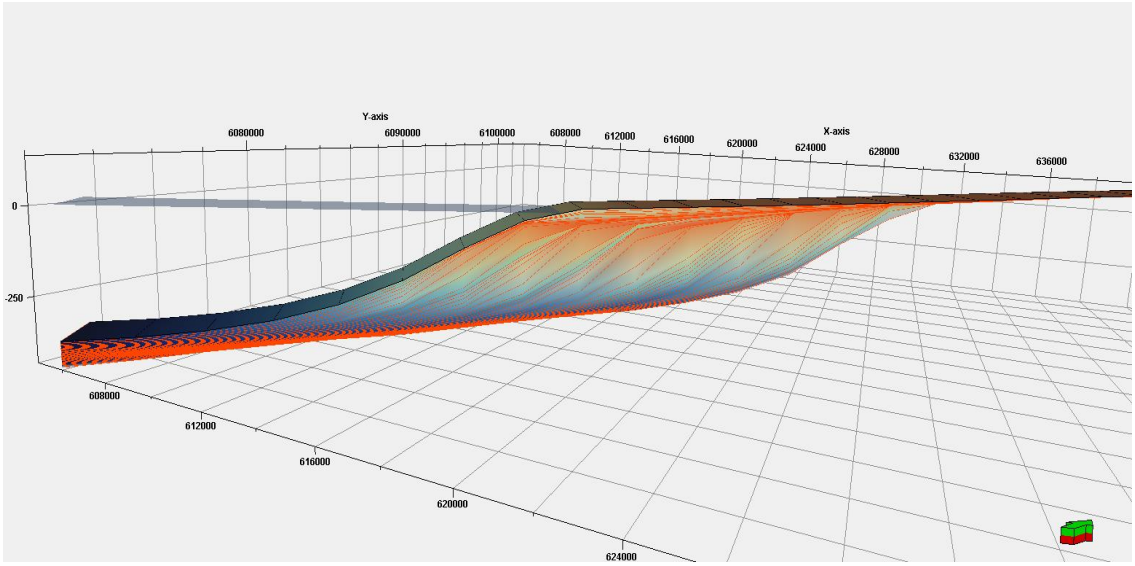

Figure 33. scenario (b) GPM model with diffusion coefficient of 5m²/y

When using a lower diffusion coefficient (5), the model shows increased erosion, sediment transport, and deposition along the slope region compared to the distal part, where it lacks sediments. Thereby the volume of sediments being transported into the basin is not enough and the basin is likely to not be filled with enough sediment within the specified time frame compared with the first model where a diffusion coefficient of (15) was used.

- ✓ Varying the diffusion function significantly impacts and alters the entire GPM simulation result; affecting both the overall shape of the slope and bringing lots more sediments into the basin

3.7.3 Scenario c: Impact of the diffusion function

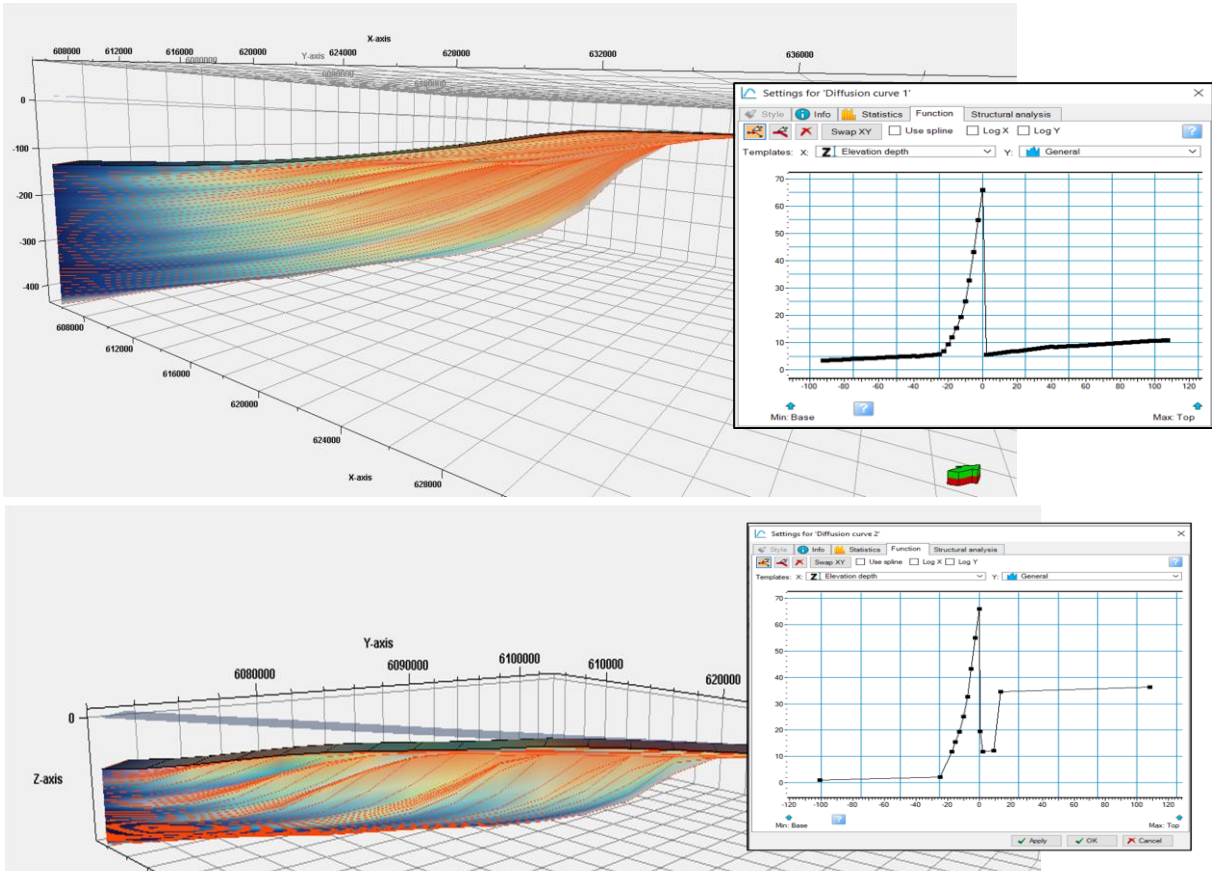

Figure 34. GPM model after varying the diffusion function, Top model showing an aggradational pattern, bottom showing a progradational pattern

As observed earlier, a constant diffusion function does not alter the shape of the slope, while a varying diffusion function significantly impacts its resulting shape.

Different diffusion functions influence the resulting Geological Process Modeling (GPM) model by altering accommodation space and sediment input patterns. The changes in these patterns can induce an aggradational pattern due to changes in accommodation space compared to the progradational pattern observed in the base model.

Both models (fig 34) demonstrate that even with the same amount of sediment being transported into the basin, the resulting stratigraphic patterns and sediment distributions are markedly different. Specifically, smaller values and steeper slopes in the diffusion function result in higher slope dips in the final equilibrium profile and shorter sediment transport distances before deposition. This first instance drives the filling of most of the accommodation space, whereas the second promotes sediment accumulation in only half of the accommodation space, primarily closest to the shore.

3.7.4 Scenario d: No tectonics

To understand the impact of tectonic movements, a scenario was simulated in which tectonic events were removed (fig 35 TOP). We can observe the impact of tectonics here by observing the same geological model (base model) with and without tectonic movements.

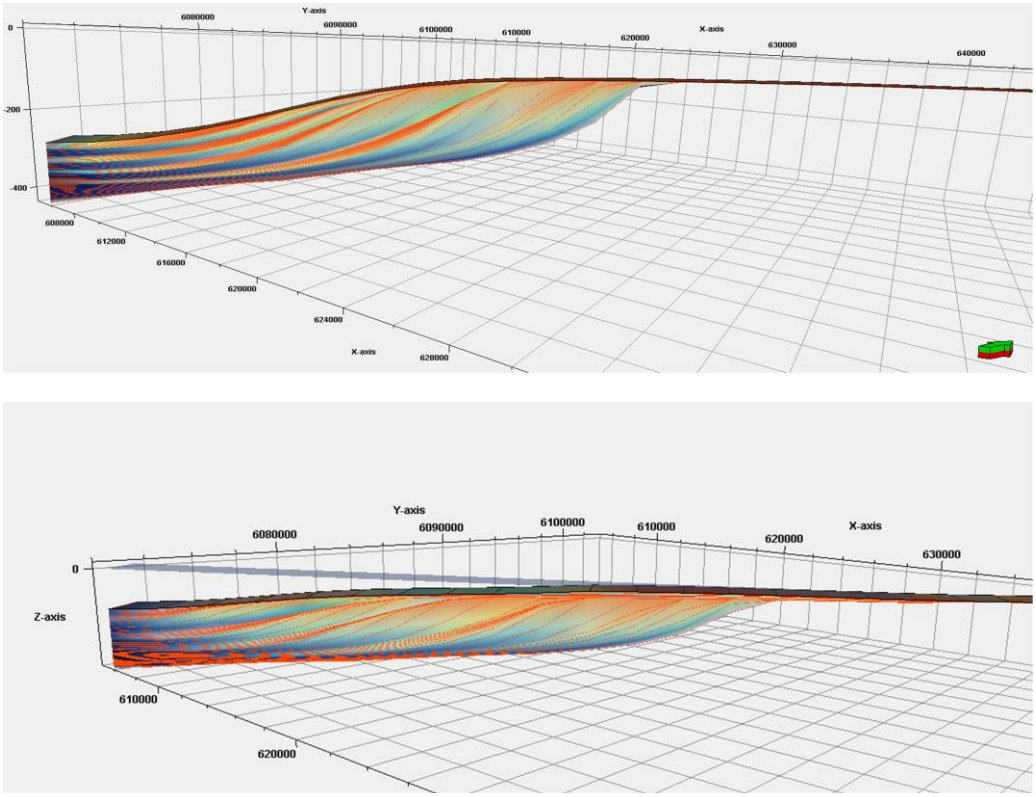

Figure 35. Top: GPM model without the influence of tectonic movements. Bottom: GPM model affected by uplift to the Eastern part.

The tectonic rate is applied to the basement only, affecting the basin's final shape and controlling the accommodation space, sediment supply area.

The overlying sediment column is moved up, according to the uplifted movement of the basement.

By providing further material from the source from an uplift tectonic event to the east, we observe a change in the stratigraphic patterns and sediments distributions, as well as the overall thickness of the sediment column.

3.7.5 Scenario E: Varying the sea level curve

In this experiment, we replaced the Haq global sea level curve by the Exxon global sea level curve.

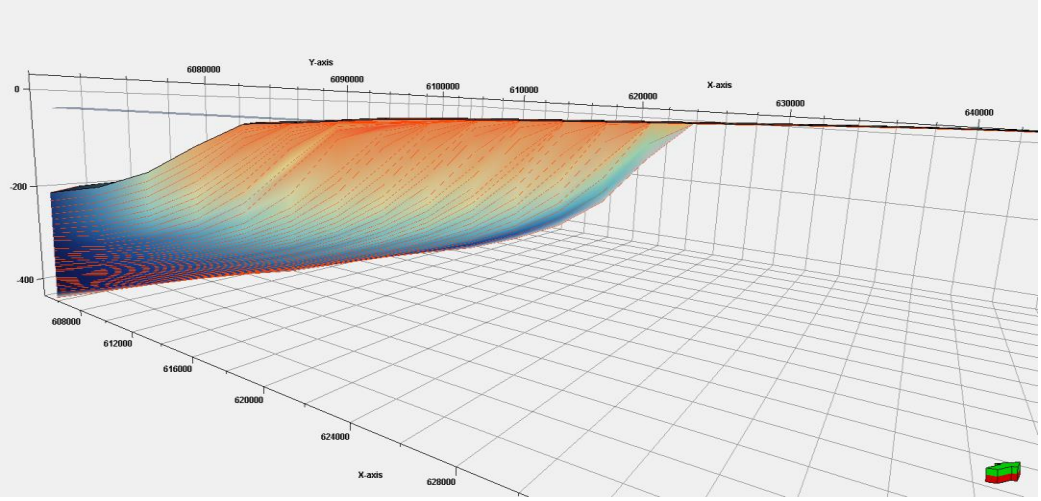

Figure 36. GPM model varying the sea level curve input

Sea level changes did not significantly alter the general geometry of the model, but they did impact sediment transport pathways. The model using the Exxon curve (fig 36) changes the accommodation space in the distal areas of the model and fails to capture the stacking patterns and sequence boundaries of the desired model.

In contrast, employing the Haq global sea level curve in the GPM model accurately reflected the desired level of detail. It emphasized sequence boundaries and systems tracts, enhancing understanding of sedimentary sequences and their organization. The model dynamically adjusted accommodation space to reflect frequent sea level changes, leading to a finer representation of sedimentary processes.

We applied the trimming process used on the base model previously to trim the simulations into the right position and age in order to compare the resulting models with the depth-converted seismic data.

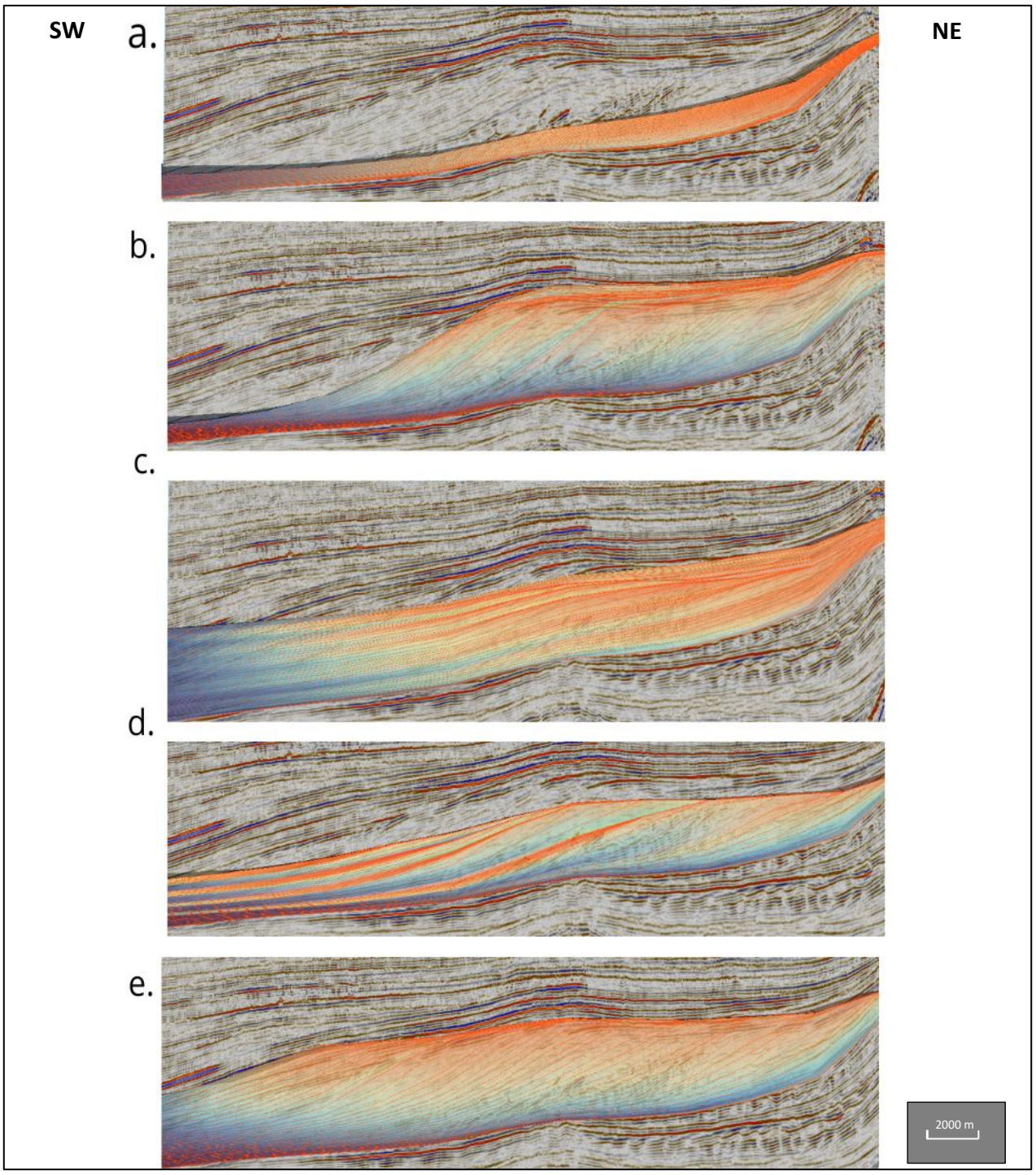

Figure 37. trimmed simulations result of the previous scenarios overlaid on seismic 2D line

3.8 Conclusion:

The application of Geological Process Modeling within the F3 Block of the North Sea has provided the following significant insights into the geological evolution and sedimentary processes:

The deposition within the F3 Block is characterized by three principal sedimentary units: an initial prograding unit from the early Pliocene, followed by a second unit from the late Pliocene, and an aggradational third unit from the Pleistocene. These units were primarily influenced by sediment diffusion driven by gravitational forces and sea-level fluctuations.

The stratigraphic sequences, mainly Sequences 1 and 2, show progradation and regression patterns consistent with seismic data.

-Sequence 1 exhibits a clear forced regression (FR) formed sigmoid oblique prograding clinoforms due to low subsidence rates and reduced sea level, leading to sediment accumulation and shallower parasequences.

- Sequence 2 represents normal transgressive system tracts.

- Sequence 3 displays an aggradational pattern.

The model displays lateral changing textures from coarser to finer moving southwest with a deepening trend. This variability allows for different sediment accumulations, replicating reservoir architecture and honoring well data.

Through the integration of GPM with seismic data, a comprehensive reconstruction of the complex depositional history has been achieved, enhancing our understanding of subsurface architecture. The model's capabilities extend beyond sediment source identification and transport mechanisms to include the prediction of facies variations essential for delineating potential reservoir zones.

CHAPTER IV
GPM CASE APPLICATION IN ALGERIA
Block 401a/402a, Berkin basin

4 Introduction:

In the previous chapters, we introduced Geological Process Modeling (GPM) technology and its applications. This chapter marks the first implementation of GPM in the Berkin Basin of Algeria, and more specifically in the TAGI reservoir. We will outline the geological background of the Berkin Basin, describe the methodology for applying GPM, and present the results of our simulations. Our findings will provide new insights into the basin's evolution and potential for hydrocarbon exploration.

4.1 Geological setting:

4.1.1 Berkine basin:

The Berkine Basin is an intra-cratonic basin that developed during the Middle to Late Triassic on the northeastern part of the Algerian Saharan platform. Covering an area of 102 395 km², it is one of Algeria's most important hydrocarbon-producing basins. The Berkine basin is bounded to the North by the Saharan flexure and the allochthonous units of the Saharan and Tellian Atlas Mountains (Guiraud, 1998). The western margin of the basin is bounded by the Hassi-Messaoud and El Biod palaeohighs which together form a broad ridge separating Berkine basin from the neighboring Oued Mya Basin. To the south, it is separated by the Ahara from the Illizi Basin. (Fig. 38).

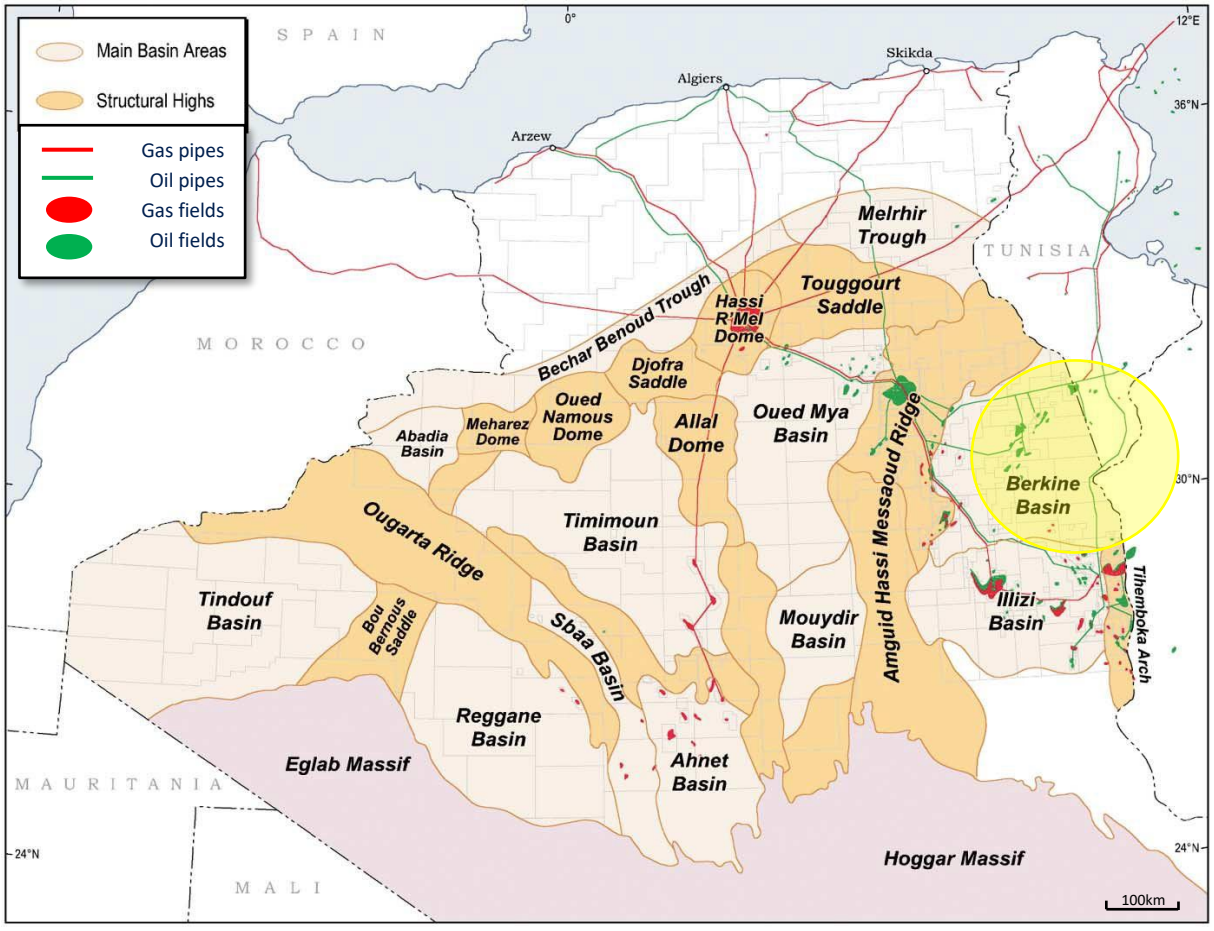

Figure 38. Map showing the location of the Berkine Basin (yellow circle) on the northern part of the Saharan Platform, related structural highs and the main oil and gas fields of Algeria, modified from Turner et al 2001.

The Berkine Basin, more subsident in the north, contains deposits referred to as 'distal'. The sedimentary inputs mainly came from the south and the Hoggar massif, with a low sedimentation rate estimated at 10 m/Ma, which is typical of intracratonic basins.
The structure of the Triassic basins is largely controlled by the reactivation of NE-SW and NW-SE, Pan-African, and late Paleozoic basement lineaments (Nedjari, 1994). The Middle Cretaceous extensional reactivation of the NW-SE cross-cutting faults played a key role in the formation of several giant Lower Triassic Argilo-Gréseux (TAGI) reservoir oil fields (Pink, Carney, Drumheller, & Okbi, 1999). Late Cretaceous/early Tertiary compressional inversion accounts for several other fields, including the El Borma oil field. Due to the significant subsidence that has affected it during its evolution, the Berkine Basin has the most complete sedimentary series (over 6,000 m), with three sedimentary cycles: Paleozoic, Mesozoic, and Cenozoic. The Paleozoic (Cambrian to Early Carboniferous) consists of a predominantly siliciclastic succession reaching up to 3.5 km in thickness (Askri et al., 1995) (Fig. 39).

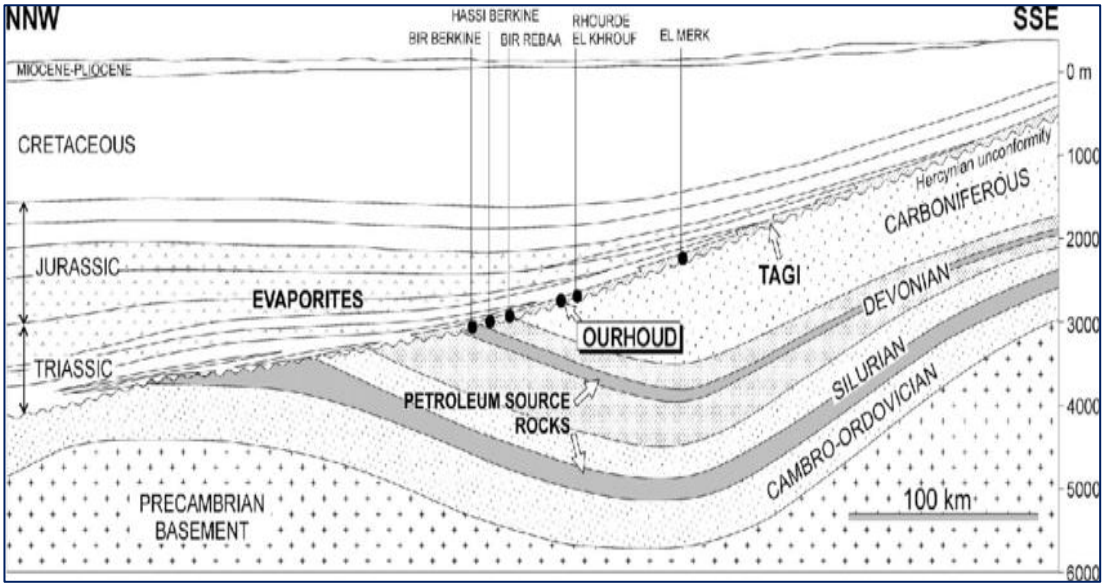

Figure 39. NNW-SSW generalized cross section through the Berkine Basin, showing the location of major oil fields of the central part of the basin. Boote et al. (1998)

4.1.2 Tectonic History

The Berkine Basin is an intracratonic depositional center that originated in the Paleozoic era because of tectonic depressions brought about by Pan-African orogenesis on Gondwana. (Kröner and Stern, 2004). The continent was then uplifted by the Arenigian extension, leading to the closure and erosion of the basin, creating the metamorphic and igneous unconformity basement (Galeazzi et al., 2010). The Phanerozoic history of the Berkine Basin is marked by distinct multi-phase tectonics. The major structural event is the Hercynian orogeny: the end of the Hercynian period is characterized by a period of regional emergence, accentuated by uplift in the north, with the visible consequence being the Djeffara-Dahar highs. The Berkine Basin is the most affected by Hercynian tectonics. This was followed by a rifting period related to the emergence of the passive margin of the North African Tethys, then an extension phase during the Lias and Triassic, marked by a progressive tilting to the north of the underlying Paleozoic platform.

4.1.3 Stratigraphy

The regional stratigraphy of Lower Paleozoic section is generally continuous, but the Devonian and overlying sections show more localized depositional systems. (Fig 40).

The Paleozoic of the Berkine basin is characterized by a succession of transgressive and regressive second-order cycles whose mega-sequences are composed of extensive sandstone deposits mainly of fluvial and fluvial-deltaic origin interbedded with intervals of marine clay.

These cycles are delimited by regional discordances (Infra-Tassilian Discordance, Intra-Arenig Discordance, Hirnantian Glacial Erosion Surface, Caledonian Discordance, Frasnian Base). They all include a transgression peak associated with the regional development of offshore clays, locally anoxic and acting as cover and / or Source Rocks. Continental Triassic deposits cover the Paleozoic wedges and constitute the best reservoir in the Basin. They are surmounted by an excellent evaporite cover of Triassic and Liasic age. (Alnaft)

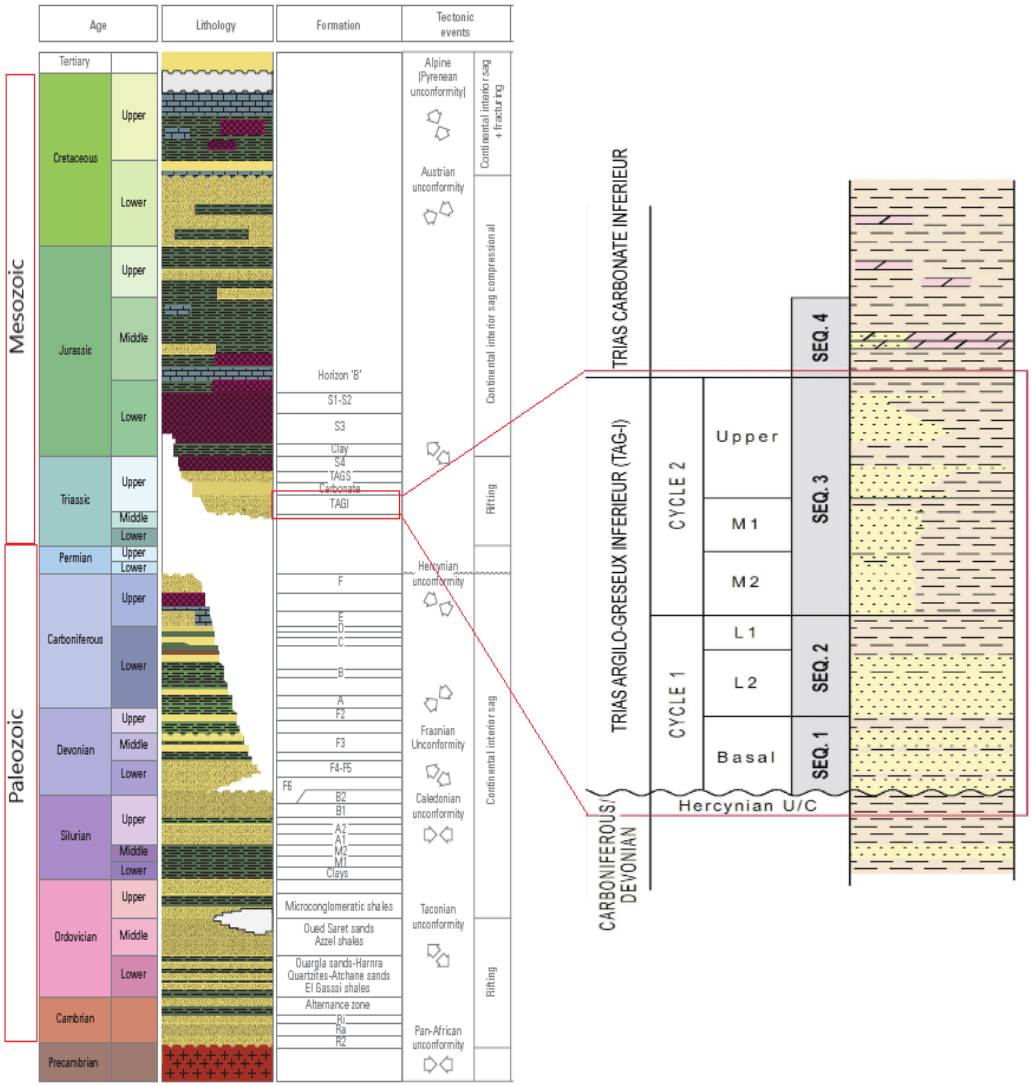

Figure 40. Generalized stratigraphy of the Berkine Basin and the different units of the TAGI. Turner et al 2001 et Schlumberger 2007

4.2 Area of study:

Our study is centered on the red section shown in the provided figure 41, which traverses both Blocks 401a and 402a of the Berkine Basin.

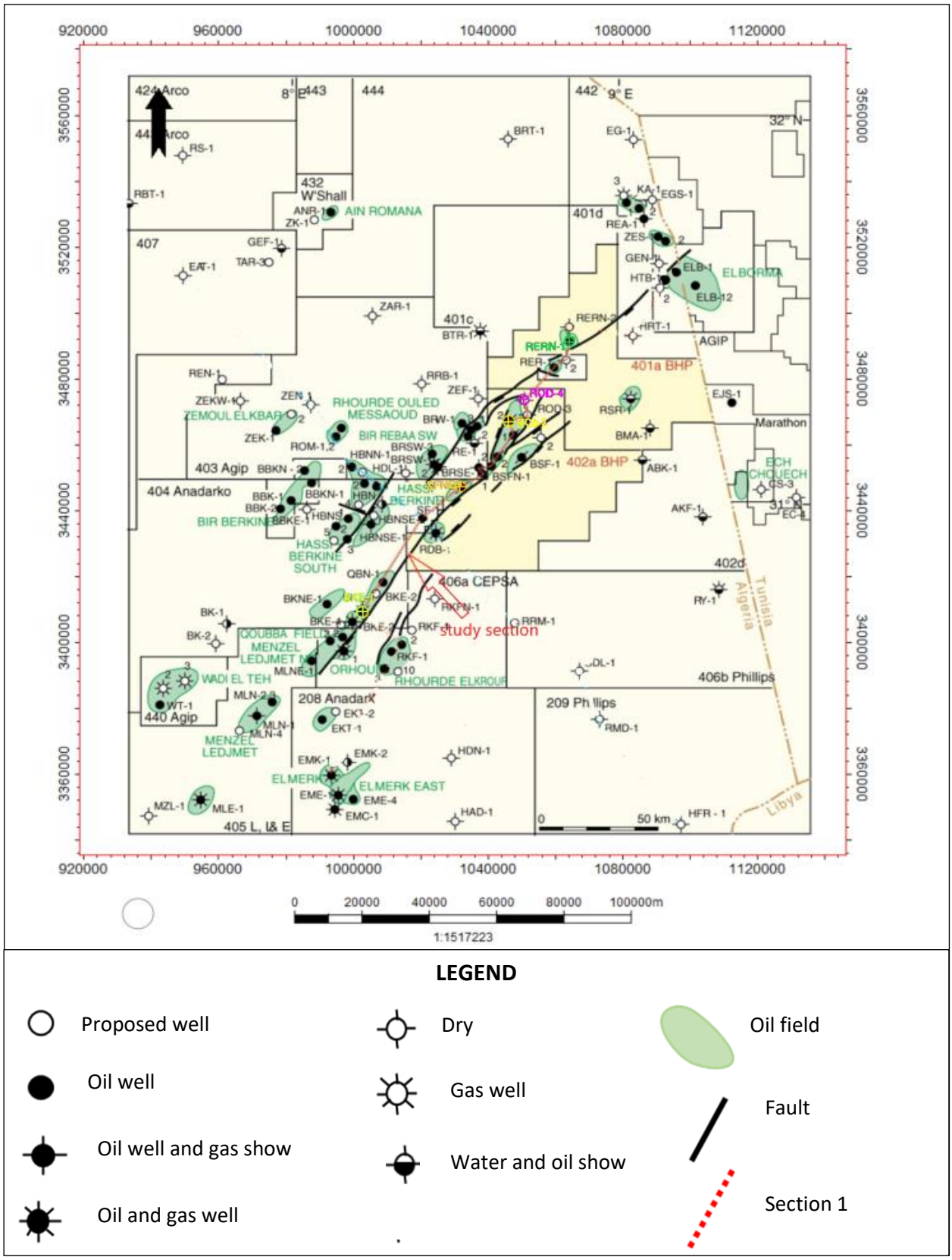

Figure 41. Location of the Blocks 401a and 402a and Hydrocarbon Accumulations in eastern part of Berkine Basin and the section of used wells for the GPM model, modified from Turner et al 2001

4.2.1 The Triassic Argilo-Gréseux Inférieur "TAGI" in the Blocks Blocks 401a and 402a

The principal hydrocarbon-bearing interval in the Berkine Basin is the "Triassic Argilo-Grèseux Inférieur" (TAGI), which in the blocks 401a and 402a is of Late Triassic age.

The TAGI rests directly on the Hercynian unconformity with a subcrop of Lower Carboniferous to Upper Devonian age in the study area. It comprises fluvio-lacustrine sediments whose style of deposition evolved through the four depositional sequences.

Triassic sandstones of the Berkine Basin in Algeria (which include the late Triassic Argilo-Gréseux Inférieur Formation, or TAGI) are a prolific hydrocarbon reservoir that is part of a SW to NE trending fluvio-lacustrine depositional system, extending eastwards from Algeria through southern Tunisia. A detailed lithostratigraphy and sedimentology of the TAGI Formation are given by Turner et al. (2001). In blocks 401a and 402, the TAGI thickness varies from 25m to 100m, where it displays lateral and vertical facies variations on a local and regional scale. it has a high net to gross ratio and is dominated by sheet flood and braided, low-sinuosity fluvial deposits, with laterally persistent sandstones and claystones. In Block 402 (which includes the ROD/BRSE/BSFN, SFNE and BSF fields), the net to gross ratio is markedly lower, typically with low thick claystone intervals.

4.2.2 Study sequence stratigraphy

In the study area, the TAGI rests unconformably on a subcrop of Carboniferous to Devonian sediments and is overlain by the Triassic Argilo Carbonaté (or Triassic Carbonates).The sedimentology of the TAGI has been described by Turner et al. (2001) to be a series of predominantly fluvio-lacustrine facies that is overlain by the estuarine to shallow marine Triassic Carbonates with a total of 23 lithofacies based on core descriptions, with the principal facies associations in the Block 402 area consisting of fluvial channel sandstones, floodplain siltstones and palaeosols, crevasse splay deposits, lacustrine sediments and shallow marine transgressive deposits (fig 43) . Regionally, the internal lithostratigraphy of the TAGI is complicated, although locally it can be layer cake in nature. While the apparent complexity is, in part, inherent in a fluvial system with a wide variety of facies associations, it is exaggerated in the case of the TAGI due to the lack of a regional stratigraphic template into which more localised schemes can be placed. Licences and field areas shown in figure 1 are operated by a number of different oil companies each having its preferred stratigraphic framework that has been internally devised. This makes stratigraphic comparisons between blocks difficult.

Turner et al. (2001) presented a semi-regional correlation of the TAGI based on core descriptions, mineralogical data and wireline log responses. They demonstrated that the TAGI thickens and becomes sandier to the SW, identifying four depositional sequences associated with the TAGI and the overlying basal Triassic Argilo-Carbonaté (also known as the Lower Carbonaté).

These four depositional sequences reflect variations in depositional style resulting from base level shifts, tectonics, and climate changes during the TAGI period. The overall increase in relative sea level was interrupted by periods of incision, likely related to rifting and erosion of the rift shoulders of the Berkine Basin. The TAGI unconformably overlays Palaeozoic

basement rocks and, together with the basal Lower Carbonate, comprises a megasequence that is variable both laterally and vertically and that can be separated into 4 sequences.

The initial valley fill (Sequence 1) was deposited under relatively arid or semi-arid conditions, forming an unconformity-bounded, ephemeral fluvial interval that fills the palaeorelief on the Hercynian unconformity surface. This fluvial package, bounded by unconformities or disconformities, infills the inherited palaeorelief on the Hercynian unconformity. The upper boundary of Sequence 1 is marked by a regional disconformity, indicating a probable hiatus. In the study area, the thickness of this sequence varies significantly, ranging from 8 meters to 25 meters, reflecting the influence of pre-existing topographic variations.

During Sequence 2 and 3, perennial fluvial systems with anastomosed channels and floodplain lakes became dominant and the climate increasingly humid. At this time a major longitudinal drainage, divide developed due to intrabasinal rifting. sequence 2 comprises an initially upward-fining, and subsequently upward-coarsening package of perennial fluvial sandstones and floodbasin shales with thin crevasse splay elements and interfluve palaeosols. The thickness of this sequence ranges between 25m and 30m in the study area.

Sequence 3 (TAGI) This erosive-based, fluvio-lacustrine sequence is dominated by channel sediments with associated crevasse sandstones and floodplain/lacustrine shales. The top of the sequence is interpreted as a marine transgressive surface of erosion (TSE), formed in response to a marine transgression from the NE. This sequence is the main hydrocarbon reservoir section and is divided into two main packages 3A and 3B; the base of 3B is distinguished by basin-wide fluvial incision and the widespread channel sand deposition. The thickness of this sequence ranges between 33m and 50m in the study area.

Sequence 4 (Lower Carbonate) is a coastal plain and shallow marine system consists of green and grey dolomitic shales, claystones and siltstones, interbedded with dolomite and occasional estuarine sandstones as well as sabkha-type evaporites. The base of the sequence is characterised by a thin transgressive lag of bone fragments and shell debris, and is overlain by occasionally fossiliferous claystones interpreted as a flooding surface, which is a part of a transgressive system tract. The sequence top is picked at a unit informally known as the “Double Dolomite” which represents the maximum flooding surface in the area. The thickness of this sequence ranges between 20m and 37m in the study area.

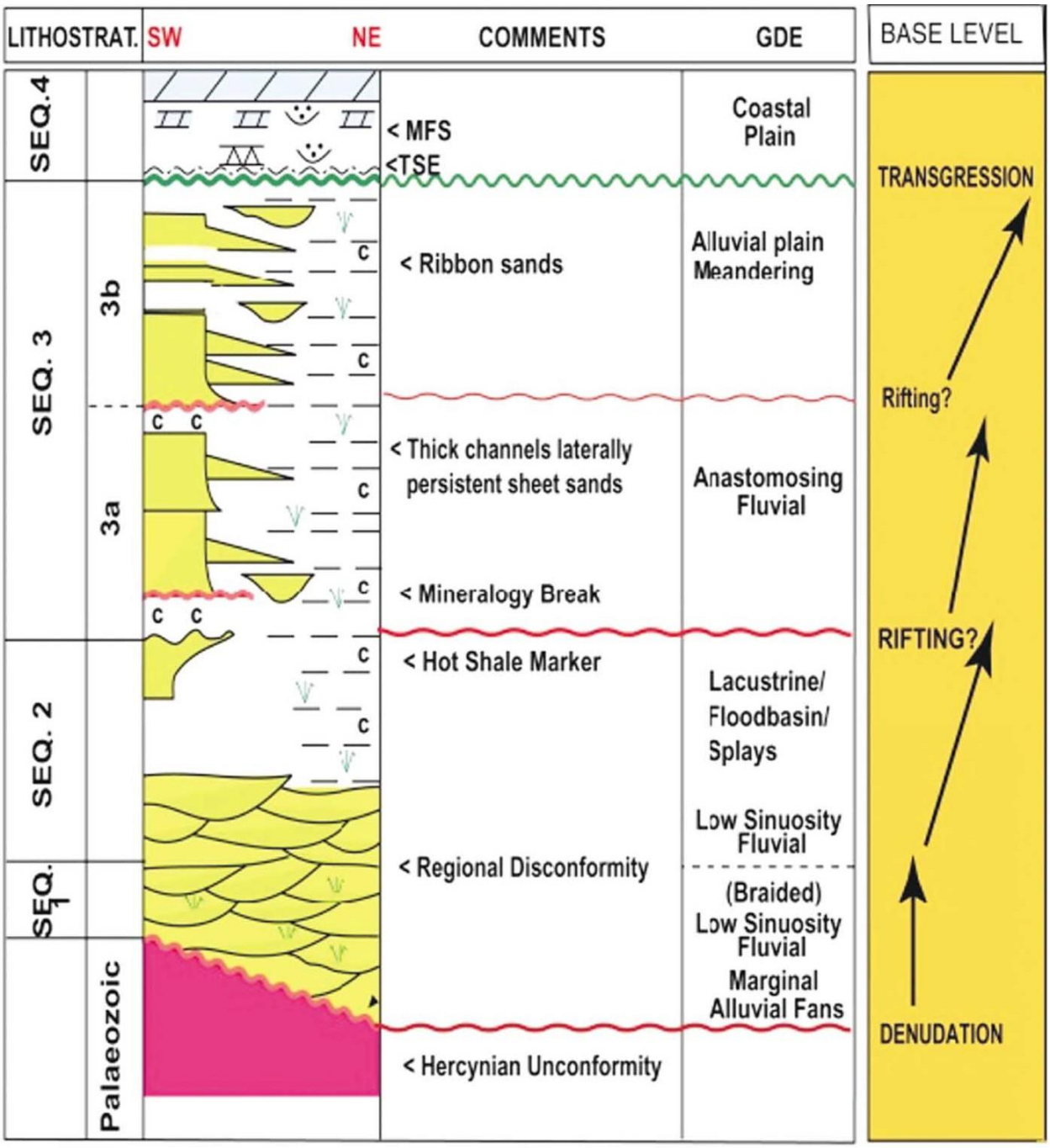

Figure 42. Sequence stratigraphy of the TAGI based on Blocks 401a and 402a Turner et al (2001)

4.3 Data preparation and experiments

To have a better understanding of the subsurface, we integrated the available data into Petrel software. This data mainly included well logs with the gamma ray log accessible for the correlation of all wells. The geological background served as soft data, with the technical report and findings from P. Turner et al in the article « Sequence stratigraphy and sedimentology of the late Triassic TAGI (Blocks 401/402, Berkine Basin, Algeria) », being crucial for understanding the sedimentary sequences and their organization in our study area.

the project was set to UTM84-31N coordinate reference system CRS and six representative wells were selected (BKE-1 SFNE-1 ROD-2 ROD-4 RER-1 RERN-1) oriented in the SW-NE direction.

4.3.1 Importing data for the initialization of the simulation model

Prior to initiating any modeling, it is imperative to prepare the required data for the study area. These data have been sourced from research conducted on the TAGI reservoir comprising geological, sedimentological and geophysical data.

A number of data types can be entered into Petrel™, including points, lines, 2D and 3D grids, well data and seismic data. The data identified and included in the study are:

1. Paleogeographic maps
2. Wellheads (well location map): Surface locations and target measured depths for every well. contains information about top position, well path length, and well name
3. Well tops: Points along the path of each well, indicating the depth of each zone within the formation
4. Well logs and core data: This includes raw and interpreted data specific to Y- Formation

NOTE: Each data must be imported in a specific format that must be followed as showed in the figure 43.

Data Type	Format	Type	Template
Fault polygons	Zmap+lines(ASCII)	Polygons	Elevation time
Isochores	Zmap+grid(ASCII)	Surface	Thickness Depth
Data Type	**Format**	**Type**	**Template**
3D seismic	SEG-Y seismic data (*.*)	3D seismic	Elevation time
3D seismic interpretation	Seisworks 3D interpretation (ASCII)	Seismic horizon	Elevation Time
Data Type	**Format**	**Type**	**Template**
Wells – Well header	Well heads	Points	Well symbol
Wells – Deviation	Well path/deviation (ASCII)	Well trace	Match well trace with file name
Wells – Logs	Well logs (ASCII)	Well trace	One for each log loaded
Well tops	Petrel Well tops (ASCII)	Points	Different attributes can be displayed

Figure 43. Petrel data types with their formats, categories, and template

After creating a new project in Petrel, paleogeographic maps (see appendix) describing the development of the Berkine Basin during the TAGI and basal Lower Triassic Carbonate periods, were imported using a triangulation method. A regional correlation map showing well locations used in the study was also imported to aid well implementation. Bitmap images were added to the Input pane, and georeferencing information were specified for all maps to ensure precise spatial alignment with the project's reference projection (fig 44).

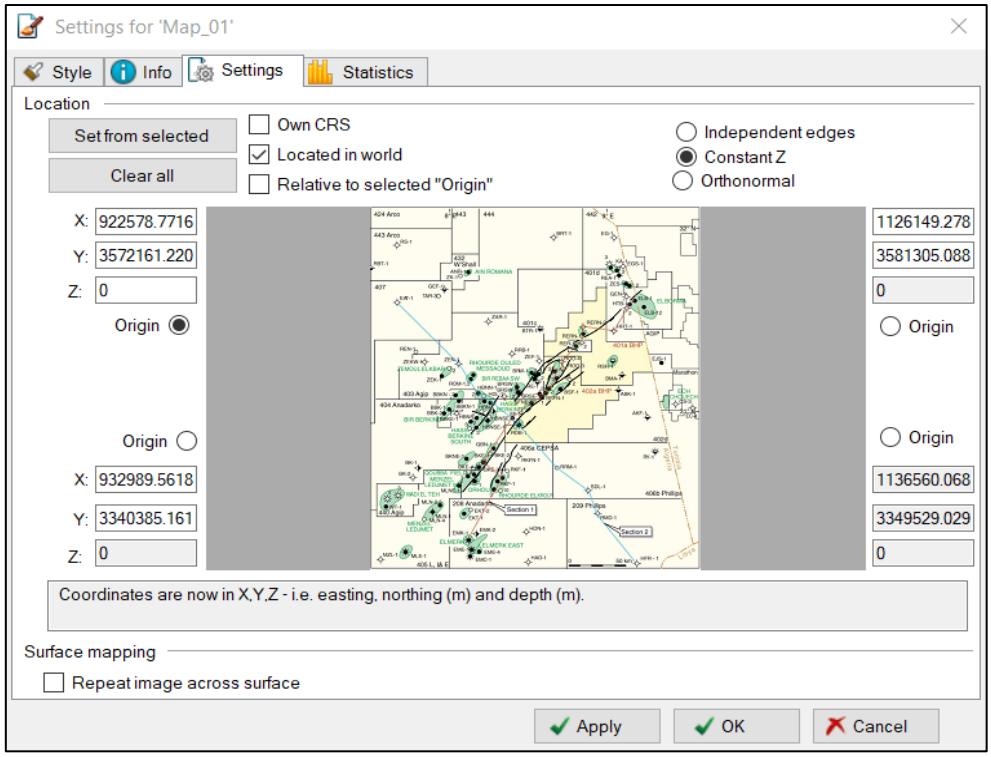

Figure 44. Map georeferencing information in PETREL

4.3.2 Implementing wells

4.3.2.1 Well heads:

The process involved plotting the position of wells, Total Measured Depth along their paths, and assigning names and symbols. This was achieved by digitalizing the wells using their coordinates in LAS format. The Coordinate Reference System (CRS) was set to UTM84-31N and configured in the General settings. The well coordinates were manually entered into the inputs pane. However, well deviation data for the paths was not available at this stage.

Well name	X-coordinate (m)	Y-coordinate (m)
BKE-1	999692.625	3412489.5
SFNE-1	1027646.5	3451458
ROD-2	1040728.63	3472344.25
ROD-4	1045208.13	3478031.5
RER-1	1053597	3489448.25
RERN-1	1057850.25	3497521

Table 3. Used wells names and coordinates

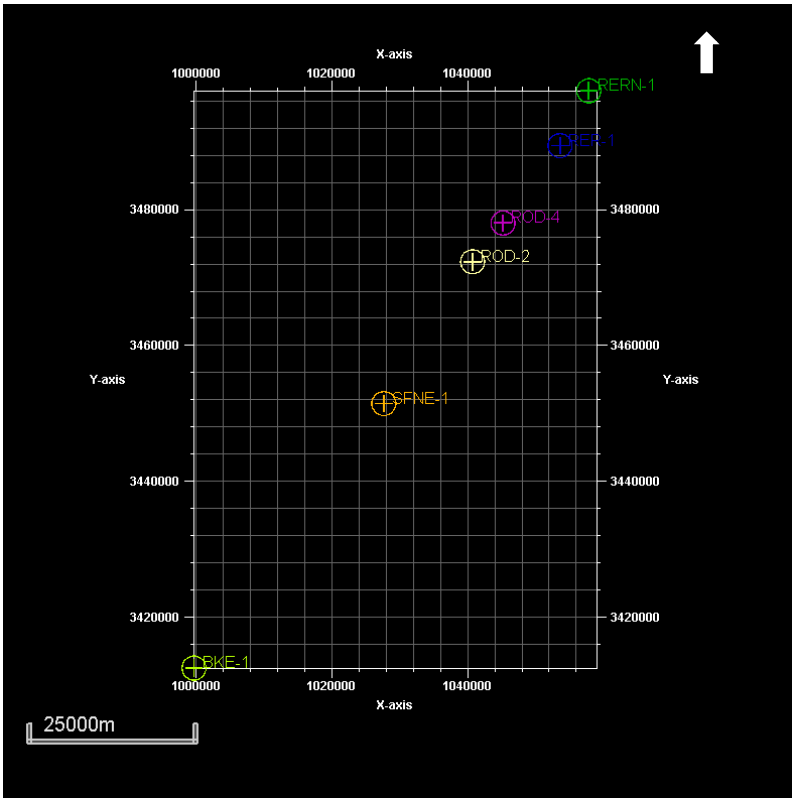

Figure 45. the location of the wells BKE-1, SFNE-1, ROD-2, ROD-4, RER-1, RERN-1 in Petrel 2D window

4.3.2.2 Establishing well tops*:*

Well tops were meticulously defined to demarcate upper and lower boundaries of the lower series, housing the reservoir, across each well's trajectory.

The identification of formation tops was possible due to the Gamma Ray log from the turner et al. 2001 article, these well tops allowed the creation of the formation zones and definition of their boundaries based on the already identified tops (fig 46).

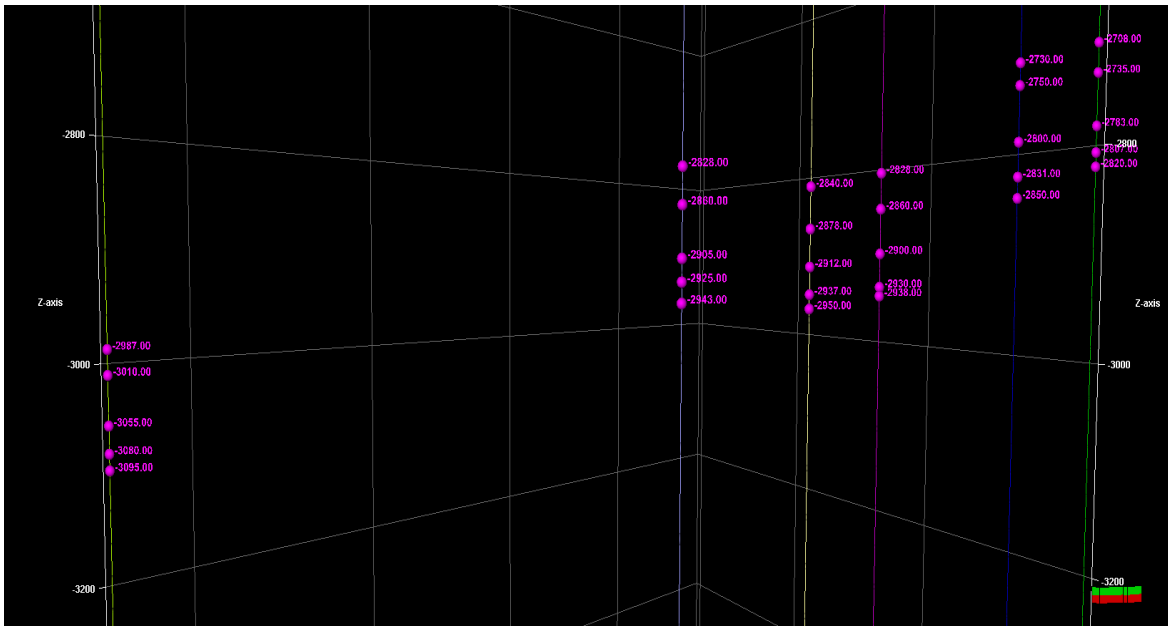

Figure 46. well tops position on studied wells representing the sequence boundaries

4.3.2.3 Surface creation:

The **Make/Edit Surface** utility in Petrel enables the construction of a surface (grid) from various types of input data (fig 47). Initially, a rectangular polygon representing the grid area was created and entered into the primary input and designated as the boundary within the Make/Edit Surfaces process. Under the Geometry tab, appropriate settings were selected, including a grid increment of 400x400 meters. The surfaces were subsequently generated (fig 49) using the convergent interpolation algorithm, ensuring accurate and reliable surface modeling based on the provided input data.

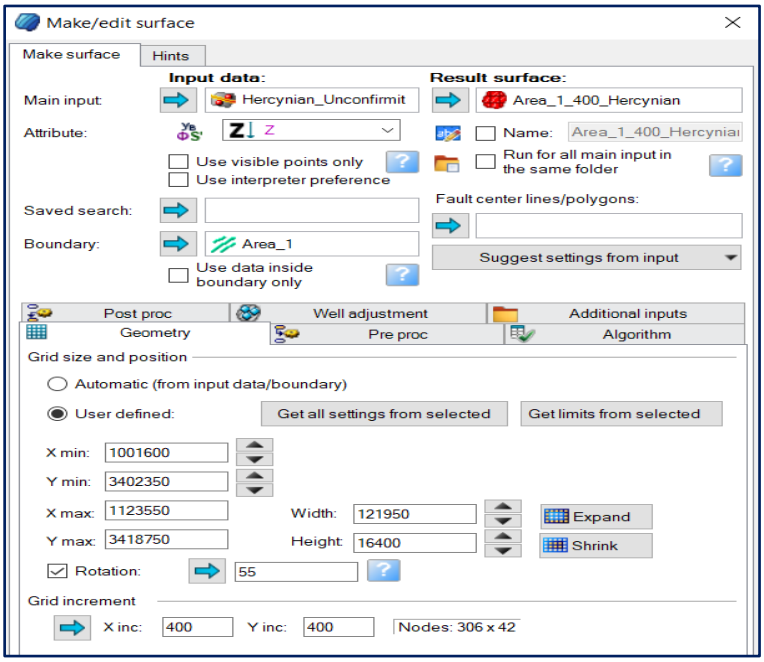

Figure 47. Make/edit Surface process in PETREL

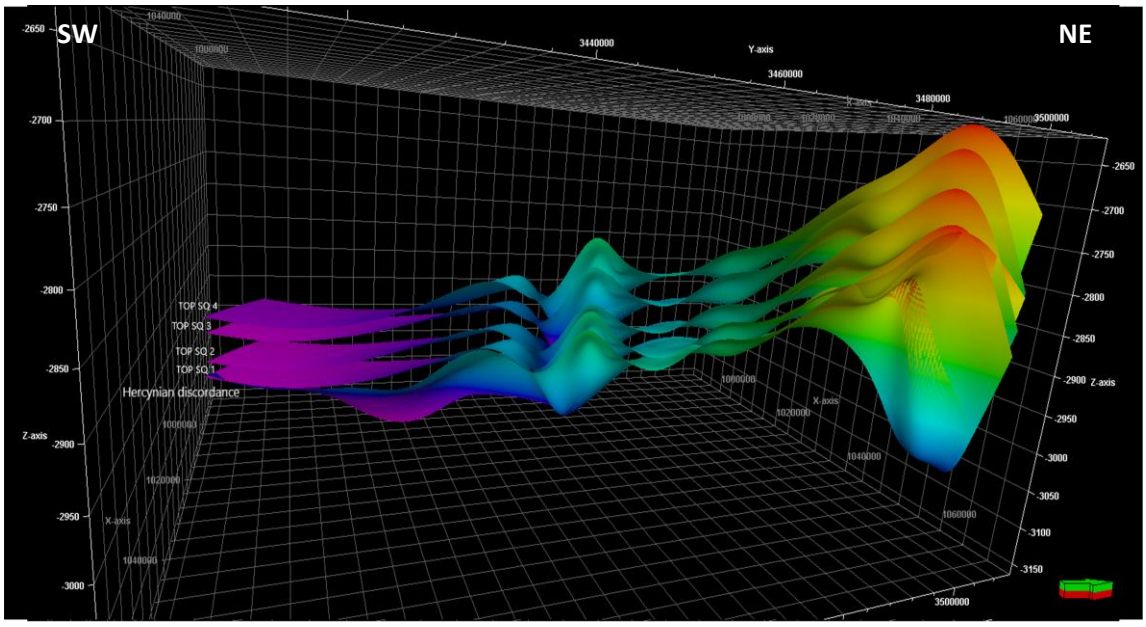

Figure 48. Surfaces corresponding to sequence boundaries

4.3.3 Well correlations:

Once data were imported, wells were correlated to visualize changes in TAGI unit thickness and responses to base level, climatic, and tectonic variations during the Triassic. The correlation along a SW-NE direction through the study area, intersecting BKE-1, SFNE-1, ROD-2, ROD-4, RER-1, and RERN-1 wells, revealed insights into the sedimentary sequences' characteristics (fig 49), the indicated color codes for different simplified facies are shown in figure 50.

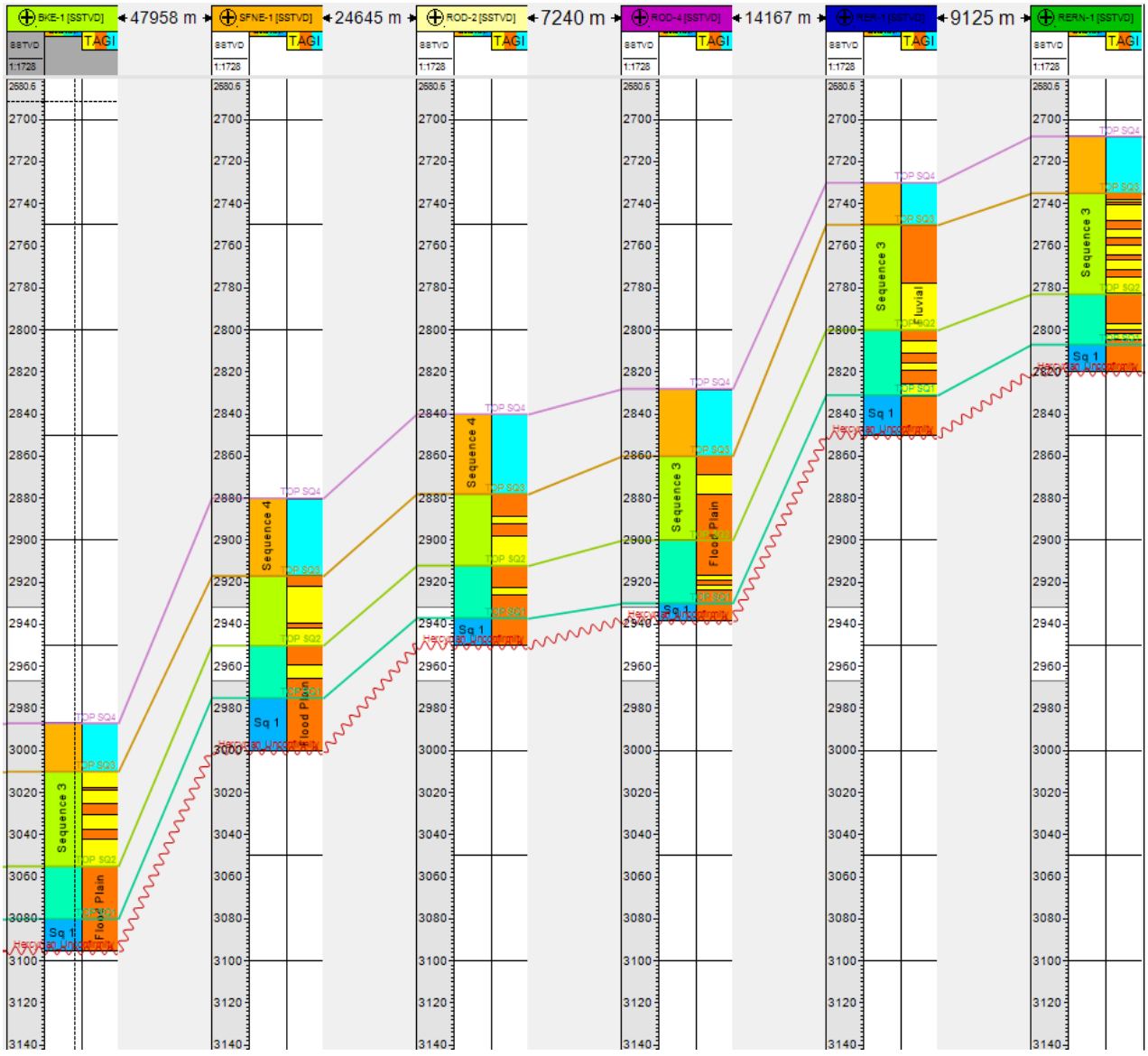

Figure 49. well correlation SW-NE through the wells (BKE-1, SFNE-1, ROD-2, ROD-4, RER-1, RERN-1)

Code	Name	Parent	Background	Lines	Pattern
0	Fluvial				
1	Flood Plain				
2	Marine Dolomite				

Figure 50. Color codes for different facies of the studied area

The correlation along the SW-NE direction through the study area, passing through the wells (BKE-1, SFNE-1, ROD-2, ROD-4, RER-1, RERN-1) with the analysis of the sequence stratigraphy column , reveals the following:
The TAGI is unconformably deposited either on the Middle-Upper Devonian formations or on the basal Carboniferous. The TAGI begins with Sequence 1, represented by fluvial sandstones filling paleovalleys inherited from Hercynian denudation (erosion). These deposits are characterized by channels sandstones; poorly sorted medium coarse kaolinitic sandstones, cross strafied sandstones and immature floodplains, indicating an arid to semi-arid continental environment with low sinuosity fluvial sandstones.

Sequence 1 has a minimum thickness of 8 meters in the central region at the ROD-4 well and shows variable thicknesses ranging from 8 to 25 meters, depending on the inherited zones of the Hercynian unconformity, where it thickens in the lower and subsiding areas corresponding to paleovalleys and thins in the higher regions.
Sequence 2 exhibits a relatively constant thickness ranging from 25m to 30m. The scarcity of fluvial sand bodies in certain areas, such as around the BKE- 1 and ROD-4 well, is also noted, with the deposition of discontinuous sandstone lenses and the presence of marker hot shales indicating the major development of lacustrine and floodplain conditions in this region.

Sequence 3 is characterized by the deposition of clay interbedded with lenticular sandstones, showing reduced thickness in the central part at the SFNE-1, ROD-2, and ROD-4 wells with a minimal thickness of 33m, and thickening towards the SW near the BKE-1 well and the NE around the RER-1 and RERN-1 wells until it reached the maximal value of 50m.
The basal part of Sequence 3 displays thick channels indicative of an anastomosing fluvial environment, while the upper part consists of ribbon sands from a meandering alluvial plain.

The lower clay-sandstone Triassic is overlaid by a clay-carbonate cover that thickens in the center ROD-2 (37m) SFNE-1 (36m) and thins towards the SW and NE and represented by sequence 4

The presence of paleovalleys during the Triassic, particularly in Sequences 1, 2, and 3, has facilitated the development of fluvial-origin sandstone lenses, which constitute potential reservoirs for hydrocarbon accumulation in the Berkine Basin. Indeed, numerous significant hydrocarbon accumulations were identified during the 1990s and 2000s, such as the Hassi berkine south, ourhoud, el merk, Hassi messaoud fields. Frequently, in the Berkine Basin and the study region, these accumulations are aligned along structural axes and major faults-oriented SW-NE (see fig 49).

4.4 Model building:

The objective is to develop a detailed model capturing vertical and lateral heterogeneity at a regional scale to replicate the stratigraphic sequence based on field observations such as rock samples, well-log responses, and publications. The spatial extent covers a rectangle of 168.4 km x 4.4 km, with a grid increment of 400 x 400 meters, spanning 5 million years from 252 to 247 million years before present, with outputs specified every 50,000 years, resulting in 100 layers.

4.4.1 Initial topography:

Initially, a rectangular polygon representing the grid area, covering an area of 168,400 x 4,400 square meters, was created and entered into the primary input area (fig 51). This polygon served as the main input and boundary in the Make/Edit Surfaces process to generate the desired surface. Under the Geometry tab, appropriate settings were selected, including a grid increment of 400 x 400 meters and a rotation of 50 degrees. The surface was subsequently generated using the convergent interpolation algorithm.

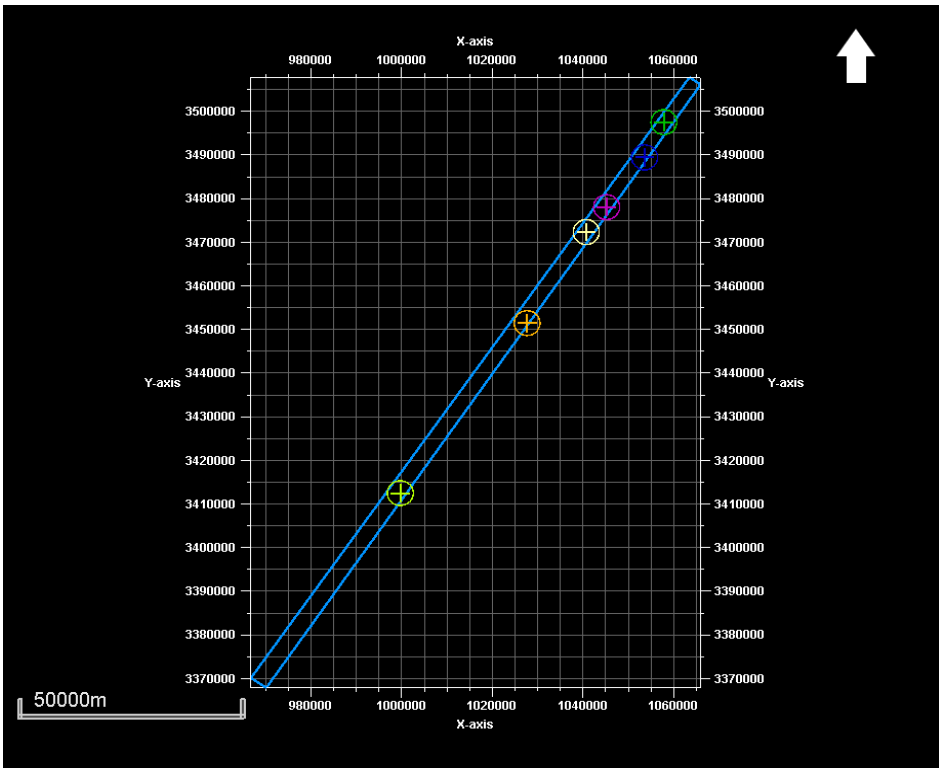

Figure 51. Study area polygon in 2D window

Well data from Turner et al. (2001) were used within Petrel to construct a stratigraphic framework, with digitized and georeferenced well correlations matched to the well data. In the absence of seismic depth profile data, paleo-topography was approximated using well markers for ground-truth validation

The entire surface was elevated to paleo-sea level at the age of deposition, correcting for an estimated total subsidence of 110 meters, assuming minimal deformation events in the TAGI-I reservoir.

The topography was iteratively refined in the topography editor (fig 52), adjusting the basin area to -50 meters to align with the sea level during the initial deposition period (252 million years ago). The slope area of the topography was extrapolated southwest, following the sediment supply trajectory and incorporating exaggerated uplift to facilitate sediment supply into the basin, creating accommodation space for sediment deposition.

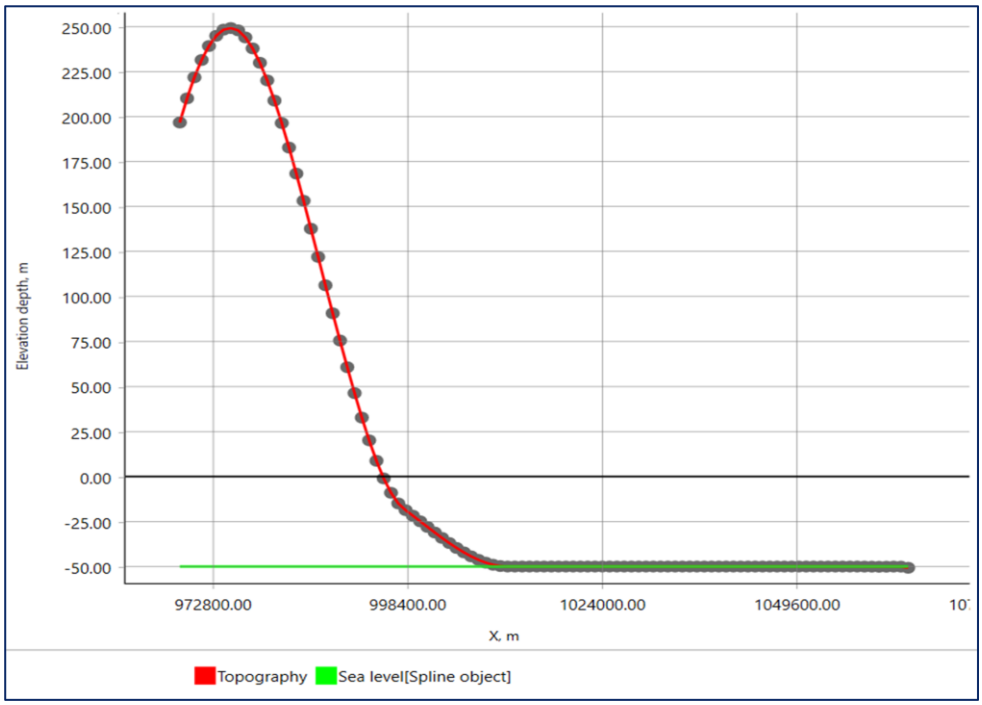

Figure 52. Base model topography elevation variations in the topography editor

4.4.2 Sea level:

For this simulation, the pre-existing Exxon global sea-level curve was chosen due to its comprehensive coverage of the requisite geological period for our study. This stratigraphic curve presents age in millions of years alongside sea level in meters (fig 53).

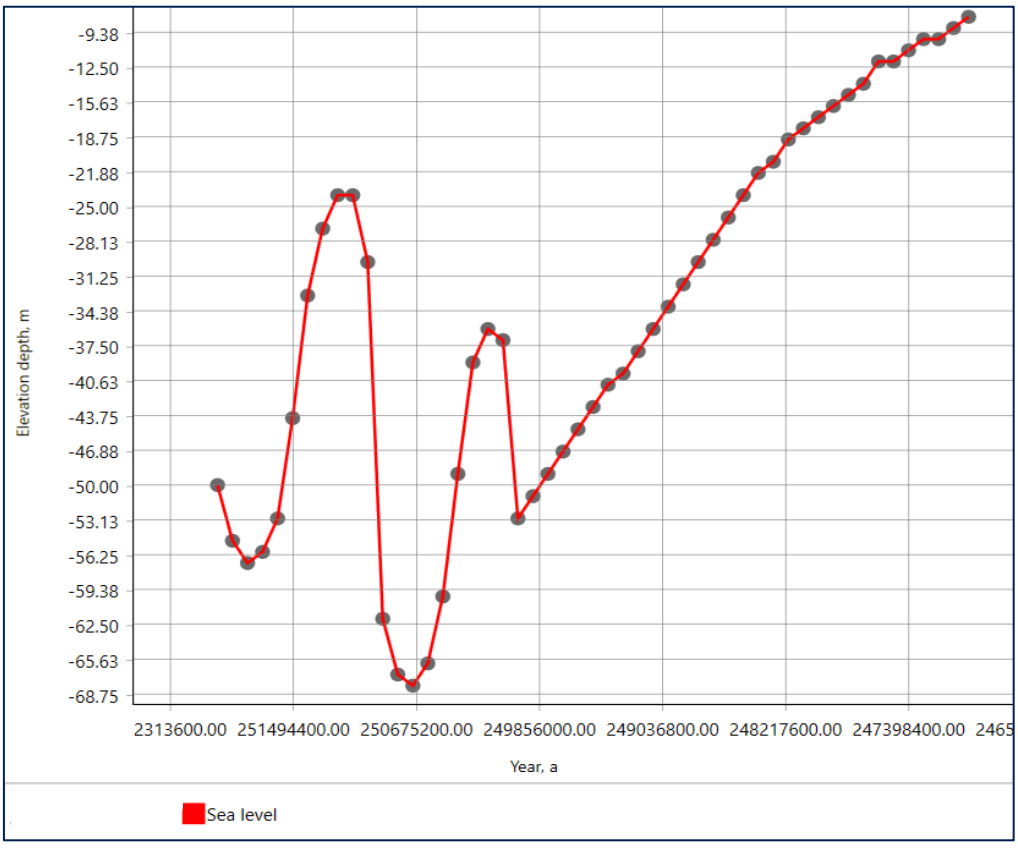

Figure 53. Exxon global sea-level curve of the simulation interval in GPM software

4.4.3 Sediment types:

Based on our geological understanding of the region, we classified five sediment types: fine sand, coarse sand, silt, shale, and dolomites (table 4). The fractions of each sediment type were determined using data from previous well correlations (fig 54).

Lithology	Grain Properties		
	Diameter (mm)	Density (g/cm^3)	Transportability
Coarse Sand	1	2.7	0.8
Fine Sand	0.5	2.65	1.6
Silt	0.01	2.6	3.2
Clay	0.02	2.55	6.4
Dolomites	0.001	2.8	6.4

Table 4. Sediment types and properties

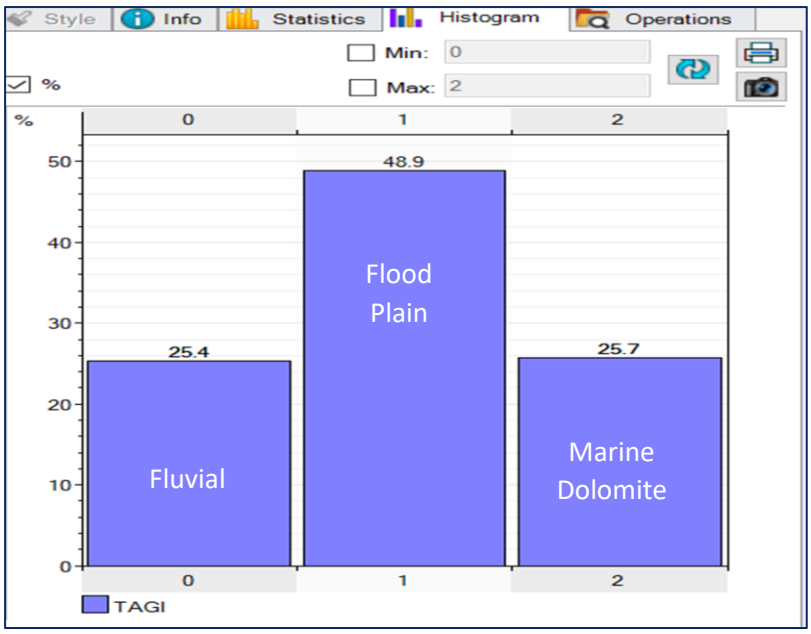

Figure 54. Sediment proportions and corresponding code names

GPM sediment accumulation was used to reproduce the dolomitic interval of sequence 4 to produce vertical thickness of uniform lithology as interpreted from well and outcrop data. The areal input rates for each sediment type (coarse-grained, fine-grained sediments) use the value of the map (topographic surface) at each cell in the model and multiply it by a value from a unitless curve at each time step in the simulation to estimate the thickness of sediments accumulated or eroded from a cell to another. In doing so, the accumulation process accounts for the different sediments involved in the simulation.

This approach ensures that the accumulation process within the simulation accurately reflects the diverse sedimentary compositions involved. By accounting for the unique characteristics of each sediment type and their distribution across the model grid, the simulation achieves a nuanced representation of sediment dynamics, including deposition and erosion processes.

Consequently, for each time increment, the accommodation space resulting from subsidence was progressively filled with sediment. Sediment input rate curves were designed to account for specific geological events, notably the deposition of 40 meters of dolomites between 247 million years ago (Ma) and 246 Ma, corresponding to an average sedimentation rate of 0.4 millimeters per annum (mm/a).

4.4.4 Tectonics:

To simulate the deposition of the lower TAGI formation within the studied area, it was imperative to create an accommodation space of approximately 110 meters by uplift and incision associated with Triassic rifting using tectonic maps (fig 55). As well as subsidence movements achieved by incorporating an average subsidence rate of 0.02 to 0.03 millimeters per annum (mm/a) into the modeling framework (figure 56).

Regarding the uplift rate, it was iteratively refined to achieve an optimal outcome. The uplift rates utilized in the model are presented in the table 5.

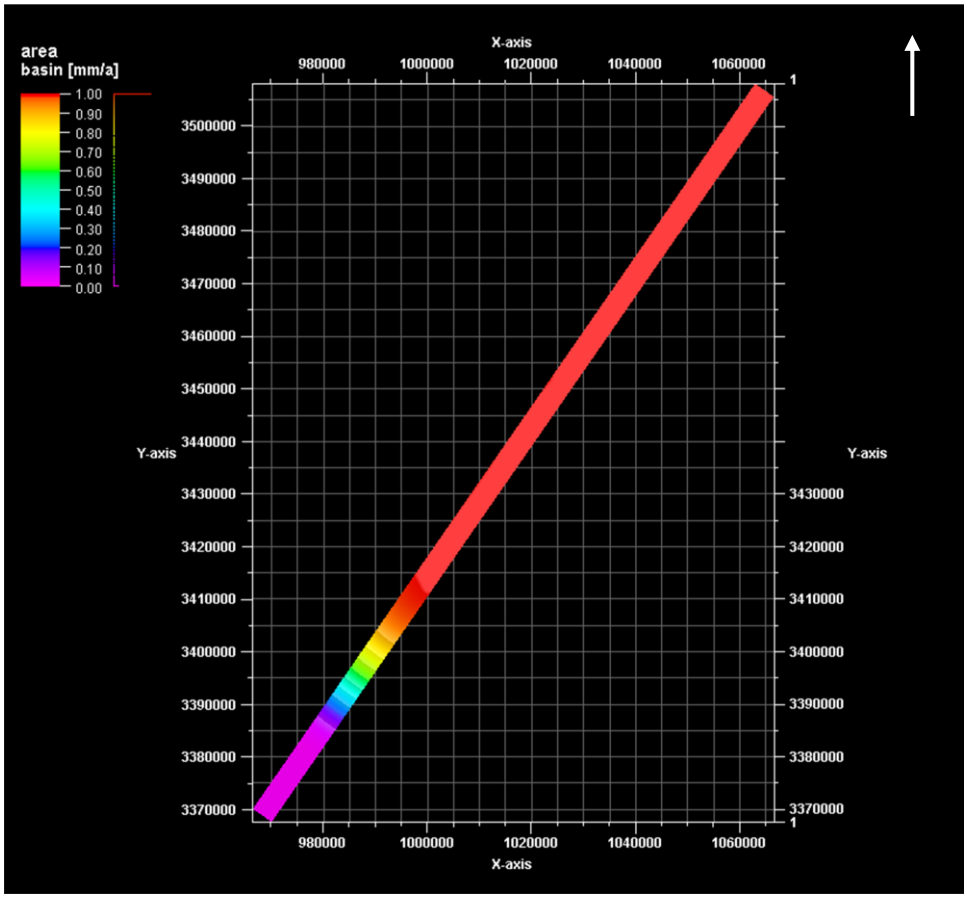

Figure 55. subsidence map rates in mm/a

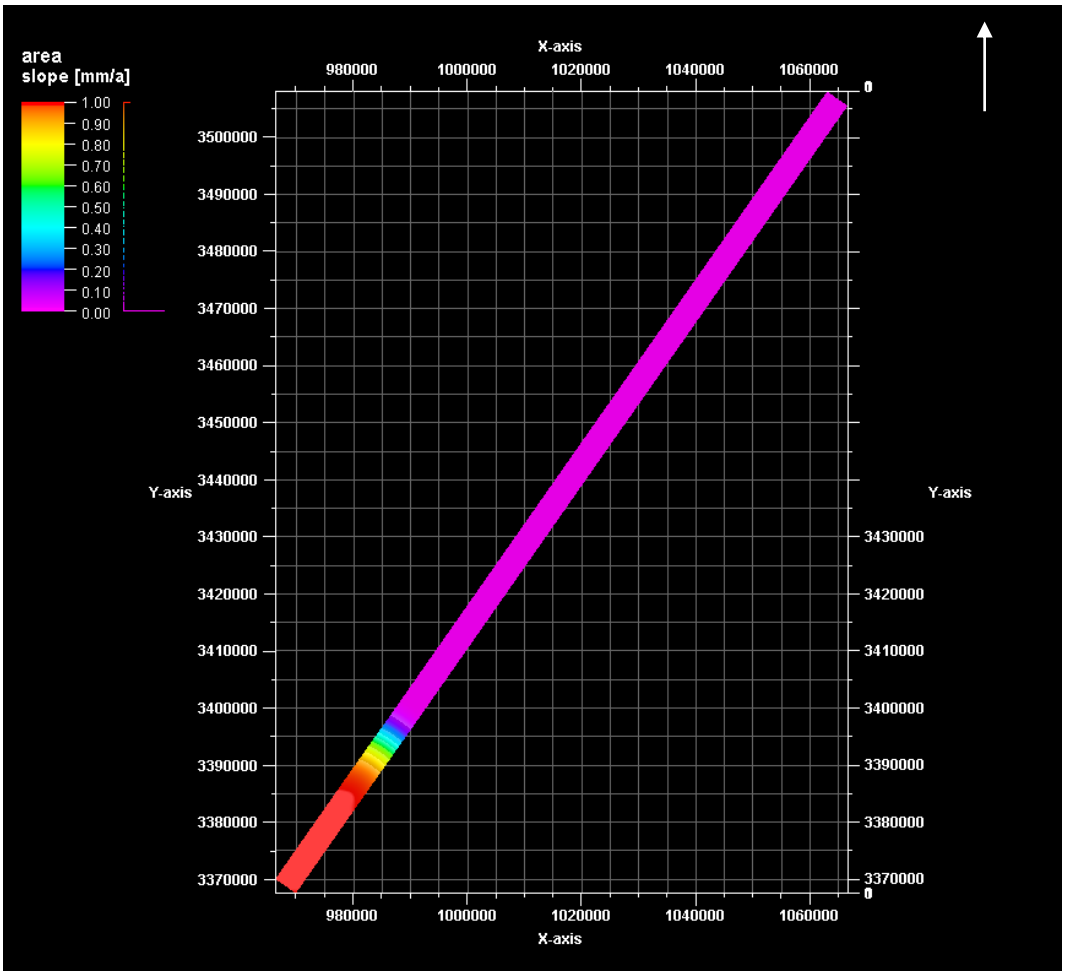

Figure 56. Uplift event map rates in mm/a

X, a	Value
247000000.00	0.0300
248500000.00	0.0300
250750000.00	0.0200
252000000.00	0.0200

Table 5. Tectonic rates along geological times

Sediment diffusion: A varying diffusion coefficient, expressed in square meters per year (m^2/year), was employed to regulate the strength and intensity of diffusion processes as required. The values of this coefficient across different time periods are presented in the table below. Additionally, a dimensionless diffusion function was utilized to illustrate how diffusion varies with elevation and depth.

The diffusion function (fig 57) exhibits high values above sea level due to enhanced weathering effects. It reaches very high values near sea level, influenced by wave actions and storm activities. Conversely, it shows low values below sea level, corresponding to a lower energy environment.
This function was iteratively adjusted to accurately replicate observed sediment volumes, as well as the slopes and shapes of clinoforms observed real data.

X, a	Value, m2/a
247000000000000.00	10.00
248500000000000.00	20.00
250000000000000.00	20.00
251500000000000.00	10.00
252000000000000.00	10.00

Table 6. Sediment diffusion values in m2/y

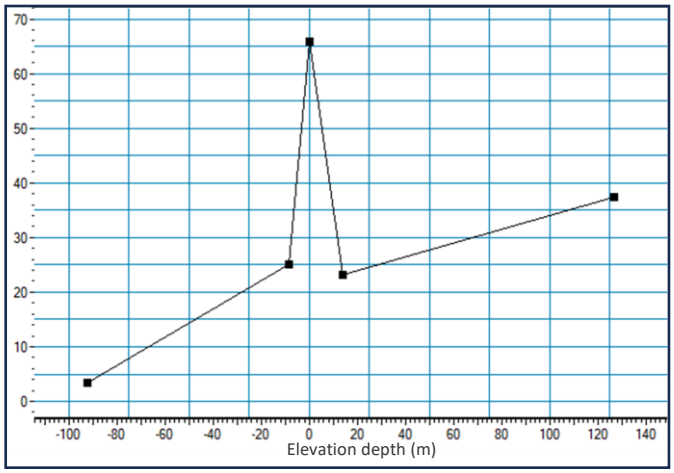

Figure 57. Diffusion function

4.5 Simulation result and discussion

The previously employed trimming process was applied to the base model to appropriately adjust the simulations in the right position and age. Using the calculator tool, the base of the model was specified to be the Hercynian discontinuity surface that had been previously delineated, the resulting model is shown in the figure 58 below and the major phases are delignated in figure 59.

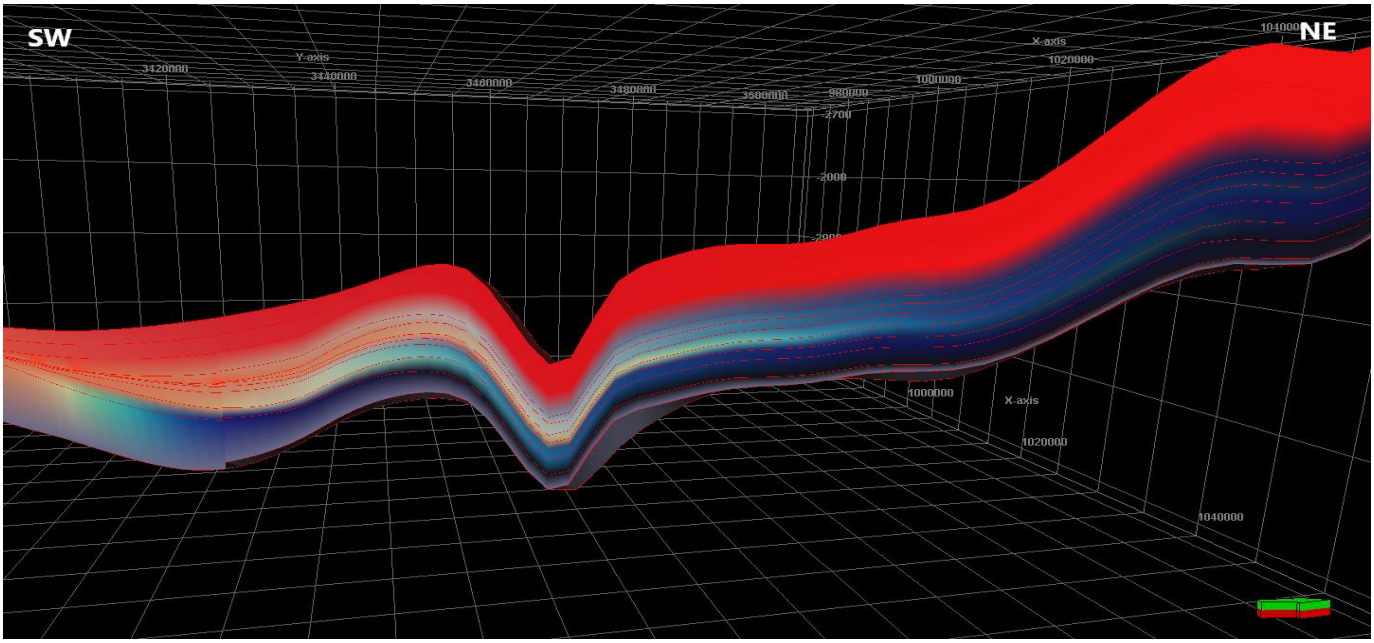

Figure 58. GPM model for the TAGI reservoir in the study area

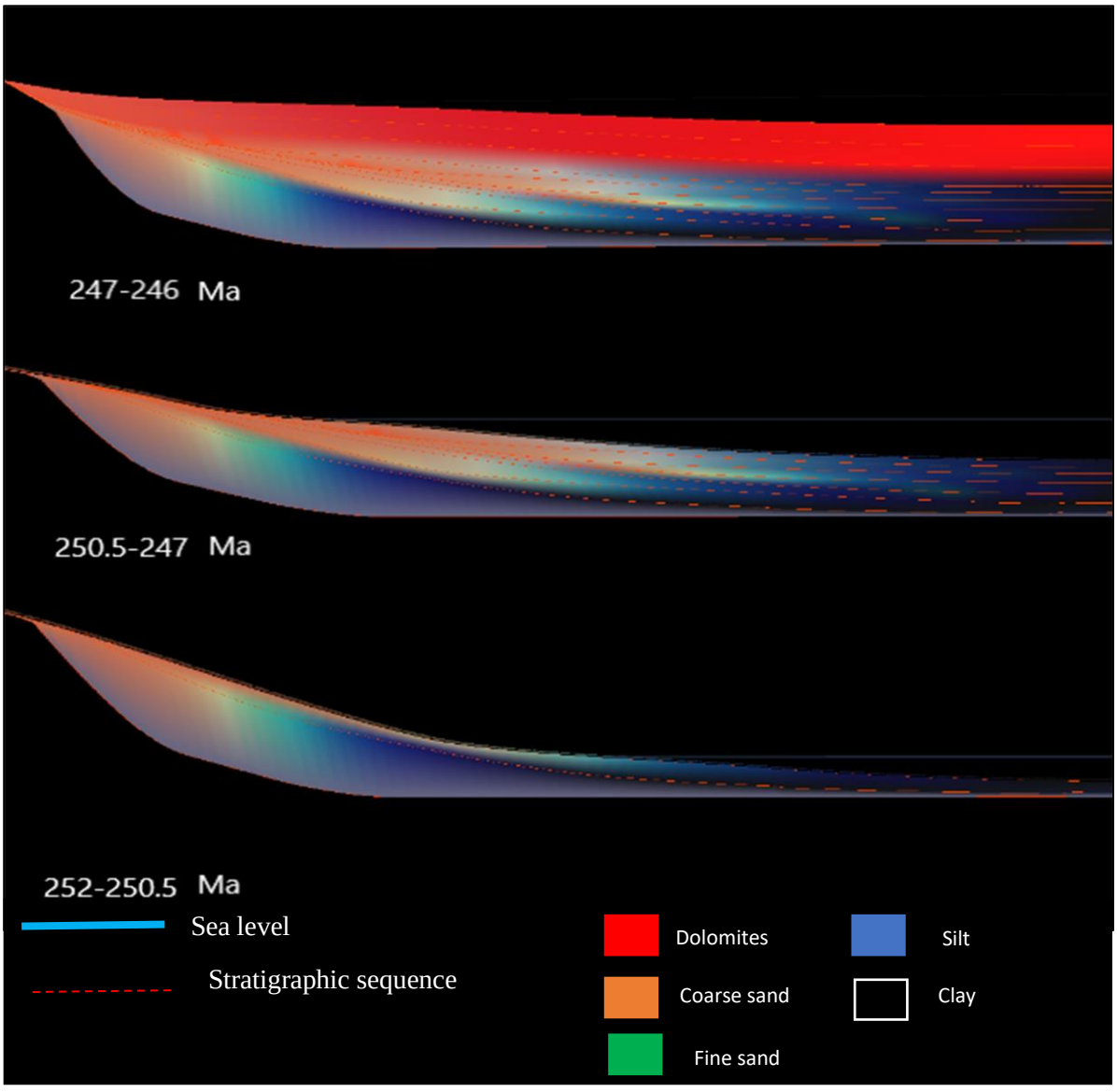

Figure 59. GPM dynamic evolution of TAGI reservoir in different time intervals

The lithologies are indirectly validated through the definition of depositional facies for each cell, based on its depositional properties. Sediments are represented by a single color if the lithology is homogenous: coarse sand (yellow), fine sand (green), silt (blue), clay (black), and dolomites (red). Mixed lithologies are represented as additive color mixtures.

252-250.5Ma:
The simulation starts with a transgression of the sea level guiding more sediments into the basin and corresponds to the filling of sequence 1 and 2;
Sequence 1 consists of well-sorted, fine- to medium-grained sandstones deposited in dynamic fluvial environments. These sandstones are frequently interbedded with clay layers, representing floodplain deposits where depositional conditions were calmer. The lithological variations within this sequence reflect depositional cycles influenced by climatic variations, base level fluctuations, and local tectonic dynamics.
Sequence 2 is predominantly composed of interbedded sandstones, siltstones, and claystones. The sandstones are generally well-sorted and fine- to medium-grained, deposited in fluvial channels and floodplains depositional environments, intercalated with siltstones and claystones.

250.5-247 Ma:
The lithology of Sequence 3 shows sandstones is fine- to medium-grained and moderately sorted deposited in deltaic to shallow marine environments interbedded with siltstones and mudstones. These layers can function as effective seals, forming stratigraphic traps for hydrocarbons., with conditions varying from moderately energetic: anastomosing channels, to calm: prodelta and shallow marine settings.

247-246 Ma:
The upper sequence (corresponds of the basal marine unit of the Triassic Lower Carbonate.) is dolomite-rich layer indicating the transgressive inundation of the Berkine Basin

Well-sorted, fine- to medium-grained sandstones form high-quality reservoirs, offering excellent porosity and permeability for hydrocarbon storage. The presence of intercalated clay and siltstone layers can act as sealing horizons for sandstone reservoirs, creating stratigraphic traps for hydrocarbons.

4.6 Experiment 2: modeling sequences separately

A second experiment was conducted by modeling geological sequences separately using Geological Process Modeling (GPM) to understand the influence of these variations. The parameters varied in this experiment are summarized in the table 7 and the resulting model is shown in figure 60:

Simulations	Base topography	Period (Ma)	Sediment contribution	Subsidence value (mm/y)
Sequence 1 and 2	Hercynian unconformity	252-250	Coarse sand 0.15 Fine sand 0.15 Clay 0.7	0.01
Sequence 3	Top of Sequence 2	250-248.5	Coarse sand 0.24 Fine sand 0.24 Clay 0.5 Dolomites 0.02	0.03
Sequence 4	Top of sequence 3	248.5-247	Coarse sand 0.025 Fine sand 0.025 Clay 0.05 Dolomites 0.9	0.03

Table 7. Input parameters for the simulation of experiment 2 with GPM

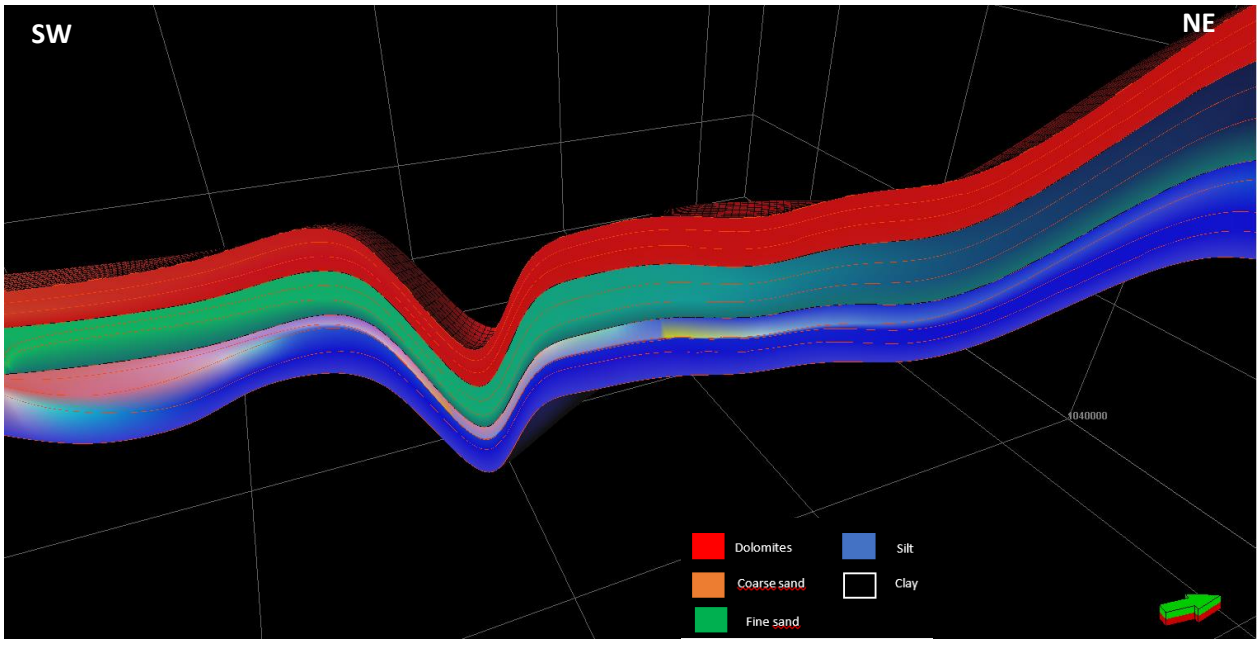

Figure 60. GPM model for the TAGI reservoir with each sequence simulated separately

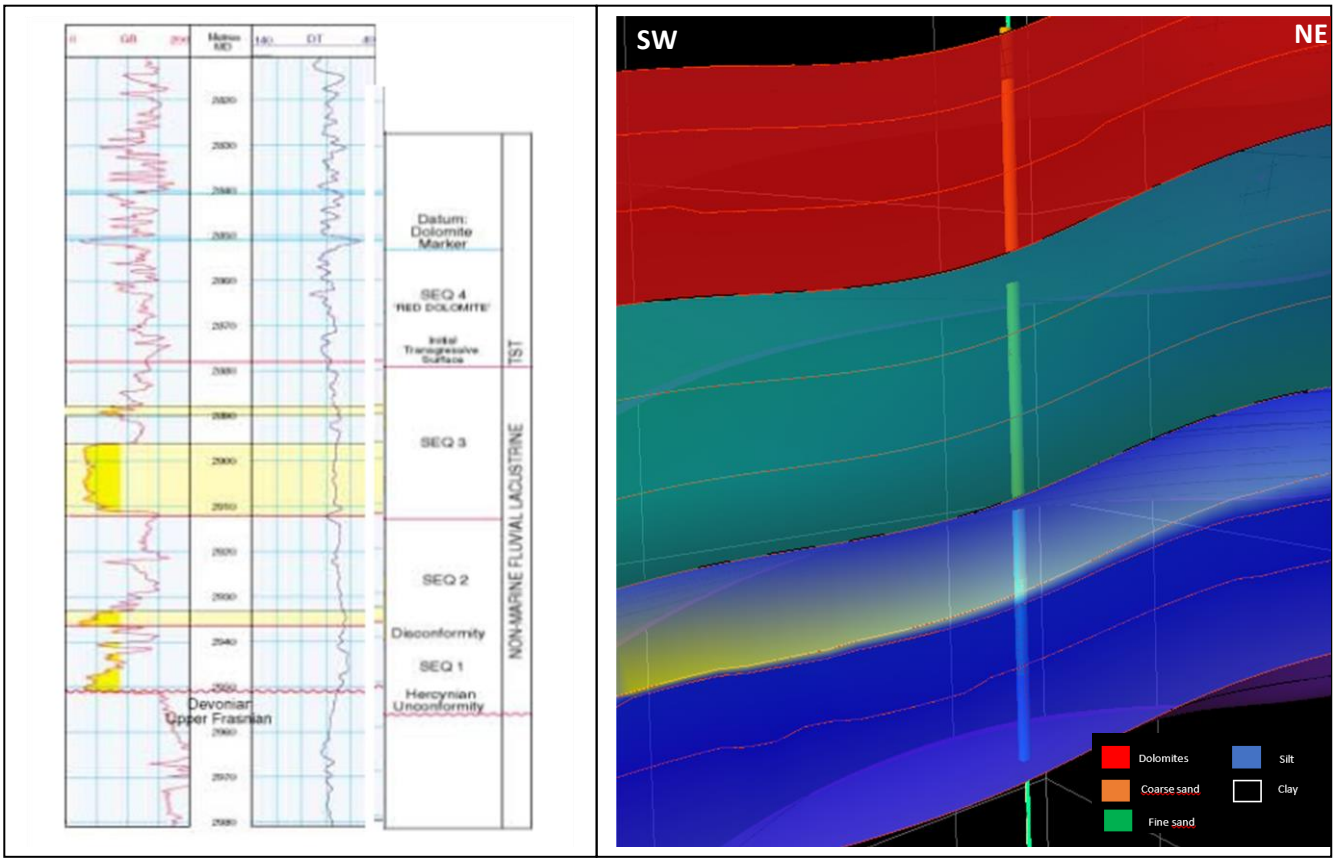

Figure 61. left: Stratigraphic column of TAGI from ROD-2 logs right: GPM model of TAGI at the level of ROD-2

The comparison between the stratigraphic column derived from the interpretation of the Gamma and DT logs (Figure 61 on the left) and the one constructed using the GPM model (on the right) shows a strong correlation in terms of lithology and the thickness of the different TAGI sequences (sequences 1, 2, and 3) as well as sequence 4, which corresponds to the lower part of the Triassic carbonate sequence.

Conducting a second experiment by modeling the geological sequences separately with GPM allows for a more nuanced and detailed analysis of sedimentary processes. By isolating the individual sequences, this approach enables the examination of specific depositional environments, their evolution over time, and the factors influencing their formation. This method offers a clearer understanding of the stratigraphic architecture and lithological variations within each sequence, facilitating the identification of patterns and trends that might be obscured in a more general model. By integrating these detailed sequence models, a comprehensive picture of the geological history can be constructed, providing valuable insights for academic research and practical applications in the upstream industry.

4.7 Conclusion

The GPM model descriptions and correlations along the SW-NE direction across the study area, including wells BKE-1, SFNE-1, ROD-2, ROD-4, RER-1, and RERN-1, reveal the following:

- TAGI begins with Sequence 1, displaying variable thicknesses (8 to 25 meters) of fluvial sandstones filling paleovalleys from Hercynian denudation.
- Sequence 2 has a more consistent thickness (25m to 30m) with significant lacustrine and floodplain development.
- Sequence 3's lower part shows thick channels from anastomosing fluvial environments, transitioning to ribbon sands from meandering alluvial plains in the upper part.
- The Triassic lower clay-sandstone is overlaid by a clay-carbonate cover, thickening in central wells and thinning towards the SW and NE, represented by sequence 4.
- The shift from coarse to fine sediments in TAGI indicates a transition from fluvial channels to floodplain sediments, influenced by the lateral heterogeneity in channel sinuosity and orientation. This sedimentary pattern suggests deposition in a fluvial environment.

The integration of GPM technology in TAGI facilitated reservoir characterization, including facies distributions and lithology variations, leading to optimized reservoir management strategies. The model identified reservoir heterogeneities and enabled predictive analyses under different production scenarios.

General conclusion & Recommendations

5 General conclusion

The simulations resulting from an extensive literature review combined with Geological Process Modeling (GPM) software using the diffusion process alone enabled us to accurately reconstruct the siliciclastic deposits known in the study region. These simulations produced consistent outcomes with the primary sequences and lithology as interpreted from seismic and well logs. This methodology marks a significant advancement in the upstream industry, serving not only in reservoir modeling but also aiding exploration plans by forecasting sediment accumulation beyond the reservoir scale. An important advantage of this method is its ability to preserve stratigraphic and sedimentological relationships, enabling precise replication of physically plausible sedimentary body geometries and internal structures.

The first reference case stratigraphic model presented provides a foundational understanding of the F3 block and its evolution over geological time. It helps establish a preliminary understanding of the system's overall behavior and its response to various factors influencing sequence stratigraphic geometries, including sedimentation rates, eustatic sea levels, and synsedimentary tectonics and consequently a better evaluation of its economic interests. The model accurately captures sedimentary geometries at a third-order stratigraphic level, depicting bathymetry from shallow to deep and preserving sediment grain size distribution and revealing its sand-rich nature and potential for shallow stratigraphic and structural traps forming shallow gas pockets.

Additionally, this study introduces a GPM model for the principal hydrocarbon-bearing interval in the Berkine Basin, the "Triassic Argilo-Grèseux Inférieur" (TAGI), of Late Triassic age. The TAGI interval lies directly on the Hercynian unconformity with a subcrop of Lower Carboniferous to Upper Devonian age in the study area. The study sheds light on the basin's evolution, comprising fluvio-lacustrine sediments whose deposition style evolved across the three depositional sequences and overlaid by the basal Lower Triassic Carbonate sequence.

We conducted a second experiment by modeling geological sequences separately with GPM for a more nuanced and detailed analysis of sedimentary processes. this approach enables the examination of specific depositional environments, their evolution over time, and the factors influencing their formation. Furthermore, separate modeling helps in testing and refining hypotheses about basin evolution, sediment transport mechanisms, and facies distribution, thereby enhancing the accuracy and reliability of subsurface predictions crucial for petroleum exploration

While the GPM simulation results can be compared to seismic and well data to a certain extent, it is essential to acknowledge the uncertainties in input parameters. Fully honoring the hard data is often physically unfeasible due to these uncertainties. However, what remains crucial is ensuring that the processes and results remain geologically consistent and plausible. Improved input data and refinement of simulation parameters are expected to enhance the model's resolution and accuracy in future iterations.

The project can be accessed via the following link: https://doi.org/10.7910/DVN/2ADETF

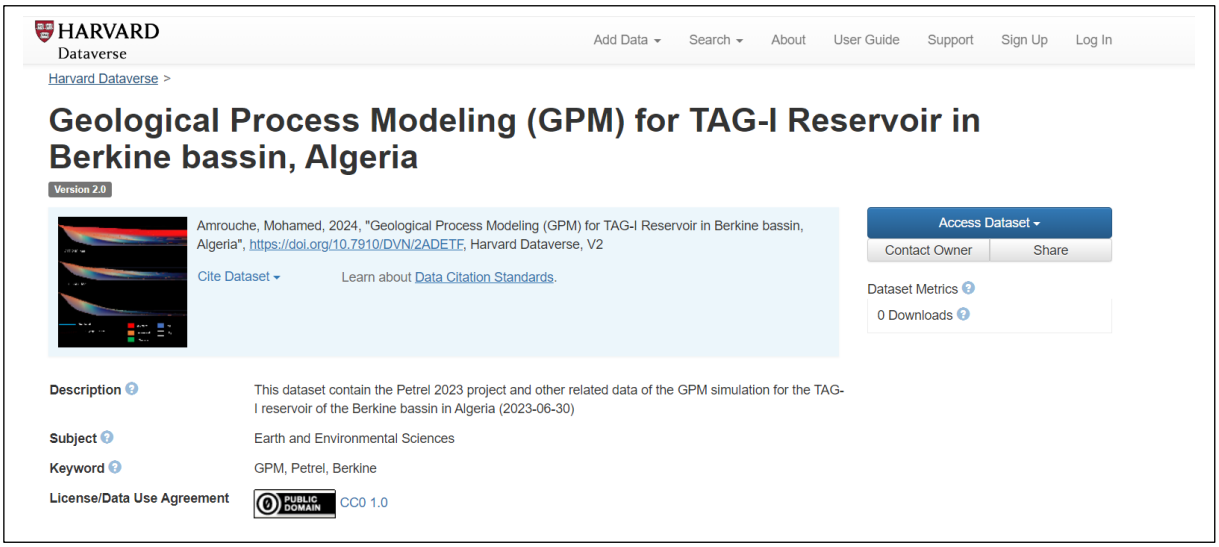

5.1 Recommendations:

1. The projects have been made publicly accessible (via the following link: https://doi.org/10.7910/DVN/2ADETF or QR code below) to facilate further refinements through including additional data from the region and integrating seismic data.
2. Incorporate water flow velocity to drive sediment movement and simulate the dynamics of channels and rivers using the steady flow process in Geological Process Modeling (GPM) for both study cases.
3. Utilize the unsteady flow process to account for turbidite events during the delta progradation of the F3 block.
4. These findings can serve as inputs for geostatistical models aimed at reservoir characterization, facilitating quantitative predictions for reservoir connectivity, porosity, and broader play definitions.

References

Alnaft.dz, saharan-domain https://www.alnaft.dz/en/842/saharan-domain

Ben Habel, W., & Dubey, S. (2022, mars 18). Towards a Multidisciplinary Approach in Play Characterisation: An Integrated Case Study from Browse Basin, NW Shelf, Australia. Day 2 Wed, March 23, 2022.

Burgess, P. M. (2012). A brief review of developments in stratigraphic forward modelling, 2000–2009. Phanerozoic Regional Geology of the World, 378-404.

Christ, Alina-Berenice & Schenk, Oliver & Salomonsen, Per. (2016). Using Stratigraphic Forward Modeling to Model the Brookian Sequence of the Alaska North Slope.

Courtade, S. F., Warren, C., Salomonsen, P., & Tveiten, J. (2017, juin 12). Use of Stratigraphic Modelling for Prediction of Reservoir Continuity in Coastal Environments. Proceedings.

Daniel M. Tetzlaff. (1986). Computer Simulation Model of Clastic Sedimentary Processes : ABSTRACT. AAPG Bulletin, 70.

Daniel Tetzlaff, W. G. (2001). FROM ACADEMIA TO INDUSTRY. Texaco, Houston, Texas US.

Dashtgard, S. E., White, R. O., Butler, K. E., & Gingras, M. K. (2007). Effects of relative sea level change on the depositional character of an embayed beach, Bay of Fundy, Canada. Marine Geology, 239(3-4), 143-161.

Eva K. Halland, The Norwegian North Sea Eva K. Halland

Galeazzi, S., Point, O., Haddadi, N., Mather, J., & Druesne, D. (2010). Regional geology and petroleum systems of the Illizi–Berkine area of the Algerian Saharan Platform : An overview. Marine and Petroleum Geology, 27(1), 143-178.

Kröner, A., & Stern, R. J. (2005). AFRICA | Pan-African Orogeny. Encyclopedia of Geology, 1-12.

Liechoscki de Paula Faria, D., Tadeu dos Reis, A., & Gomes de Souza, O. (2017). Three-dimensional stratigraphic-sedimentological forward modeling of an Aptian carbonate reservoir deposited during the sag stage in the Santos basin, Brazil. Marine and Petroleum Geology, 88, 676-695.

Liner, C. L. (2016). Elements of 3D Seismology. Society of Exploration Geophysicists.

LYONS, W. B. (2002). Geologic Modeling and Simulation : Sedimentary Systems edited by Daniel F. Merriam and John C. Davis. Geographical Analysis, 34(4), 376-376.

Mosher, S. (2002). Exploring Earth : An Introduction to Physical Geology, Second Edition. Eos, Transactions American Geophysical Union, 83(31), 344-344.

Schlumberger. (2007). ALGERIA WEC, Well Evaluation Conference - Algérie, p. 16 – 18.

Overeem, I., Weltje, G. J., Bishop-Kay, C., & Kroonenberg, S. B. (2001). The Late Cenozoic Eridanos delta system in the Southern North Sea Basin : A climate signal in sediment supply? Basin Research, 13(3), 293-312.

Petrel Geological Process Modeling (GPM) GUIDE, Next, 2023

Qayyum, F., de Groot, P., & Hemstra, N. (2012). Using 3D Wheeler diagrams in seismic interpretation – the HorizonCube method. First Break, 30(3).

Qayyum, F., N. Hemstra, and S. Raman, 2013, A modern approach to build 3D sequence stratigraphic framework: Oil & Gas Journal, 111, 46-46

Radzi, M.R. & Habel, W. & Jirim, S. & Syed Khastudin, Syarifah Nur Ain. (2019). AN INTEGRATED APPROACH OF 3D STRATIGRAPHIC FORWARD MODELLING AND SEQUENCE STRATIGRAPHY TO PREDICT RESERVOIR HETEROGENEITY IN SUBMARINE FAN OF DEEPWATER SABAH. 1-5.

Sabaou, N., Lawton, D. E., Turner, P., & Pilling, D. (2005). FLOODPLAIN DEPOSITS AND SOIL CLASSIFICATION: THE PREDICTION OF CHANNEL SAND DISTRIBUTION WITHIN THE TRIASSIC ARGILOGRESEUX INFERIEUR, BERKINE BASIN, ALGERIA. Journal of Petroleum Geology, 28(3), 223-239.

Tetzlaff, D., & Priddy, G. (2001). Sedimentary Process Modeling : From Academia to Industry. Geologic Modeling and Simulation, 45-69.

Tetzlaff, D. M., J. Tveiten, P. Salomonsen, A. Christ, and W. Athmer, 2014, Geologic process modeling, in IX Congreso De Exploración Y Desarrollo De Hidrocarburos: Insttituto Argentino del Petroleo y del Gas, p. 155–174.

Turner, P., Pilling, D., Walker, D., Exton, J., Binnie, J., & Sabaou, N. (2001). Sequence stratigraphy and sedimentology of the late Triassic TAG-I (Blocks 401/402, Berkine Basin, Algeria). Marine and Petroleum Geology, 18(9), 959-981.

Warrlich, G., Bosence, D., Waltham, D., Wood, C., Boylan, A., & Badenas, B. (2008). 3D stratigraphic forward modelling for analysis and prediction of carbonate platform stratigraphies in exploration and production. Marine and Petroleum Geology, 25(1), 35-58.

APPENDIX

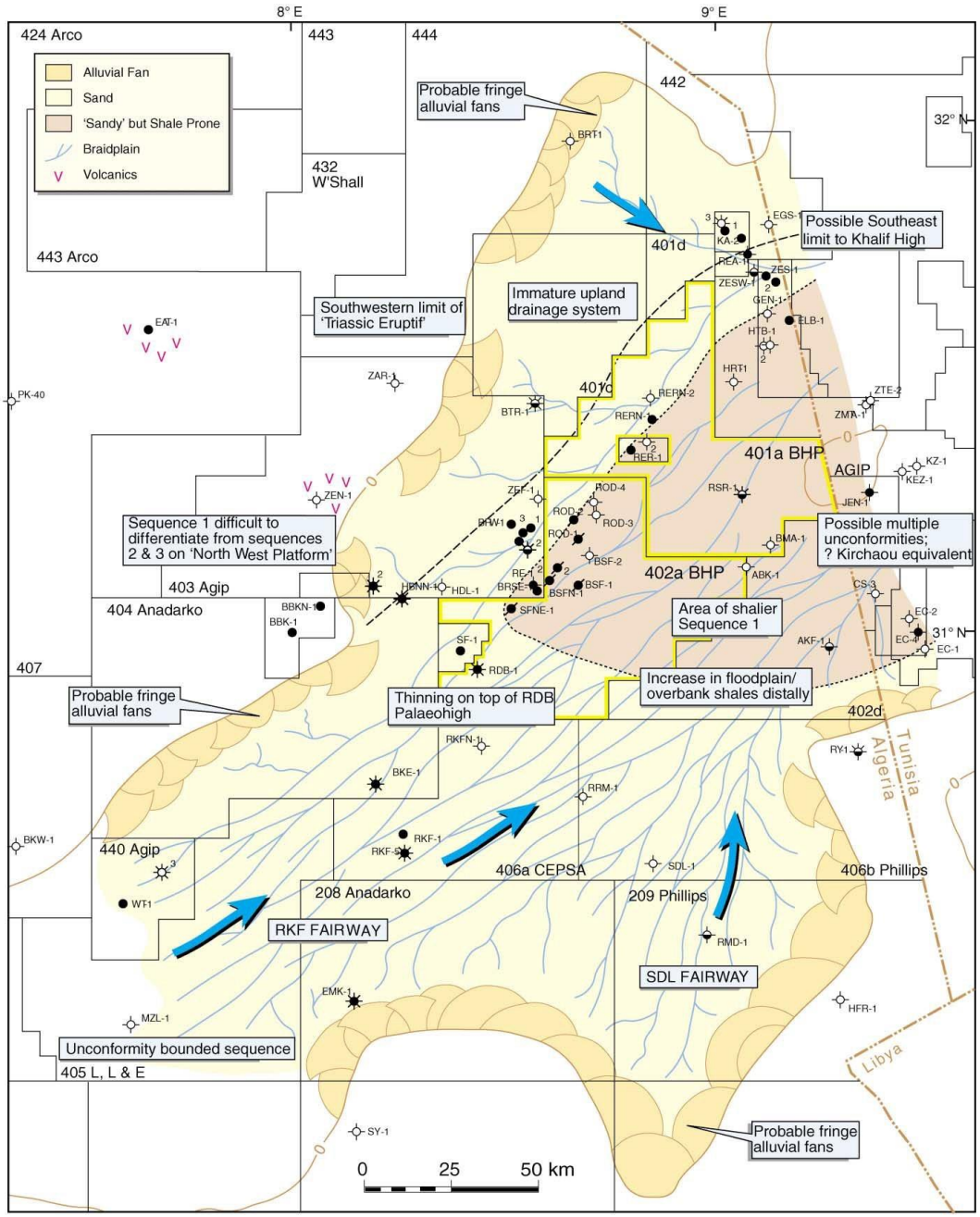

Appendix 1 . Palaeogeography of mid Sequence 1, Turner et al 2001

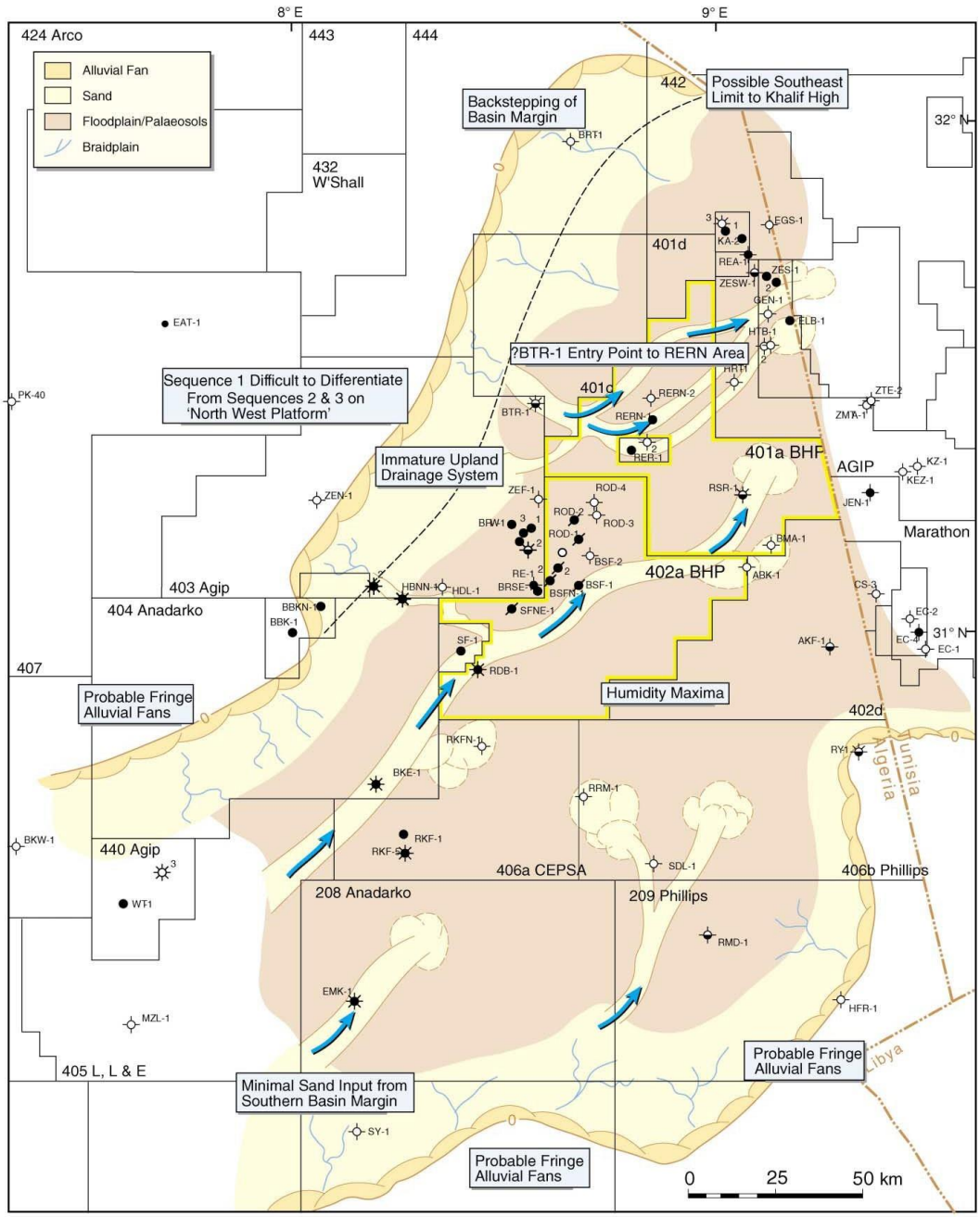

Appendix 2 . Palaeogeography of mid Sequence 2, Turner et al 2001

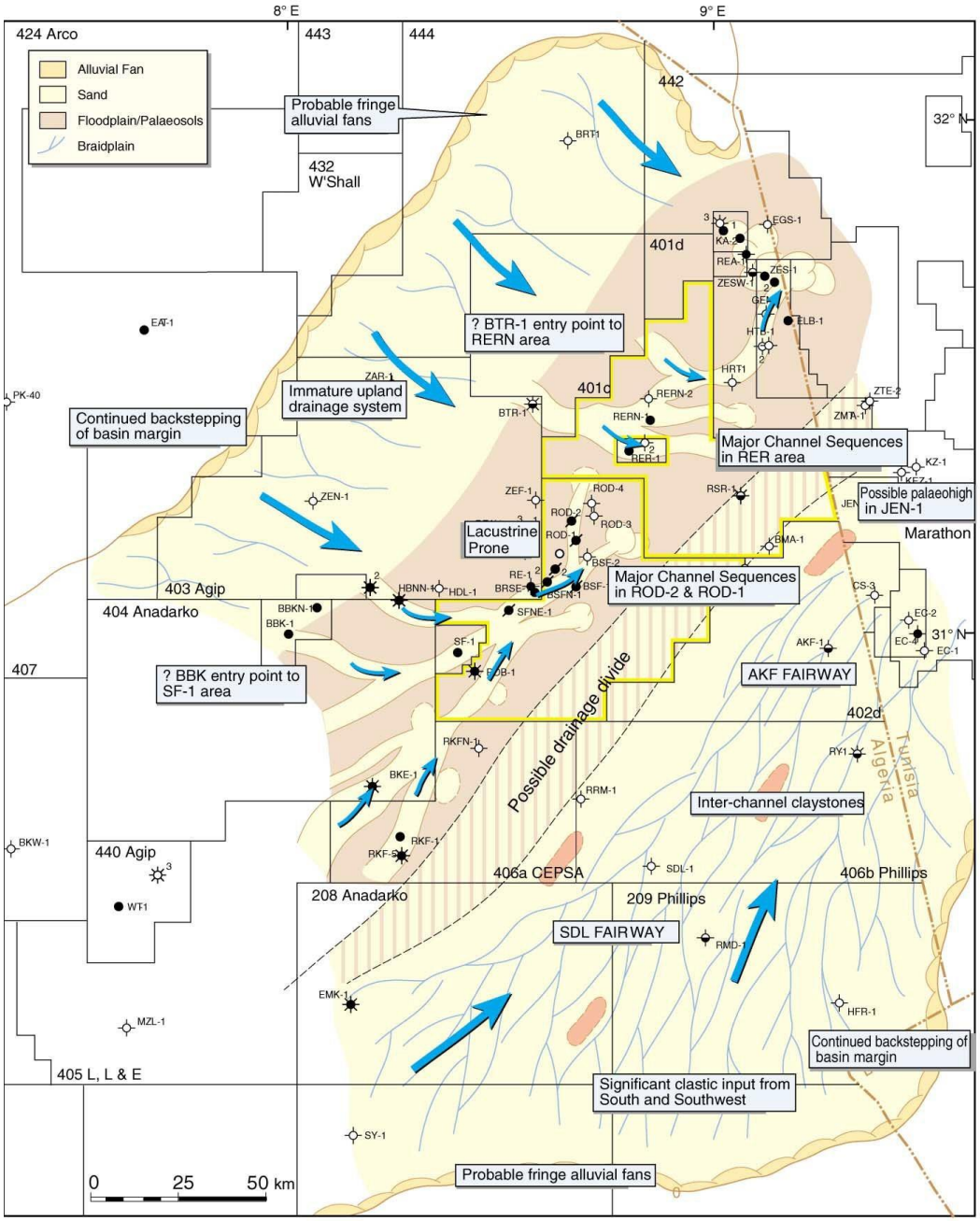

Appendix 3. Palaeogeography of mid Sequence 3, Turner et al 2001

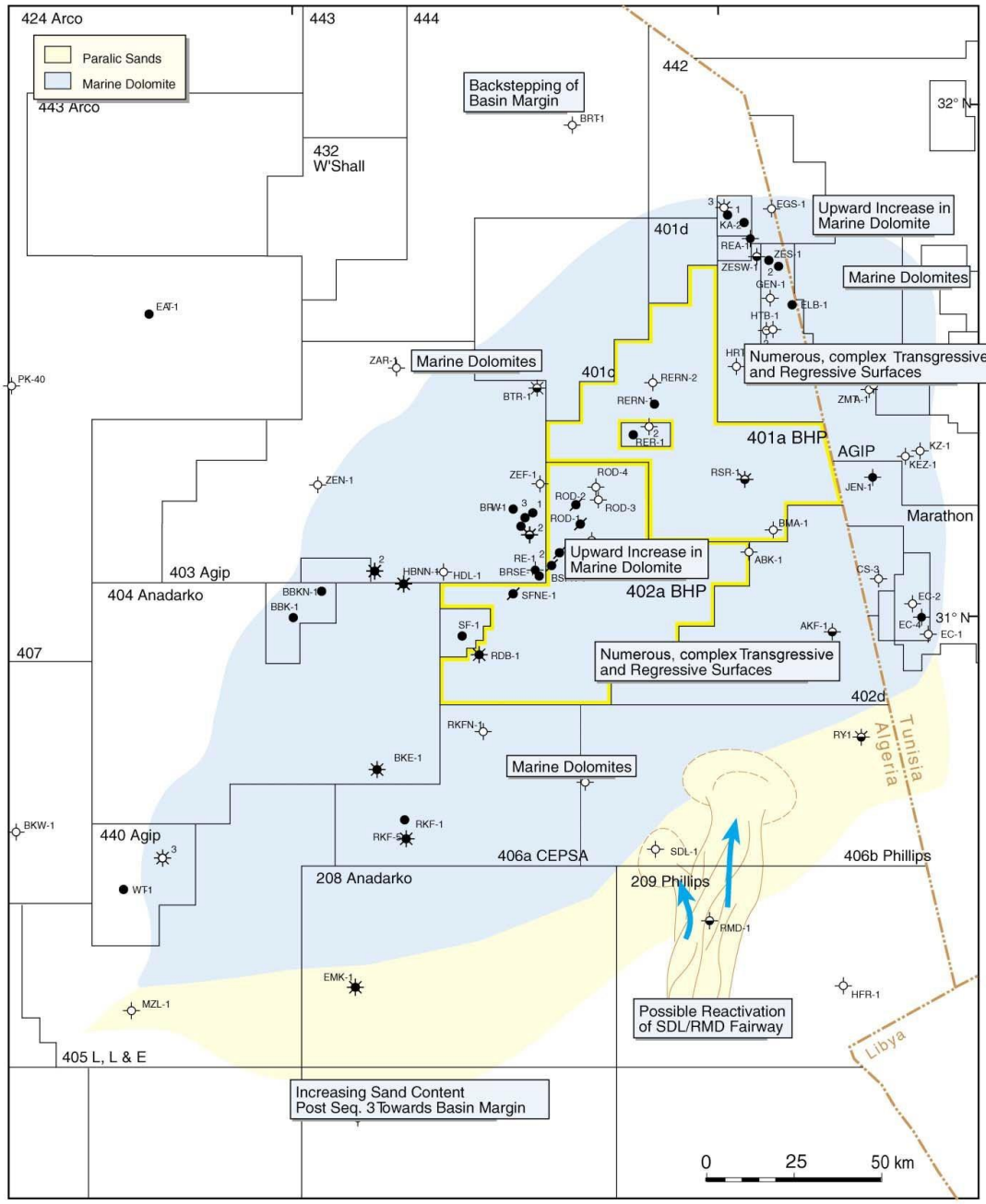

Appendix 4. Palaeogeography near/mid-top Sequence 4, Turner et al 2001